THE UNIVERSITY OF MANITOBA

THE CLIMATOLOGY OF MULTIPLY REFLECTED GLOBAL RADIATION AT TORONTO, CANADA 1 JAN. - 30 JUNE, 1970: A CASE STUDY OF A CLIMATONOMICAL APPLICATION

by

ALLAN M. SAWCHUK

A THESIS

SUBMITTED TO THE FACULTY OF GRADUATE STUDIES

IN PARTIAL FULFILMENT OF THE REQUIREMENTS FOR THE DEGREE

OF MASTER OF ARTS

DEPARTMENT OF GEOGRAPHY

WINNIPEG, MANITOBA

October, 1974

ACKNOWLEDGEMENTS

The author would like to express his sincere gratitude to Dr. A. J. W. Catchpole of the Department of Geography, University of Manitoba, who served as the major advisor for this research. Grateful appreciation is also extended to him for his financial assistance that originated from the National Research Council of Canada and the University of Manitoba. Thanks are also due to D. J. Milton, Department of Geography, and Dr. N. Losey, Department of Mathematics, for their helpful advice during the course during this research.

The author is also indebted to Caroline Trottier, for a commendable job of the cartography, and to Gabriel Tam and Wilfred Falk for their assistance in the computer programming aspects of the study.

Finally, sincere appreciation is extended to all those, both faculty and students, particularly to members of the 'GFA', who offered both their assistance and encouragement to expedite this research.

THE CLIMATOLOGY OF MULTIPLY REFLECTED GLOBAL RADIATION AT TORONTO, CANADA 1 JAN. - 30 JUNE, 1970: A CASE STUDY OF A CLIMATONOMICAL APPLICATION

by

ALLAN M. SAWCHUK

A dissertation submitted to the Faculty of Graduate Studies of the University of Manitoba in partial fulfillment of the requirements of the degree of

MASTER OF ARTS

TABLE OF CONTENTS

LIST OF TABLES

LIST OF ILLUSTRATIONS

FIGURE Page

CHAPTER I

INTRODUCTION AND THE PROBLEM

Introduction

The scattering and absorptive properties of the atmosphere ensure that a certain proportion of the incident solar radiation will be depleted upon its arrival at the earth's surface. Under certain circumstances, however, these properties may act to enhance the receipt of global radiation (i.e., total radiation from sun and sky).

The process responsible for this increase has been denoted by various terms, including: 'multiple reflection' (Ångström and Tryselius[1]; Catchpole and Moodie[2]), 'multiple scattering' (Deirmendjian and Sekera)[3], and 'backscatterance of the sky' (Möller)[4].

While multiple scattering refers more strictly to multiple particulate scattering and multiple reflection to the reflections occurring between the earth's surface and the atmosphere, no loss of generality is incurred by considering the two terms synonomous. This thesis employs the term multiple reflection. This term therefore encompasses both particulate scattering of global radiation and reflection of global radiation at the earth's surface. Backscatterance of the sky represents

---

1. Ångström, A., and Tryselius, O., 1934: Total Radiation from Sun and Sky at Abisko, Geografiska Annaller, V. 16, pp. 53-69.

2. Catchpole, A.J.W., and Moodie, W., 1971: Multiple Reflection in Arctic Regions, Weather, V. 26, No. 4, pp. 157-163.

3. Deirmendjian, D., and Sekera, Z., 1954: Global Radiation Resulting from Multiple Scattering in a Rayleigh Atmosphere, Tellus, V. 6, pp. 382-398.

4. Möller, F., 1965: On the Backscattering of Global Radiation by the Sky, Tellus, V. 17(3), pp. 350-355.

that portion of the scattered and earth-reflected radiation that is reflected back to the earth's surface by the atmosphere. It is thus an important component of the multiple reflection process.

By multiple reflection is meant the case where global radiation, incident at some point at the earth's surface, is reflected upwards to the atmosphere, then reflected downwards to the earth's surface, etc. The situation is outlined schematically in FIG. 1.

In the absence of absorption and assuming complete forward-scattering (i.e., in a direction towards the earth's surface) an infinite number of such cyclic reflections would be possible. In the real-world, however, such a conceptualization is never realized. This is because absorption and scattering do attenuate the reflected radiation sufficiently such that after a certain number of cyclic reflections have occurred further reflections result in a negligible contribution to the global radiation receipt. Nevertheless, under certain circumstances, the contribution of multiply reflected global radiation to the global radiation receipt may be significant.

Theoretical modelling of the multiple reflection process has presented some formidable problems. The main difficulty encountered arises from the complicated nature of radiative transfer in the atmosphere, which, in the most general case, is rather inaccessible to mathematical solutions in general form (Deirmendjian and Sekera)[5].

The solution to this problem becomes nearly intractable for the case of cloudy atmosphere. Clouds are complex entities possessing certain optical properties not present in the cloudless atmosphere. It is not

---

5. Deirmendjian and Sekera, 1954, op. cit.

Figure 1

A SCHEMATIC MODEL FOR MULTIPLE REFLECTION

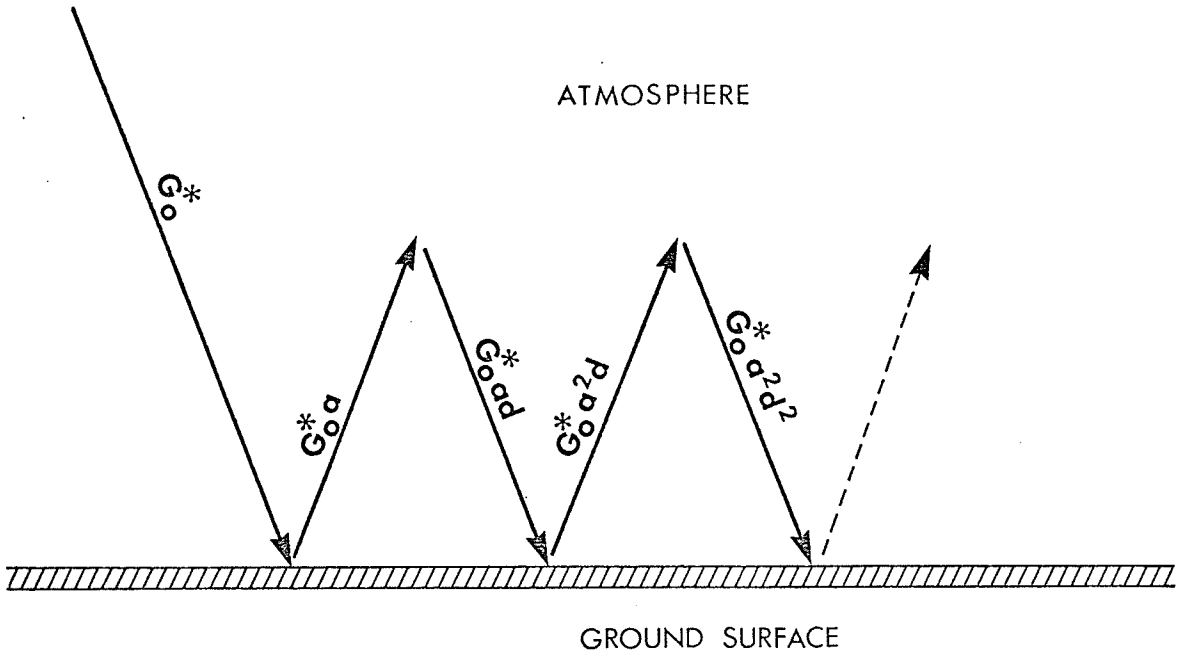

G_o^* global radiation prior to multiple reflection

a surface albedo

d backscatterance of the sky

After Catchpole and Moodie, 1971, op.cit.

surprising to find therefore that theoretical modelling has been, more or less, restricted to ideal cases, such as a Rayleigh atmosphere[6], and a turbid[7], but cloudless, atmosphere. Analyses of multiple reflection have been attempted for the case of cloudy atmosphere, as will be indicated later on. But such analyses are invariably made in the light of certain assumptions regarding the cloud model. The relation between the degree of multiple reflection and various cloud parameters, such as cloud height and thickness, do not appear to be very well understood.

Climatologically, the main interest in this flux would appear to lie in the degree to which the global radiation is intensified as a result of multiple reflection. Thus, if it is possible to calculate the global radiation prior to multiple reflection, and if the actual global radiation is known from, say, pyrheliometric readings, then the ratio of global radiation with multiple reflection to the global radiation prior to multiple reflection can be formed.

Ångström and Tryselius[8] were apparently the first researchers to propose such a relationship. Recalling FIG. 1, let

G^* = actual global radiation receipt for some surface with $a > 0$,
G_o^* = global radiation receipt over an ideally black earth's surface (i.e., $a = 0$),
a = surface albedo,
d = backscatterance of the sky.

---

6. A Rayleigh atmosphere may be defined as a homogeneous atmosphere containing only spherical particles whose diameter is much smaller than the wavelength of the incident radiation. Mathematically, $a\lambda^{-1} \ll 1$, where a is the diameter of the particle, and λ is the wavelength of the incident radiation.

7. A turbid atmosphere may be defined as a heterogeneous atmosphere containing an entire spectrum of particle-size characteristics ranging from small ions to giant nuclei and including haze and industrial aerosols. Mathematically, $a/\lambda \geq 1$. The necessity of distinguishing between the Rayleigh and turbid cases will be shown in Chapter II.

8. Ångström and Tryselius, 1934, op. cit.

Then at any point on the earth's surface the total receipt of global radiation, G^*, may be expressed as an infinite series, or,

$$G^* = G_o^* - G_o^* a + G_o^* ad - G_o^* a^2 + G_o^* a^2 d^2 - \ldots \qquad (1)$$

It is easy to demonstrate that this is a convergent series whose limit is given by $(1 - ad)^{-1}$. Thus

$$G^*/G_o^* = (1 - ad)^{-1} \qquad (2)$$

Eqn. (2) is the form originally proposed by Ångström and Tryselius. The ratio G^*/G_o^* shall here be denoted as the intensification ratio. Parenthetically, it is interesting to note that eqn. (2) can be derived from the principles of climatonomy which is discussed in greater detail in Chapter III.

According to Sellers[9], Budyko[10], and others, the global radiation, G^*, may be expressed as the sum of two components: Q, the direct radiation, and q, the diffuse flux. The latter flux in turn may be viewed as being comprised of two fluxes: q_p, primary scattering from the direct beam, and q_m, the flux of diffuse radiation which has experienced reflection from the earth's surface at least once. The term G_o^* may be similarly partitioned. It represents the sum of $(Q + q_p)$. It is possible to invest the following physical interpretation to the ratio G^*/G_o^*: it represents the intensification of global radiation due to the flux of multiply reflected global radiation.

---

9. Sellers, W.D., 1969: Physical Climatology, The University of Chicago Press, Chicago and London, 272 pp.

10. Budyko, M.I., 1956: The Heat Balance of the Earth's Surface (Trans. from the Russian by N.A.Stepanova, U.S. Dept. of Commerce, Washington, D.C., 1958), GMID, Lenningrad, U.S.S.R., 1956.

It is instructive to note that, by definition, $\{0 \leq a,d \leq 1\}$. Substitution of these limit values into eqn. (2) yields the following.

When $\{a = d = 0\}$, eqn. (2) reduces to the form

$$G^* = G_o^* \quad \text{or, alternatively, as} \quad G^*/G_o^* = 1.000$$

When $\{a = d = 1\}$, the denominator of the r.h.s. of eqn. (2) vanishes so that $G^*/G_o^* \longrightarrow \infty$.

The domain of definition for G^*/G_o^* is therefore the interval $(1, \infty)$.

While these limiting values rarely occur in nature, the discussion does indicate some of the climatological features of the intensification ratio. Thus maximum values of the intensification ratio when maximum values of surface albedo and backscatterance occur synchronously. Physically, such a situation is likely to arise in nature when dense clouds of large optical thickness overlie a highly reflecting snow surface.

Conversely, when $\{a,d\}$ = minimum, minimum values of G^*/G_o^* result. Such situations may be given during anticyclonic spells in summer. In this case a greater absorption, both in the atmosphere and at the earth's surface, and a low backscatterance from clear skies, result in minimum values of the intensification ratio.

Conceptualization of multiple reflection as a reflecting boundries problem is thus of some climatological utility, but only to the extent that the variables a and d are accurately known. In turn, surface albedo and backscatterance are complex expressions of the earth's surface and atmosphere, respectively. Both variables are characterized by diurnal, and in mid- and high-latitudes, seasonal regimes. Moreover,

instrumentation offers little in the way of assistance. For whereas values for surface albedo may be deduced from measurements of the components of solar radiation, backscatterance cannot be measured at all. This is because current instrumentation employed in measuring the diffuse flux cannot distinguish between q_p and q_m. Consequently, any inquiry into the multiple reflection process necessitates consideration of those processes that determine a and d for any given set of atmospheric and surface conditions. Of paramount importance in this respect are the processes of scattering and absorption.

Theoretical calculations by Deirmendjian and Sekera[11] indicate values of G^*/G_o^*, for a Rayleigh atmosphere, ranging from 1.011 to 1.042, corresponding to backscatterances of 0.044 to 0.073. For the turbid, but cloudless, atmosphere Feigel'son et al[12] have calculated a range of values for G^*/G_o^* of 1.064 - 1.180, corresponding to backscatterances of 0.120 - 0.305. These values reflect differences in solar zenith angles, the optical thickness of the atmosphere, and the particular scattering function that is assumed. In passing it is noted that these values are not strictly comparable, not only because different models are assumed, but also because the values are calculated employing different values for the surface albedo. The salient feature in these comparisons is that with increasing turbidity the intensification ratio increases. Even higher values of the ratio G^*/G_o^* may be expected for the case of cloudy atmosphere, because backscatterance from a cloud base is always greater

---

11. Deirmendjian and Sekera, 1954, op. cit.

12. Feigel'son, E.M., Malchevich, M.S., Kogan, S.Ya., Koronotova, T.D., Glazova, K.S., and Jutznetsova, M.A., 1960: Calculations of the Brightness of Light in the Case of Anisotropic Scattering, Part I (Trans. from the Russian by Consul. Bureau, New York, U.S.A.).

than that from a cloud-free atmosphere.

Ångström and Tryselius[13] evaluated G^*/G_o^* at Abisko (68°21' N, 18°49' E), for illustrative purposes, by assigning 'typical' values of a and d. For overcast skies it was assumed that d = 0.75, while for clear skies it was assumed that d = 0.25. Similarly, for a snow-covered surface it was assumed that a = 0.70, while for a snow-free surface it was assumed that a = 0.10. These assumptions permit G^*/G_o^* to vary between 1.025 (clear-sky) - 1.081 (overcast) in summer and 1.212 (clear-sky) - 2.105 (overcast) in winter.

Statistical comparison of radiation data by Möller[14] for the Canadian stations Moosonee (51°16' N, 83°39' W) and Toronto-Scarborough (43°43' N, 79°14' W) indicate intensification ratios (and corresponding backscatterance values) ranging from 1.14 (0.28) - 1.19 (0.36) for overcast sky at Toronto-Scarborough to 1.46 (0.58) - 1.60 (0.69) for overcast sky at Moosonee. For cloudy and cloudless conditions Möller finds values of 1.05 (0.11) - 1.19 (0.36) for Toronto-Scarborough and 1.20 (0.31) - 1.23 (0.34) for Moosonee. These values were obtained by comparing the global radiation receipt during the period of snow-covered surface to that during the snow-free period for several zenith angle intervals. And since Möller could compute the values for surface albedo, the intensification ratios refer to the ratios $G^*_{0.71}/G^*_{0.168}$ at Moosonee and $G^*_{0.65}/G^*_{0.21}$ at Toronto-Scarborough.

Several considerations cast some doubt as to the utility of these methodologies. In the first instance, comparison of global radiation receipts over a snow-covered surface to a snow-free surface is not strictly justified because of varying degrees of absorption of (global) radiation

---

13. Ångström and Tryselius, 1934, op. cit.

14. Möller, 1965, op. cit.

and (possible) changes in atmospheric backscattering characteristics. Möller's and Ångström's and Tryselius' values refer to the net effect of several changes, not that necessarily due to changes in surface albedo.

Secondly, while these values indicate the magnitude of the seasonal differences, they are too explicit to ascertain the actual seasonal regime of G^*/G_o^* at a locality. Yet in mid- and high latitudes both surface albedo and atmospheric backscatterance experience pronounced variations. This leads one to conclude that the intensification ratio must also exhibit a distinct seasonal regime.

There would appear to be strong motivation for obtaining the actual seasonal regime of G^*/G_o^*. Such motivation stems from an examination of the relationship between the multiple reflection process and the global solar radiation estimation equations.

The problem of estimating global radiation receipts at the earth's surface from other more extensively recorded parameters has drawn the attention of a number of climatologists, engineers, architects, and scientists from many other disciplines. Two parameters in particular, that of cloudiness and the duration of bright sunshine, have been utilized for this purpose. Haurwitz[15], Neuman[16], and others have investigated the relationship between cloudiness and (relative) global radiation receipt. These relationships do not appear to have gained wide recognition.

Other researchers, eg., Kimball[17], Ångström[18], Black, Bonython, and

---

15. Haurwitz, B., 1945: Insolation in Relation to Cloudiness and Cloud Density, J. Meteor., V. 2, pp. 154-166.

16. Neuman, J., 1954: Insolation in Relation to Cloud Amount, Mon.Weath. Rev., V. 82, pp. 317-319.

Prescott[19], Fritz and McDonald[20], and others, have devoted their efforts to formulating empirical relationships between global solar radiation and bright sunshine. The duration of bright sunshine appears to be a better estimator of global radiation than cloudiness because: it is recorded continuously whereas cloud measurements are instantaneous measurements; it is measured instrumentally whereas clouds are not; moreover, the duration of bright sunshine may be taken as a measure of cloudiness since this type of information does take into account the optical density of the clouds at a certain stage (Robinson)[21].

The relationship has generally taken the form of a (simple) linear regression equation, viz.,[22]

$$Q/Q_o = \hat{a} + \hat{b}n/N \qquad (3)$$

where Q = the global radiation receipt,
Q_o = corresponding clear sky radiation,

---

17. Kimball, H.H., 1919: Variations in Total and Luminous Radiation with Geographical Position in the United States, Mon.Weath.Rev., V. 47, pp. 769-793.

18. Ångström, A., 1924: Solar and Terrestrial Radiation, Quart. J. Roy. Met. Soc., V. 20, pp. 121-125.

19. Black, N.J., Bonython, C.W., and Prescott, J.A., 1954: Solar Radiation and the Duration of Bright Sunshine, Quart. J. Roy. Met. Soc., V. 80, pp. 231-235.

20. Fritz, S., and McDonald, T.H., 1949: Average Solar Radiation in the United States, Heating and Ventilating V. 46, pp. 61-64.

21. Robinson, N., 1966: Solar Radiation, Elsevier, Amsterdam, 347 pp.

22. Unfortunately some variable names have been duplicated. To avoid ambiguity statistical variables and constants are denoted by the symbol $\hat{}$.

n = actual hours of bright sunshine,
N = Maximum number of possible hours of bright sunshine,
a,b = empirical constants to be determined.

The form of eqn. (3) was originally proposed by Ångström[23]. He obtained, from data at Stockholm, the relationship

$$Q_s = Q_o(0.25 + 0.75n/N) \qquad (4)$$

By definition $\hat{a}$ and $\hat{b}$ total to unity, since on clear days $Q_s = Q_o$[24]. Since $\hat{a}$ was determined, by comparison of pyrheliometric records, to be 0.25 it follows that $\hat{b} = 0.75$. Ångström further stated that his results corroborated almost exactly with those of Kimball[25]. Unfortunately, this agreement may have been purely fortuitous.

Black et al[26], utilizing data from widely disparate geographical regions and records varying in length from three to sixty years, obtained

$$Q/Q_o = 0.23 + 0.48n/N \qquad (5)$$

In eqn. (5) Q_o represents the extra-atmospheric flux. Thus eqn. (5) is not strictly comparable to the other equations.

Fritz and McDonald[27], using data from continental United States,

---

23. Ångström, 1925, op. cit.

24. It is instructive to note that Ångström did not use regression analysis to determine a and b. a was determined by comparing pyrheliometric records of overcast to clear sky conditions. Statistically, there is no reason why these constants should total to unity.

25. Kimball, 1919. op. cit.

26. Black et al, 1954, op. cit.

27. Fritz and McDonald, 1949, op. cit.

obtained

$$Q/Q_o = 0.35 + 0.61n/N \qquad (6)$$

Mateer[28], using Canadian data, obtained the relationship

$$Q/Q_o = 0.43 + 0.58n/N\ (1.00 + 5.54w^2) \qquad (7)$$

where w is a correction term applied for the time when the sun was less than five degrees above the horizon.

When the predicted values are compared to the actual values some consistent discrepancies emerge. Mateer, for instance, has noted that his equation consistently underestimates global radiation receipts for the winter months, while radiation receipts for the summer months are overestimated. He invoked multiple reflection as an explanation for the underestimated winter months. According to Mateer

> "When snow cover is present along with thin high cloud and/or 'scattered' or 'broken' middle or even low cloud, some solar radiation may be trapped between the highly reflecting snow surface and the cloud. Multiple reflections may then increase the observed insolation to somewhere near the cloudless day value. However, the cloud will cause interruptions in the sunshine record and may even stop the record entirely. Thus we may have a relatively high value of Q/Q_o associated with a relatively low value of n/N."

Mateer corrected for this effect by developing a set of equations:

$$Q/Q_o = \begin{cases} 0.450 + 0.78n/N(1.00 + 2.78w^2) & \text{for winter months} \\ 0.355 + 0.68n/N & \text{for summer months} \end{cases} \qquad (8)$$

---

28. Mateer, C.L., 1955: A Preliminary Estimate of Average Insolation in Canada, Can. J. Agric. Sci., V. 35, pp. 579-594.

Subsequent research, eg., Bennett[29], Titus and Truhlar[30], have followed this procedure.

It may be postulated that these discrepancies are statistical. For instance, a curvelinear regression may have yielded a better fit to the data. However, the fact that these discrepancies reveal a seasonal bias leads one to conclude that the problem is more climatological in nature.

Dreidger[31], in a detailed examination of the (linear) relationship between the relative global radiation receipt (i.e., Q/Q_o) and relative sunshine duration (i.e., n/N) at Winnipeg (49°54' N, 97°35' W), found that when the constants $\hat{a}$ and $\hat{b}$, when plotted as a function of time of year, were inversely related and may be functionally described as parabolic. This is indicated in FIG. 2 for the 29-day period.

Dreidger and Catchpole[32] have noted that the abrupt decrease in the constant $\hat{a}$ in spring is coincident with the median date of snow-pack decay at Winnipeg. This led these authors to conclude that the magnitude that the magnitude of $\hat{a}$ is influenced by the multiple reflection process.

On the other hand, the behaviour of $\hat{a}$ during late autumn and early winter is somewhat less distinct. This may be related to the fact that the establishment of the winter snow-cover is not a decisive event.

---

29. Bennett, I., 1965: A Method for Preparing Maps of Mean Daily Global Radiation, Arch. Met. Geophys. Biokl., Ser. B, V. 13, pp. 216-248.

30. Titus, R.L., and Truhlar, E., 1969: A New Estimate of Average Global Solar Radiation in Canada, Dept. of the Environment (formerly Dept. of Transport), Meteorological Branch

31. Dreidger, H.L., 1969: An Analysis of the Relationship between Total Daily Solar Radiation Receipt and Total Daily Duration of Sunshine at Winnipeg, 1950-1967. Unpublished M.A. Thesis, University of Manitoba, Winnipeg, Canada.

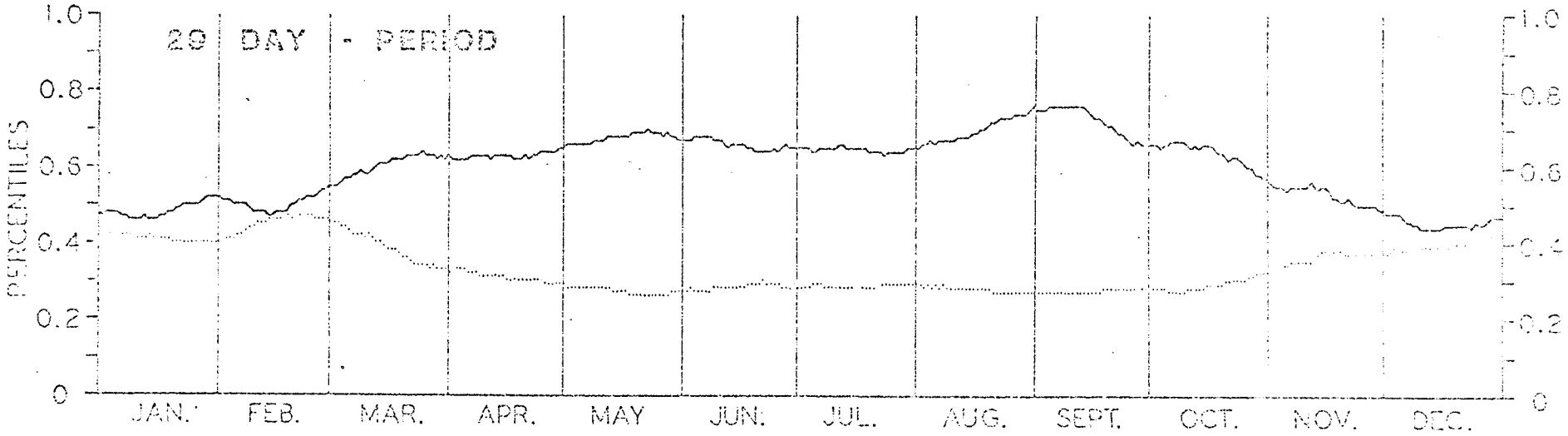

FIG. 2 - The parameters a and b for the regression of Q/Q_o on n/N at Winnipeg, 1950-1967, for the 29-day period plotted for the entire year. The dotted line represents a and the solid line represents b. From Dreidger, 1969, op. cit.

During the period of snow build-up discontinuities in the snow-pack may result from incursions of warm air from travelling depressions. In this event significant fluctuations may arise in surface albedo and culminating in a reduction in the contribution of multiply reflected radiation to the total global radiation receipt. Considering the parameter $\hat{a}$ alone leads to the conclusion that the relationship is rather sensitive to changes in surface albedo.

On the other hand, if the parameter $\hat{b}$ is considered, i.e., the slope, or, mathematically, d (Q/Q_o) / d (n/N), one is led to conclude that changes in sunshine duration, which consequently implies changes in cloudiness, over a snow-free surface are the important factor, since both $\hat{b}$ and the magnitude of the variability of $\hat{b}$ are greater over a snow-free surface than over a snow-covered surface.

Summary - The Problem

In order to elucidate the relationship between multiple reflection and the global radiation estimation equations it is apparent that a more detailed knowledge of the climatology of G^*/G_o^* must be given. In particular, it would be desireable to know how the intensification ratio varies with both surface and atmospheric conditions.

Empirical estimates, such as by Ångström and Tryselius, and Müller, are too crude to ascertain the actual regime. Such empirical work, cannot, for instance, evaluate the instantaneous value of G^*/G_o^* for a given set of conditions. In any event, such empirical analyses can only guage the magnitude of the seasonal differences that exist at a locality, and thus

---

32. Dreidger, H.L., and Catchpole, A.J.W., 1970: Estimation of Solar Radiation Receipt from Sunshine Duration at Winnipeg, Met. Mag., V. 99, pp. 285-291.

are not well suited to the particular problem of evaluating the actual seasonal regime. On the other hand, theoretical models require specific information on the size-density-and material-nature characteristics of the particulate matter in the atmosphere. This type of information is rarely available, particularly on a routine basis.

This thesis has, as its principle objective, the evaluation of the climatology of G^*/G^*_o for Toronto Meteorological Research Station (Toronto MRS) ($43^o18'$ N, $79^o33'$ W), for the period 1 Jan. - 30 June/ 70.The methodology employed was the principles of climatonomy, which might here be described as a set of equations parameterizing short-wave solar radiation relations. This is described in greater detail in Chapter III. The application of this methodolgy encountered a number a difficulties of a fundamental nature. This study might be described, therefore, as a case study of a climatonomical evaluation of the climatology of multiply reflected global radiation at Toronto.

The structure of the thesis is trichotomous. The first part (Chapter II) examines the multiple reflection from a theoretical viewpoint. The second part (Chapters III and IV) discusses, respectively, the methodology and the results. The third part (Chapter V) reconsiders some of the methodological problems that were encountered in this application of climatonomy and how they might be potentially resolved.

CHAPTER II

THE MULTIPLE REFLECTION PROCESS

The multiple reflection process is a fundamental consequence of the interaction of particulate matter with the solar radiation field. This particulate matter, whose size distribution ranges from small ions and air molecules to giant nuclei and raindrops, affects the incident solar radiation in two principle ways: scattering and absorption. The latter process represents an extraction of energy and thus affects the amount of radiation that is able to enter into the multiple reflection process. In contrast, scattering represents a dispersion of radiation and is the principle mechanism through which the diffuse flux arises. It is of some importance therefore to examine these processes in greater detail.

With regard to scattering, it is instructive to differentiate between those particles such that $a\lambda^{-1} \ll 1$ and those particles where the condition $a\lambda^{-1} \geq 1$ holds true. The former class consists of small spherical particles such as air molecules. An atmosphere consisting solely of such matter is termed a Rayleigh atmosphere. The latter class consists of particles such as dust, aerosols, water vapor molecules, etc. Such an atmosphere is often termed a turbid atmosphere. The distinction between these classes is necessary because these classes obey quite different scattering laws.

This Chapter will focus attention on scattering in a Rayleigh atmosphere. While there does not exist any physical correspondence to a Rayleigh atmosphere on the planet Earth, certain geographical regions

do represent fair approximations to the Rayleigh case. Moreover, differences between Rayleigh and aerosol scattering (i.e., scattering in a turbid atmosphere) are not so much in kind as they are in degree.

Given this description of scattering in a Rayleigh atmosphere, the implications of more realistic models, such as aerosol scattering, scattering in cloudy media, and absorption, etc., will be discussed.

1. Scattering in a Rayleigh Atmosphere

This section consists of two parts. The first part presents a derivation of the scattering coefficient for a Rayleigh atmosphere. This represents q_p in the terminology of Chapter I. The second part illustrates how this quantity is employed to calculate q_m, i.e., the flux of multiply reflected global radiation. The derivation of the scattering coefficient follows that given by Johnson[33].

Rayleigh's principle assumption that $a\lambda^{-1} \ll 1$ allows one to consider the scattering center as an oscillating dipole[34]. Consider a scatterer of energy to be surrounded by an (imaginary) sphere of radius r. r shall be chosen so large that the scatterer may be considered to be a point source. The situation is portrayed schematically in FIG. 3.

As the energy, or total power, F, is conserved in passing from source to the spherical surface

---

33. Johnson, J.C., 1954: Physical Meteorology, The M.I.T. Press, Cambridge, Mass., 393 pp.

34. When the centers of electric charges of equal and opposite magnitudes are separated by a measurable distance, the product of one of the poles and the distance between the two is the dipole moment, and the entire system is termed the dipole. When the magnitude of the dipole moment changes in a periodic fashion, the system is termed an oscillating electric dipole.

Figure 3

A SCHEMATIC INTERPRETATION OF EQNS. (9)-(12)

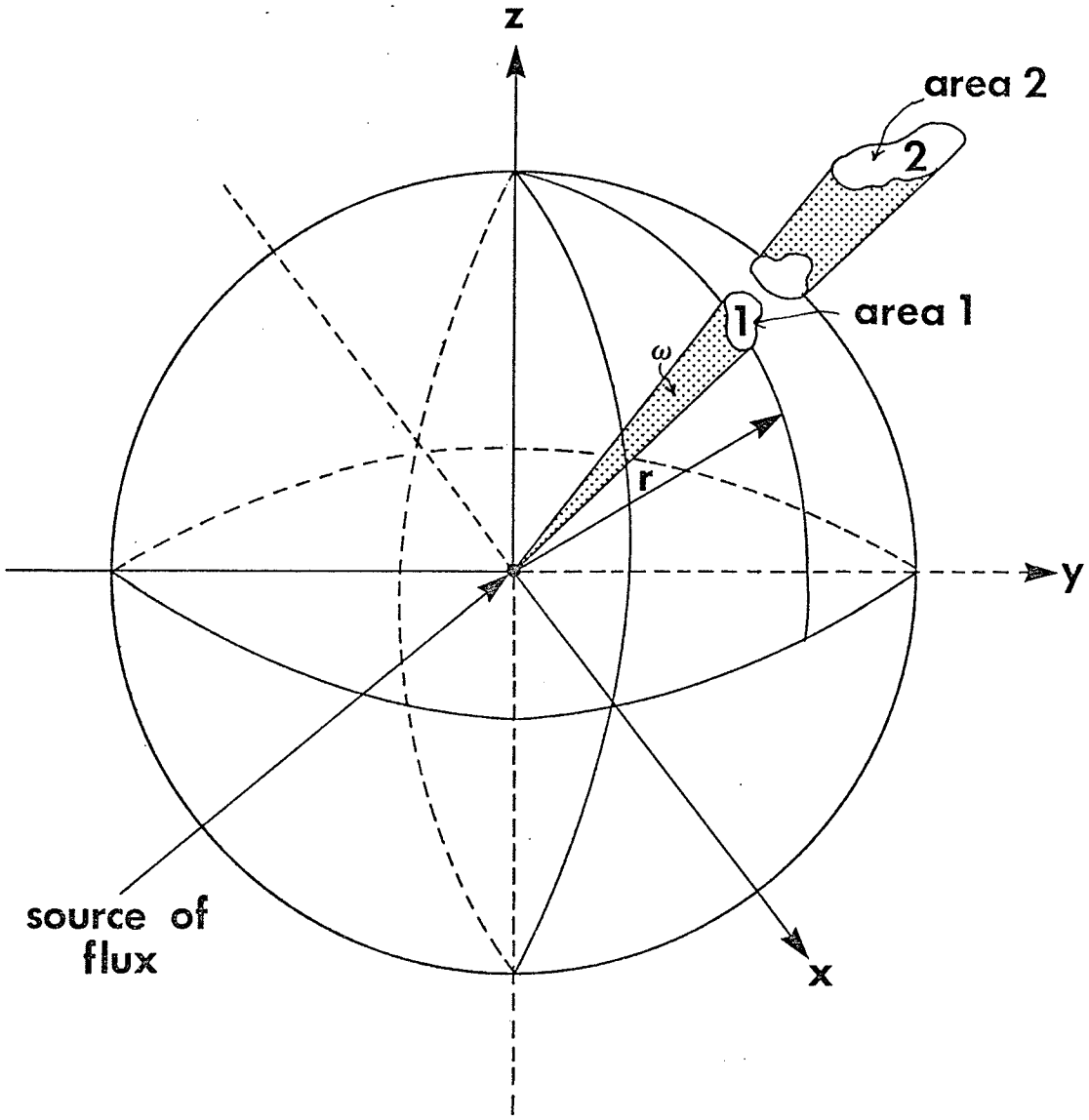

Area 2 has any orientation in space. Area 1 is the projection of Area 2 on a sphere of radius, r. $F_1 = F_2; E_1 > E_2; \omega_1 = \omega_2;$ and $I_1 = I_2$.

From Johnson, 1954, op.cit.

$$F = 4\pi r^2 E \qquad (9)$$

where E is the flux density.

By definition, the number of steradians in a sphere of solid angle ω is

$$\omega = \frac{4\pi r^2}{r^2} = 4\pi \qquad (10)$$

The intensity becomes therefore

$$I = \frac{F}{\omega} = \frac{4\pi r^2 E}{4\pi} = Er^2 \qquad (11)$$

The intensity may also be expressed in differential form as

$$I = \frac{dF}{d\omega} \qquad (12)$$

where $d\omega$ represents the differential of solid angle. The intensity in differential form represents the instantaneous flux density. As such it can also be rewritten as the magnitude of the power flow of an electromagnetic wave travelling with the speed of light, c, whose electric vector is $\mathbf{E}$. In this notation, E is the magnitude of the Poynting vector, which vector is equal to the power flow. This makes[35]

$$E = \frac{c}{4\pi}\left|\mathbf{E}^2\right| \qquad (13)$$

Eqn.(13) states that E is the instantaneous flux density of the scattered electromagnetic wave, and $\mathbf{E}$ is the instantaneous magnitude of the electric vector of this scattered wave.

The oscillating dipole is the source of the scattered flux. Since periodically changing motion is implied E must be proportional to a force, which in this case, is the acceleration of the dipole moment.

Since E, the flux density, falls off as the square of the distance, E must also be proportional to r^{-1}. And, since both the scattered flux and polarization of the dipole are vectors, the component of the radiation from the oscillating dipole along a given radius vector of magnitude r varies as $\sin\alpha$, where α is the angle between the electric vector E of the incident light and the direction along which the scattered flux is detected.

Expressing E as a function of the variables mentioned above gives

$$E = \frac{1}{c^2} \frac{d^2P}{dt^2} \frac{\sin \alpha}{r} \qquad (14)$$

where d^2P/dt^2 is the acceleration of the dipole moment and c^{-2} is the constant of proportionality.

---

35 As stated previously, E is an instantaneous value and is defined on the interval $\left(0, \frac{c}{4\pi} \left| E^2_{max} \right|\right)$. The average value of E is found by replacing $|E^2|$ by the square of the root mean square value of the electric vector. Thus

$$E_{rms} = \frac{E_{max}}{\sqrt{2}}$$

and thus

$$\bar{E} = \frac{c}{8\pi} \left| E^2_{max} \right|$$

It is assumed that

$$E = E_{max} \sin \frac{2\pi c}{\lambda} t$$

where E_{max} is the amplitude of the electric vector

The induced dipole moment P is related to the index of refraction, m, through the Lorenz-Lorentz law. The strength of this induced dipole is directly proportional to the amplitude of the incident electric vector E_o. The amplitude of the induced dipole moment is

$$P_o = \frac{3E}{4\pi}\left(\frac{m^2-1}{m^2+2}\right) V \qquad (15)$$

where V is the volume of a scatterer.

Assuming a simple sinusoidal variation for P, the instantaneous dipole moment, yields

$$P = P_o \frac{\sin^2 \pi c}{\lambda} t \qquad (16)$$

Differentiating eqn.(16) twice yields the acceleration of the dipole moment, namely,

$$\frac{d^2P}{dt^2} = -\left(\frac{2\pi c}{\lambda}\right)^2 P_o \sin \frac{2\pi c}{\lambda} t \qquad (17)$$

Substitution and re-arrangment of terms gives

$$E = \frac{-3\pi E_o}{r}\left(\frac{m^2-1}{m^2+2}\right)\frac{V}{\lambda^2} \sin \frac{2\pi c}{\lambda} t \sin\alpha \qquad (18)$$

As has already been stated E is an instantaneous value. It is the mean value of this quantity that is required here, i.e.,

$$E^2_{rms} = \frac{9\pi^2 E_o^2}{r^2}\left(\frac{m^2-1}{m^2+2}\right)^2 \frac{V^2}{\lambda^4} \sin^2\alpha \overline{\sin \frac{2\pi c}{\lambda} t} \qquad (19)$$

where the bar over the quantity $(\sin(2\pi c\lambda^{-1}t))$ indicates the mean value of the quantity. It can be shown that the mean value is $\frac{1}{2}$. Substitution back into eqn.(19) yields

$$E_{rms}^2 = \frac{9\pi^2}{2r^2} E_o^2 \left(\frac{m^2-1}{m^2+2}\right)^2 \frac{V^2}{\lambda^4} \sin^2\alpha \qquad (20)$$

which, in view of footnote 35 can be rewritten as

$$\bar{E} = \frac{9\pi^2}{r^2} \left(\frac{c}{8\pi} E_o^2\right) \left(\frac{m^2-1}{m^2+2}\right)^2 \frac{V^2}{\lambda^4} \sin^2\alpha \qquad (21)$$

Analogous to eqn.(13), therefore,

$$\frac{c}{8\pi} E_o^2 = \frac{c}{4\pi} \left|E_{rms}^2\right| = \bar{E}_o \qquad (22)$$

the mean flux density of the incident radiation.

Substitution of eqn.(22) back into eqn.(21) yields

$$\bar{E} = \frac{9\pi^2 \bar{E}_o}{r^2} \left(\frac{m^2-1}{m^2+2}\right)^2 \frac{V^2}{\lambda^4} \sin^2\alpha \qquad (23)$$

Eqn.(23) represents the scattering of (polarized) radiation by non-absorbing particles such that $a\lambda^{-1} \ll 1$.

The total scattered flux can be obtained by multiplying both sides of eqn.(23) by the area of a sphere, $r^2 d\omega$. This yields

$$\bar{F} = 9\pi^2 \bar{E}_o \left(\frac{m^2-1}{m^2+2}\right)^2 \frac{V^2}{\lambda^4} \int_0^{4\pi} \sin^2\alpha \, d\omega \qquad (24)$$

Changing $d\omega$ to spherical coördinates and the limits of integration to the corresponding limits of α, the integral of eqn.(24) can be easily evaluated. It can be shown that this value is 4/3. Eqn.(24) then becomes

$$\frac{\bar{F}}{\bar{E}_o} = 24\pi^3 \left(\frac{m^2-1}{m^2+2}\right)^2 \frac{V^2}{\lambda^4} \qquad (25)$$

Eqn.(25) represents the total flux scattered out of a beam of radiant energy of unit flux density by a single scatterer. If there are n such scatterers per unit volume of space, then the energy scattered out of a beam per unit length, called the scattering coefficient, k_s, is then eqn.(25) multiplied by n, or,

$$k_s = 24\pi^3 n \left(\frac{m^2-1}{m^2+2}\right)^2 \frac{V^2}{\lambda^4} \qquad (26)$$

In words, the scattering coefficient represents the ratio of the total flux scattered out of a beam of radiation in a unit length of n scatterers per unit volume of space, to the flux intercepted by the total geometric cross-sectional area of these n scatterers.

At sea-level $k_s \simeq 10^{-1}$. Some selected monochromatic values of k_s were calculated and are shown below in TABLE 1.

TABLE 1 - VALUES OF k_s FOR SELECTED WAVELENGTHS IN A RAYLEIGH ATMOSPHERE.

λ	k_s
0.30μ	0.364
0.50μ	0.135
0.70μ	0.036

TABLE 1 demonstrates that molecular scattering is most effective in the small wavelength range of the visible portion of the electromagnetic spectrum. k_s decreases quite rapidly as the infra-red portion is approached, indicating that very little diffuse radiation is generated at these wavelengths.

To conclude this discussion on the scattering coefficient, it is to be noted that Rayleigh's theory also yields the direction of the scattered light. Letting $\bar{I}$ represent the intensity of the scattered light from n particles, and $\bar{I}_o$ the initial intensity of the incident radiation, then

$$\bar{I}/\bar{I}_o = \frac{9\pi^2 n}{r^2}\left(\frac{m^2-1}{m^2+2}\right)^2 \frac{V^2}{\lambda^4} \sin^2\zeta \text{ ; for polarized } \bar{I}_o \qquad (27)$$

$$\bar{I}/\bar{I}_o = \frac{9\pi^2 n}{2r^2}\left(\frac{m^2-1}{m^2+2}\right)^2 \frac{V^2}{\lambda^4} (1+\cos^2\zeta); \text{ for unpolarized } \bar{I}_o \qquad (28)$$

The terms $\sin^2\zeta$ and $(1+\cos^2\zeta)$ are variously termed the scattering or phase functions or scattering indicatrix. These functions describe the angular distribution of the scattered radiation. FIG. 4 represents the case for eqn.(28).

In FIG. 4 the solid outer curve represents the function $(1+\cos^2\zeta)$. The diagram is so constructed that the length of the radius is proportional to the amount of radiation scattered in the direction of that radius.

FIG. 4 illustrates, that, for the Rayleigh case, the amount of radiation scattered in the forward direction ($\zeta = 0^o$) equals the amount scattered in the backward direction (i.e., $\zeta = \pi^o$).

Moreover, the amount of radiation scattered in the forward and backward directions is twice that scattered in a direction normal to

Figure 4

A SCHEMATIC REPRESENTATION OF THE MOLECULAR SCATTERING INDICATRIX

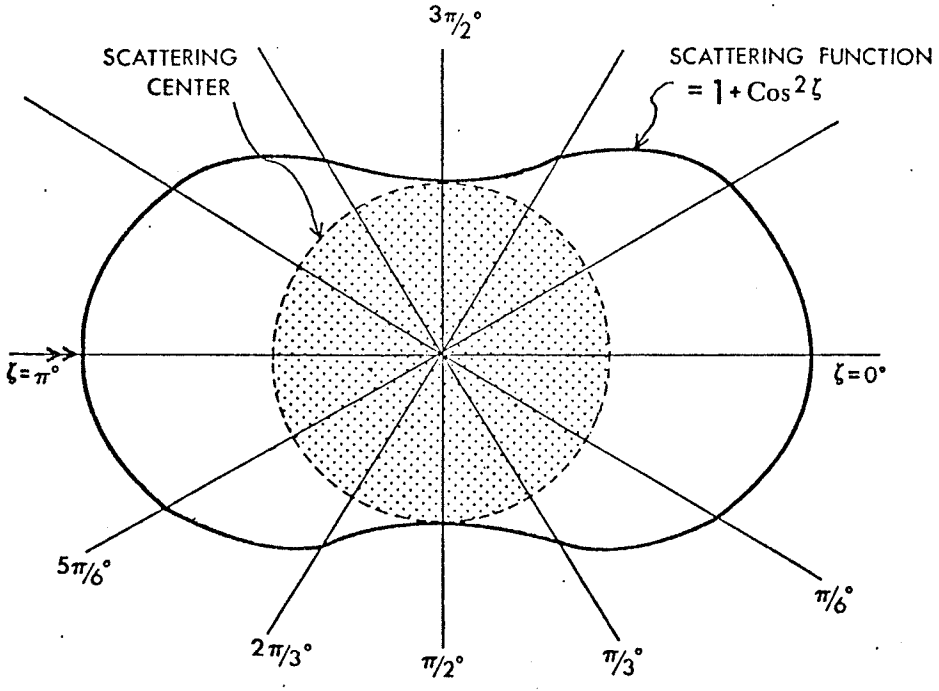

that of the incident radiation.

But just as a unit volume of space depletes the incident solar beam by an amount proportional to k_s, it may also act as a source of further diffusing of the radiation which has already experienced scattering at least once. Consequently, the radiance emanating from a unit volume of space is always greater than would be expected from consideration of k_s alone. The discrepancy, of course, is due to multiple reflection.

Unfortunately, Rayleigh's theory does not consider multiple particulate scattering or reflection of radiation at the earth's surface. Deirmendjian and Sekera[36] have used Chandrasekhars[37] theory of radiative transfer to obtain a solution to this problem.

Let πF_o be the flux of monochromatic radiation of wavelength incident at top of the atmosphere under zenith angle θ.

Then the reduced flux, πF_λ, through a unit area normal to the incoming radiation at a height z cm above the earth's surface can be shown to be

$$\pi F_\lambda = \pi F_{o\lambda} \exp\{-\tau/\mu_o\} \qquad (29)$$

where $\mu_o = \cos\theta$.

The non-dimensional parameter τ, termed the normal optical thickness, is a function of the wavelength λ, and stands for the integral

$$\tau = \int k_s dz \qquad (30)$$

where k_s is the monochromatic attenuation coefficient, i.e., the

---

36. Deirmendjian and Sekera, 1954, op. cit.

37. Chandrasekhar, S., 1950: Radiative Transfer, Clarendon Press, Oxford, U.K., in Deirmendjian and Sekera, 1954, op. cit.

scattering coefficient.

For a given distribution of air density with height, τ can be determined. At some fixed level z cm above sea-level,

$$\tau = f(\lambda) \qquad (31)$$

and can therefore serve as a dimensionless parameter defining the wavelength of the incident radiation.

Thus the flux of the direct component at wavelength λ is given by

$$S_\lambda = \pi F_\lambda \mu_o \exp\{-\tau/\mu_o\} \qquad (32)$$

which reduces to eqn.(29) when the sun is exactly at the zenith (i.e., $\theta = 0$).

The monochromatic radiation received from a unit cone of solid angle $d\omega$ and from a direction making an angle θ with the vertical will contribute to the net flux, through a horizontal unit area, by the amount $I\cos\theta d\omega$, where, in general, $I = I(\theta_o, \varphi_o, \theta, \varphi)$ is the specific intensity of the diffuse sky radiation. The sky radiation, H_λ, is then given by

$$H_\lambda = \int I \cos\theta \, d\omega \qquad (33)$$

where the integration is performed over all the solid angles of the outer hemisphere only, i.e., it is assumed that the surface element is receiving radiation from one side only. Since $d\omega = \sin\theta d\theta d\varphi$ (wher φ denotes the azimuth of the particular direction) eqn.(33) can be rewritten as

$$H_\lambda = \int_0^1 \int_0^{2\pi} I\mu d\mu d\varphi \qquad (\mu = \cos\theta) \qquad (34)$$

The sky radiation is in general polarized and thus the specific intensity, I, can be expressed as the sum of the intensities of two components polarized in two directions normal to each other: normal (I_r) and parallel (I_l) to the vertical plane through the direction given by the zenith angle θ and the azimuth φ. From the general equations of radiative transfer, with all orders of scattering included, the expressions for the intensities I_r and I_l may be given as

$$I_i = I_i^o + A_i(\mu,\mu_o) \cos(\varphi - \varphi_o) + B_i(\mu,\mu_o) \cos 2(\varphi - \varphi_o) \qquad (i = l,r) \qquad (35)$$

where μ_o and φ_o specify the direction of the incident direction, and the functions A_i and B_i are linear combinations of six special functions of μ_o and μ only.

Upon substitution of eqn.(35) into eqn.(34) and performing the indicated integration, the azimuth terms vanish so that only the functions I_r^o and I_l^o (which are azimuth independent) contribute to the integration. The functions I_r^o and I_l^o are related to the incident radiation by the relationship

$$\begin{pmatrix} I_l^o \\ I_r^o \end{pmatrix} = \frac{3}{16\mu} T^o(\mu,\mu_o) \begin{pmatrix} F_l \\ F_r \end{pmatrix} \qquad (36)$$

where T^o represents the transmission matrix with elements $T^o_{i,k}$ $(i,k = r,l)$. Substitution of eqn.(36) into eqn.(35), and assuming neutral incident radiation, i.e., $F_l = F_r = F_o/2$, yields the explicit integral for the sky radiation, namely,

$$H_\lambda = \frac{3\mu F_o}{16} \int_0^1 (T^o_{ll} + T^o_{lr} + T^o_{rl} + T^o_{rr})\, d\mu \qquad (37)$$

When eqn.(37) is rewritten in terms of Chandrasekhar's γ_1 and γ_r functions, eqn.(37) becomes

$$H_\lambda = \pi F_o \mu_o \left[\tfrac{1}{2}\gamma_1(\mu_o) + \tfrac{1}{2}\gamma_r(\mu_o) - \exp\left\{ - \tau/\mu_o \right\} \right] \qquad (38)$$

Combining eqns.(37) and (32) yields

$$G_\lambda = H_\lambda + S_\lambda = \frac{\pi F_o \mu_o}{2} \left[\gamma_1(\mu_o) + \gamma_r(\mu_o) \right] \qquad (39)$$

Eqn.(39) represents the monochromatic global radiation. The functions $\frac{1}{2}\gamma_1(\mu_o)$ and $\frac{1}{2}\gamma_r(\mu_o)$ have the following physical meaning: they represent the monochromatic global radiation resulting from the components polarized normal and parallel, respectively, to the vertical plane, for unit incident flux ($\pi F_o = 1$) of neutral radiation, when there is no reflection at the earth's surface and $\theta \doteq 0$.

In general, the problem of reflection by the earth's surface may be viewed as an additional illumination which may be expressed in terms of Chandrasekhar's I_i functions. This additional intensity I_r^* and I_l^* of diffuse light due to surface reflection is also azimuth independent and has the form

$$I_r^* + I_l^* = \frac{\alpha \mu_o F_o}{4(1-\alpha \bar{s})} \left[\gamma_1(\mu_o) + \gamma_r(\mu_o) \right] \left[2 - \gamma_1(\mu) - \gamma_r(\mu) \right] \qquad (40)$$

where α is the albedo of the earth's surface and $\bar{s}$ is a quantity depending on τ only, but independent μ_o. It is connected to the γ_i functions by the relation

$$\bar{s} = 1 - \int_0^1 \left[\gamma_1(\mu) + \gamma_r(\mu) \right] \mu d\mu \qquad (41)$$

The diffuse radiation resulting from surface reflection may be computed by substituting eqn.(40) into eqn.(34) The integration, using eqn.(41) for $\bar{s}$, yields

$$\int\int (I_1^* + I_r^*)\ \mu d\mu d = \frac{\pi F_o \mu_o \alpha \bar{s}}{2(1-\alpha\bar{s})} \left\{ \gamma_1(\mu_o) + \gamma_r(\mu_o) \right\} \qquad (42)$$

Adding eqn.(42) to eqn. (38), i.e., the diffuse radiation if the earth's surface were a black body, yields an expression for the diffuse radiation which includes the effect of surface reflection, namely,

$$H_\lambda = \pi F_o \mu_o \left\{ \frac{\gamma_1(\mu_o) + \gamma_r(\mu_o)}{2(1-\alpha\bar{s})} - \exp\left\{ -\tau/\mu_o \right\} \right\} \qquad (43)$$

When eqn.(43) is in turn added to eqn.(32), i.e., the direct flux, a rather simple result is obtained, representing the monochromatic global radiation, G_λ, when the earth is reflecting with albedo α, viz,

$$G_\lambda = H_\lambda + S_\lambda = \frac{\pi F_o \mu_o}{2} \left\{ \frac{\gamma_1(\mu_o) + \gamma_r(\mu_o)}{1-\alpha\bar{s}} \right\} \qquad (44)$$

Thus the global radiation can be easily computed provided the functions $\gamma_1(\mu)$ and $\gamma_r(\mu)$ are known. However, as Deirmendjian and Sekera point out, the evaluation of these functions is not so simple. It requires the solution of two systems consisting each of two non-linear integral equations for two pairs of functions (X_1, Y_1, X_r, Y_r).

Before discussing the evaluation of eqns.(43) and (45), it is informative to note that more recent approaches to the multiple reflection problem have made extensive use of a matrix formulation of

the radiative transfer problem. Twomey et al[38] have obtained some very interesting results employing such a formulation. Tanaka[39] has presented a comprehensive listing of all matrix relationships for the radiative transfer problem. Besides the considerable facility of computation that this approach offers, the matrix formulation can incorporate many realistic features of real atmospheres such as (highly) anisotropic scattering, polarization effects, etc. Attention will, however, be focussed on the evaluation of eqns.(43) and (44).

Sekera and Blanche[40] have obtained a solution to these equations by performing successive iterations (corresponding, physically, to the inclusion of second- and higher-orders of scattering) for several normal optical thicknesses. TABLE 2 contains values of $H^{(1)}/H$ (for the case of albedo = 0) for various solar zenith angles (μ_o) and wavelengths (expressed in terms of τ). This ratio is a measure of the contribution of primary scattering to the total diffuse flux resulting from all orders of scattering.

Although uncorrected for surface reflection, TABLE 2 does indicate that multiple reflection (i.e., secondary and higher order scattering and reflection from the earth's surface) is of major importance in the visible portion of the electro-magnetic spectrum. As the near and infra-red portions are approached primary scattering accounts for nearly all of the diffuse radiation arsing in this portion

38. Twomey, S., Jacobowitz, H., and Howell, H.B., 1966: Matrix Methods for Multiple Reflection Problems, J. Atmos. Sci., V. 23, pp. 289-296.

39. Tanaka, M., 1971: Radiative Transfer in Turbid Atmospheres: (I): Matrix Analysis for the Problem of Diffuse Reflection and Transmission, J. Meteor. Soc. Japan, V. 49(4), pp. 296-311; (II): Angular Distribution of Intensity of the Solar Radiation Diffusely Reflected and Transmitted by Turbid Atmospheres, J. Meteor. Soc. Japan, V. 49(5), pp. 321-332; (III):Degree of Polarization of the Solar Radiation Reflected and Transmitted by Turbid Atmospheres, J. Meteor, Soc. Japan, V. 49(5), pp. 333-342.

TABLE 2 - $H^{(1)}/H$ FOR THE CASE OF ALBEDO = 0.0. VALUES IN PARENTHESES REPRESENT THE CORRESPONDING WAVELENGTH AT SEA-LEVEL. From Deirmendjian and Sekera, 1954, op. cit.

μ_o	τ (λ)	1.00 (0.312μ)	0.25 (0.436μ)	0.15 (0.495μ)	0.06 (0.618μ)	0.02 (0.809μ)	8.5×10^{-3} (1.000μ)	5.2×10^{-4} (2.000μ)
1.000		0.403	0.734	0.812	0.904	0.960	0.980	1.000
0.600		0.352	0.699	0.785	0.887	0.950	0.980	1.000
0.100		0.271	0.667	0.765	0.877	0.950	0.970	1.000
0.025			0.66	0.75	0.88	0.95	0.97	1.000

of the electro-magnetic spectrum. And, as TABLE 1 indicates, very little diffuse radiation arises from the infra- and near infra-red portions. Thus multiple reflection is primarily a feature of visible solar radiation.

TABLE 3 represents the evaluation of eqn.(44) for the parameters listed in TABLE 2. TABLE 3 demonstrates how the monochromatic global radiation, G_λ, increases with increasing surface albedo for all (μ_{o_i}, τ_i). An interesting feature of TABLE 3 concerns G_λ when the albedo = 0.80. When $\mu_o = 1.00$, $G_\lambda \geq 1.00$ for all τ_i. The physical interpretation of this result is that under these circumstances, G_λ, exceeds the extra-atmospheric irradiance. This indicates that multiple reflection is a rather effective process in rendering a higher global radiation receipt than would be the case if the earth's surface were a black body.

Finally, when the monochromatic functions are integrated to obtain the integrated absolute diffuse, direct, and global radiations the pattern established by the monochromatic functions are maintained. These (integrated) values have been extracted and have been used to calculate the intensification ratio G^*/G_o^*. The results are given in TABLE 4.

TABLE 4 - INTENSIFICATION RATIOS G^*/G_o^* FOR A RAYLEIGH ATMOSPHERE FOR VARIOUS SURFACE ALBEDOS AND SOLAR ZENITH ANGLES. After Deirmendjian and Sekera, 1954, op. cit.

G^*/G_o^*	0°	53.1°	84.3°	88.8°
$G_{.8}/G_{.0}$	1.058	1.055	1.046	1.044
$G_{.25}/G_{.0}$	1.016	1.015	1.016	1.011
$G_{.8}/G_{.25}$	1.041	1.039	1.029	1.032

TABLE 3 - SELECTED VALUES FOR THE RELATIVE MONOCHROMATIC GLOBAL RADIATION, G_λ, FOR SURFACE ALBEDOS OF $\alpha = 0.00$, $\alpha = 0.25$, $\alpha = 0.80$. (VALUES IN BRACKETS ARE THE CORRESPONDING WAVELENGTHS AT SEA LEVEL). FROM DEIRMENDJIAN AND SEKERA.

τ	1.00	0.25	0.15	0.06	0.02	8.5×10^{-3}	5.2×10^{-4}	1.03×10^{-4}
(λ)	(0.312μ)	(0.436½μ)	(0.495μ)	(0.618μ)	(0.809μ)	(1.00μ)	(2.00μ)	(3.00μ)
μ_o								
				$\alpha = 0.00$				
1.00	0.6597	0.8884	0.9301	0.9709	0.9901	0.9958	0.9998	0.9999
0.60	0.3250	0.4961	0.5332	0.5714	0.5902	0.5958	0.5998_5	0.5999
0.02	0.0050	0.0078	0.0086	0.0100	0.0137	0.0166	0.0197^5	0.0199
				$\alpha = 0.25$				
1.00	0.7427	0.9302	0.9587	0.9840	0.9948	0.9979	0.9999	1.0000
0.60	0.3658	0.5194	0.5495	0.5792	0.5930	0.5971	0.5998_5	0.0000
0.02	0.0056	0.0082	0.0089	0.0101	0.0138	0.0166	0.0197^5	0.0200
				$\alpha = 0.80$				
1.00	1.0269	1.0377	1.0282	1.0142	1.0054	1.0025	1.0002	1.0000
0.60	0.5058	0.5794	0.5894	0.5969	0.5993	0.5999	0.6000_5	0.6000
0.02	0.0078	0.0091	0.0095	0.0105	0.0139	0.0167	0.0197^5	0.0200

The values for the ratio $G_{.8}/G_{.25}$ indicate that, in a Rayleigh atmosphere, the increase in global radiation attributable to multiple reflection ranges from about 3 per cent for low solar altitudes to about 4 per cent when the sun is exactly at the zenith.

In summary, the salient features of scattering in a Rayleigh atmosphere may be described as follows:

(i) - A unit volume of space depletes the incident solar radiation by an amount proportional to the scattering coefficient, k_s. This decrease in intensity is directly proportional to the size and number of scattering centers and inversely proportional to the fourth power of the wavelength of the incident radiation. Moreover, the scattered flux follows an angular distribution described by the scattering function. For a Rayleigh this is the function $(1 + \cos^2\zeta)$. The consequence of this particular function is that the (global) radiation scattered in the forward (i.e., in the direction of the incident radiation) and the backwards direction is equal.

(ii) - But a unit volume of space may also act as a further source of diffusing of the radiation which has already experienced primary scattering. Consequently, the radiance emanating from a unit volume of space is always greater than would be expected from consideration of primary scattering alone. Extensive calculations by Deirmendjian and Sekera illustrate that multiple reflection is primarily a feature of visible shortwave solar radiation. When the monochromatic functions are integrated to obtain the absolute values, the basic pattern established by the monochromatic functions are maintained. Thus the diffuse flux, and consequently, the global radiation, increase with increasing surface albedo. Moreover, Deirmendjian and Sekera's calculations indicate that

$$H_{.8}/G_{.8} > H_{.25}/G_{.25} > H_{.0}/G_{.0} \qquad \forall\theta,\ \theta = 0,..,\pi/2 \qquad (45)$$

which illustrates that with increasing surface albedo the contribution of multiply reflected global radiation to the global radiation receipt becomes disproportionally larger.

(iii) - Finally, comparison of radiation fluxes of a snow-covered to snow-free surface indicates a general intensification of global radiation of the order of 3 - 4 per cent for a Rayleigh atmosphere.

The preceding results have been derived for a Rayleigh atmosphere, a concept not strictly applicable to the lowest layers of the atmosphere (See FIG. 5).

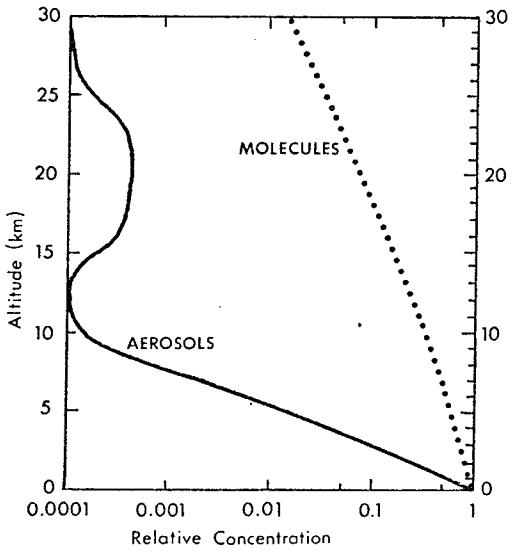

FIG. 5 - Vertical distribution of the relative concentration of aerosols and air molecules. From Tanaka, 1971 (II), op. cit.

In this portion of the atmosphere are found particles, such as larger molecules, dust, haze and industrial aerosols, etc., whose dimensions are commensurate with the wavelength of the incident radiation. The ultimate effect of such matter is that the atmosphere can no longer be assumed to scatter (nearly) isotropically, the situation

described above[41]. Consideration of these larger particles leads to what is often referred to as anisotropic or aerosol scattering.

2. Aerosol Scattering

The effect of aerosol scattering is not so much to alter the basic features of molecular scattering as it is to scatter light more selectively. A complete theoretical solution valid for all values of $a\lambda^{-1}$ was given by Mie[42]. According to Tverskoi[43]

> "Mie showed that the principle physical difference between scattering on small and large particles is the following. The field inside a particle can be regarded as uniform only when its dimensions are smaller than the wavelength of the monochromatic radiation incident upon it. The proper emission which arises in this process can then be regarded as the emission of a dipole. However, if the particle dimensions are comparable with (or greater than) the wavelength of the incident light the field around the particle can no longer be regarded as uniform and the spherical wave which it emits must be represented by a system of partial waves which become more complex as the particle dimensions increase (on the dipole field are superimposed fields of higher orders: quadruple, octuple, etc.).
>
> Mathematically, the intensity of the scattered light can then be treated as an infinite series, the terms of which characterize the intensity of the indicated partial waves."

---

41. Technically, Rayleigh scattering is not true isotropic scattering. True isotropic scattering leads to a constant flux density, or, in other words, scattering is independent of the angle of incidence of the incident radiation (c.f. FIG. 4). However, the differences between the two cases are small, so that the two cases are usually considered synonomous.

42. Mie, G., 1908: A Contribution to the Optics of Turbid Media Especially Colloidal Metalic Suspensions, Ann. Physik., (fourth series), V. 25, pp. 377-445. In Johnson, 1954, op. cit.

43. Tverskoi, P.N., 1962: Physics of the Atmosphere (Trans. from the Russian by Isreal Program for Scientific Translations (IPST), Jerusalem, 1965), GMIZ, Leningrad, 560 pp.

The series begins as

$$k_s = 24\pi^3 n \left(\frac{m^2-1}{m^2+2}\right)^2 \frac{V^2}{\lambda^4}\left[1 + \frac{6\pi^4}{5}\left(\frac{m^2-2}{m^2+2}\right)\frac{a^4}{\lambda^4} + \cdots\right] \qquad (46)$$

where k_s is defined as before. Eqn.(46) illustrates that the leading term is the molecular scattering coefficient. Rayleigh's theory may therefore be viewed as a special case of a more general theory of light scattering. However, as has been pointed out by several authors, eqn.(46) converges so slowly that it may not be used with any facility, although the availability of modern high-speed computers does not make this feature the disadvantage it once was. In any event, eqn.(46) does illustrate that "scattering by particles just slightly larger than the Rayleigh limit tends to deviate quite rapidly from the inverse fourth power law" [44].

Besides knowing k_s, it becomes critical to establish the material nature of the aerosol which is understood to be composed of all solid or liquid colloidal particles of the size of molecular complexes up to a radius of about 20μ.

According to a survey by Bullrich[45] the aerosol extends over a range of four orders of magnitude. The aerosol can thus be characterized by a size distribution which follows a power law. It will be here denoted by the symbol ϑ^*. The important aspect is the particle with the smallest radius, r_1, and the particle with the largest radius, r_u.

In theory, the distribution can be the interval $(0,\infty)$.

---

44. Johnson, 1954, op. cit.

45. Bullrich, K., 1964: Scattered Radiation in the Atmosphere, Advances in Geophysics, V. 10, pp. 99-260.

However, a more realistic definition is the interval $(0.04\mu, 10\mu)$. Assuming a concentration of small particles and a few large particles gives the result $\vartheta^* \simeq 4.0$. Assuming a distribution which contains a high concentration of large particles and few small particles gives the result $\vartheta^* \simeq 2.5$. According to a survey by Bullrich "the majority of direct aerosol and indirect optical measurements indicate that $\vartheta^* \simeq 3.0$ gives the best fit to the natural size distribution. If a graph of concentration versus the logarithm of radius is plotted, $\vartheta^* = 3.0$ represents a mass distribution with equal particle masses contained within equal logarithmic radius intervals d(log r).

ϑ^* is affected by several processes, mainly of meteorological origin. Sedimentation processes, for instance, result in maximum values of ϑ^*, while various coagulation processes minimize ϑ^*. Thus ϑ^* is a complex function of both time of year and time of day.

The significance of the parameter ϑ^* lies in the relationship between ϑ^* and the angular distribution of scattered light. Research by Bullrich and others leads to the following general conclusion: as ϑ^* decreases (i.e., as the concentration of larger particles increases) forward-scattering (i.e., in the direction of the incident radiation) becomes more prominent. Of special interest is the case of a transparent sphere corresponding to the case of scattering of light by water droplets.

Tverskoi[46] has reproduced polar diagrams constructed by Shuleikan[47] for this case. This is shown in FIG. 6. In FIG. 6(a) the case for a

---

46. Tversloi, 1962, op. cit.

47. Shuleikan, in Tverskoi, 1962, op. cit. Unfortunately, a bibliography is not included in Tverskoi's text and consequently a proper reference for Shuleikan's work cannot be given.

Figure 6

POLAR DIAGRAMS FOR THE CASE OF A WATER DROPLET

Fig. 6a

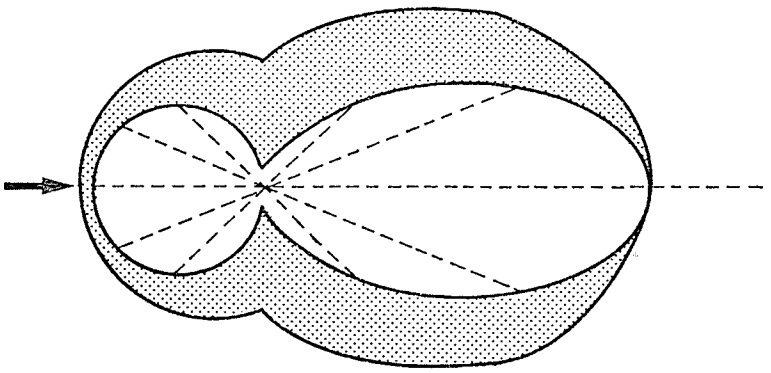

Fig. 6b

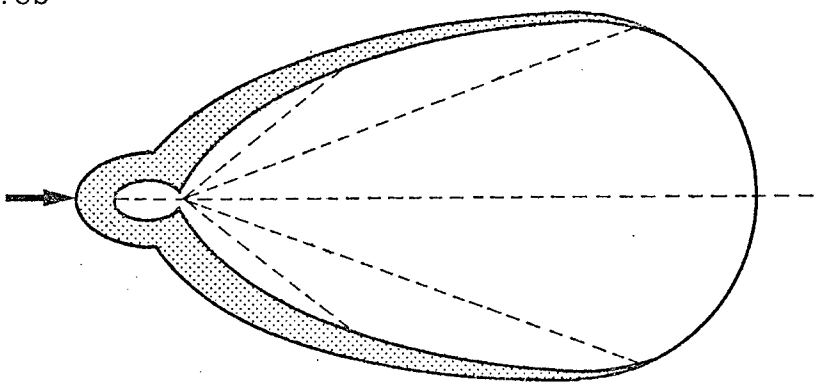

Fig. 6c

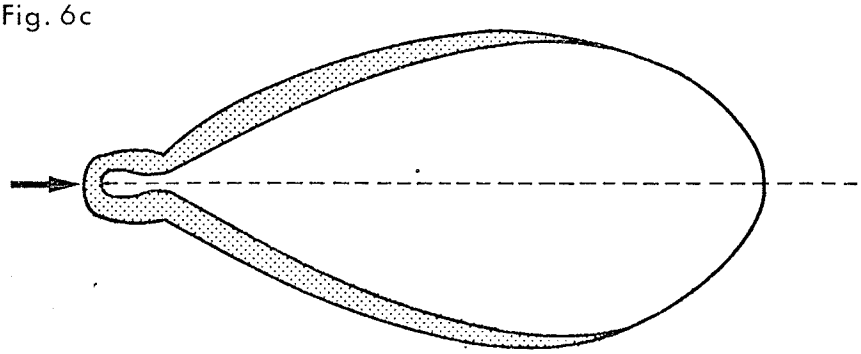

Shaded areas represent the degree of polarization

From: Tverskoi, 1965, op.cit.

water droplet is shown. The diagram illustrates two features of aerosol scattering. First, scattering is no longer symmetrical with respect to the scattering center (c.f. FIG. 4). Second, scattering in the forward direction exceeds that in the backward direction. As the particle dimensions increase, these effects become still more pronounced, and FIGS. 6(b) and 6(c) illustrate.

Now let the radiation scattered in the forward direction have a ratio ξ to that scattered in the backward direction. Feigel'son et al[48] have presented comprehensive calculations of the ratio $G^*_{.6}/G^*_{.1}$ for variable ξ. Some of these values are shown in TABLE 5. These values are characterized by the optical thickness, τ^*, and by the shape of indicatrix numbered by roman numerals. These numbers correspond to

$\xi = 0.85$(V), $\xi = 2.48$(VI), $\xi = 4.69$(VII), $\xi = 8.46$(VIII).

TABLE 5 illustrates that with increasing τ^* and ξ, G^*/G^*_o increases. Maximum values of G^*/G^*_o are, in fact, recorded under highly anisotropic conditions. In contrast to the Rayleigh case, however, G^*/G^*_o shows an increase with increasing zenith distance for a given τ^*, although these differences are small. This nevertheless has the important effect of increasing the radiance near the horizon. It is not unlikely that such considerations are the essence of such optical phenomena as the 'white-out' and 'ice-blink'[49].

In summary the multiple reflection process is a rather effective process in a turbid atmosphere. This is primarily a consequence of the greater backscatterance which obtains in a turbid atmosphere. Feigel'son et al[50] calculations indicate that multiple reflection increases the global

---

48. Feigel'son et al, 1960, op. cit.

49. Catchpole and Moodie, 1972, op. cit.

50. Feigel'son et al, 1960, op. cit.

50. Feigel'son

TABLE 5 - INTENSIFICATION RATIO $G^*_{.6} / G^*_{.1}$ AND CORRESPONDING BACKSCATTERANCES IN PARENTHESES FOR VARIOUS ZENITH DISTANCES, Z, OPTICAL THICKNESS, τ^*, AND SHAPE OF INDICATRICES. After Feigel'son et al (1960, op. cit.), in Möller, 1965, op. cit.

	30	45	60	90
τ^* = 0.2, V	1.064(.120)	1.065(.122)	1.065(.122)	1.084(.155)
= 0.2, VI	1.064(.120)	1.064(.120)	1.065(.122)	1.083(.153)
= 0.4, VI	1.116(.208)	1.116(.208)	1.116(.208)	1.124(.221)
= 0.4, VII	1.103(.187)	1.107(.194)	1.109(.197)	1.114(.205)
= 0.6, VII	1.160(.276)	1.158(.274)	1.158(.274)	1.165(.283)
= 0.6, VIII	1.117(.210)	1.117(.210)	1.116(.208)	1.120(.214)
= 0.8, VII	1.166(.284)	1.159(.274)	1.180(.305)	1.167(.286)
= 0.8, VIII	1.144(.252)	1.144(.252)	1.144(.252)	1.143(.250)

radiation from about 6 - 18 percent for a snow-covered surface.

As these values refer to the clear-sky condition, it may be expected that even greater values for the intensification ratio will be obtained for the case of cloudy and/or overcast conditions. No great extension of theory is required since, conceptually, cloudy media may be regarded as a highly anisotropic scattering medium. The feature which renders this problem so complex is the diversity of cloud-types. Even for a given cloud-type a large variability in height-thickness-density characteristics is likely to be witnessed.

The problem of radiative transfer through cloudy media has recently been subjected to a variety of approaches including: diffusion theory[51,52], numerical solution of the radiative transfer equations[53], and Monte Carlo techniques (i.e., probabilistic simulation)[54]. These approaches all yield interesting results.

The major conclusion to be drawn from such analyses, especially, from the work of Plass and Kattawar, is that as cloud models of

---

51. Fritz, S., 1954: Scattering of Solar Energy by Clouds of 'Large Drops', J. Meteor., V. 11, pp. 291-300.

52. Fritz, S., 1955: Illuminance and Luminance under Overcast Skies, J. Opt. Soc. Am., V. 45(10), pp. 820-825.

53. Feigel'son, E.M., 1964: Light and Heat Radiation in Stratus Clouds (Trans. from the Russian by IPST, Jerusalem, 1966), GMIZ, Leningrad, 1964, 244 pp.

54. Plass, G., and Kattawar, G., 1968: (I)- Influence of Single Scattering Albedo on Reflected and Transmitted Light from Clouds, J. Appl. Opt., V. 7(2), pp. 361-367; (II)- Monte Carlo Calculations of Light Scattering from Clouds, J. Appl. Opt., V. 7(3), pp. 415-419; (III)- Radiant Intensity of Light Scattered from Clouds, J. Appl. Opt., V. 7(4), pp. 699-704; (IV)- Influence of Particle Size Distribution on Reflected and Transmitted light from Clouds, J. Appl. Opt., V. 7(5), pp. 869-878; (V)-Calculations of Reflected and Transmitted Radiance for Earth's Atmosphere, J. Appl. Opt., V. 7(6), pp. 1129-1135.

increasing opacity are considered forward-scattering becomes more accentuated. Admittedly, this is a rather broad generalization and this statement is only valid in the light of several qualifications. For the sake of brevity such a discussion is omitted here.

If, in a cloudy medium, forward-scattering is more pronounced, then backscatterance must also be increasing. For this reason backscatterance is greater for the cloudy sky than the clear-sky. For illustrative purposes, TABLE 6 contains some calculated backscatterance values for overcast conditions (after Korb[55]).

TABLE 6 - BACKSCATTERANCE, d, OF OVERCAST SKIES. After Korb (in Müller, 1965, op. cit.).

Cloud	Optical Thickness	d
Low cloud, 1 km thick	5	0.48
	30	0.80
High cloud, 1 km thick	5	0.46
	30	0.78
Tall cloud, 5 km thick	25	0.78
	150	0.95

TABLE 6 illustrates two features of interest. First, the backscatterance shows a dependency on the optical thickness of the cloud, increasing as the optical thickness increases. Second, backscatterance is substantially greater for overcast conditions than it is for the case of clear-sky. Recalling eqn.(2) this can only result

55. Korb, G., 1961: Absorption von Sonnenstrahlung, Wolken. Wiss. Mitt., Meteorl. Inst., München, Nr. 6, 175 pp. in Müller, 1965, op. cit.

in greater intensification ratios being observed for cloudy atmosphere. Thus, under conditions of a high surface albedo and clouds of great optical thickness, G^*/G_o^* approaches the maximum value or, upper bound, of its interval of definition. Thus the empirical evaluation of the intensification ratio tends to confirm the theoretical model, but only to the extent that absorption can be neglected.

3. Absorption

Absorption represents an extraction of energy and is thus likely to affect the multiple reflection proces by altering the amount of radiation that is able to enter into the multiple reflection process.

Molecular absorption is a complex process resulting from transitions involving from (i) changes in rotational energy; (ii) simultaneous changes in rotational and vibrational energy; and (iii) simultaneous changes in rotational, vibrational, and electronic energy.

Various atmospheric constituents, such as water vapor, carbon dioxide, aerosols, etc., absorb (global) solar radiation. Moreover, this absorption occurs at discrete points along the radiation spectrum, in contrast to scattering which is continuous, although, as Golberg[56] has pointed out, absorption may be continuous for certain portions of the solar spectrum.

From spectral measurements carried out by Fowle[57], and others, the absorption spectra of solar radiation are fairly well known. This is represented in FIG. 7.

---

56. Goldberg, L., 1958: The Absorption Spectrum of the Atmosphere, in The Earth as a Planet, pp. 434-490, G. Kuiper (ed.), U. of Chicago Press, Chicago, 751 pp.

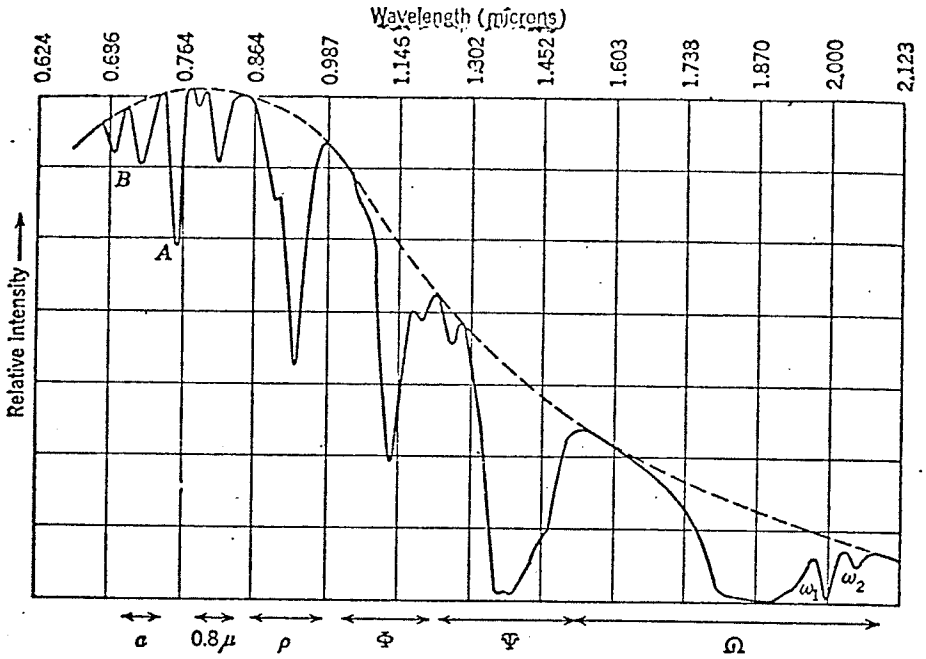

FIG. 7 - Absorption spectra of solar radiation (after Fowle). A and B refer to absorption bands of oxygen. The remaining bands are due to water vapor. From Haltiner and Martin[58].

In FIG. 7 the dashed curve represents the theoretical spectral distribution of solar radiation for $0.62\mu \leq \lambda \leq 2.123\mu$. The solid curve represents the observed distribution. The gaps may therefore be attributed to absorption, since scattering does not alter the spectral distribution. FIG. 7 demonstrates two important features of absorption of global radiation. First, the major absorption spectra occur at $\lambda = 1.00\mu$. Thus the major portion of global radiation is unaffected by absorption. Second, in this range, most of the absorption is effected by water vapor.

The latter generalization is rapidly distorted in urban-industrial

---

57. Fowle, F.E., 1915: Astrophysics Journal, V. 42.

58. Haltiner, G.J., and Martin, F.L., 1957: Dynamical and Physical Meteorology, McGraw-Hill, New York, 470 pp.

agglomerations because of various aerosols that are emmitted into the atmospheres of these areas. According to Johnson[59] the absorption spectra of such aerosols are poorly known. In any event, the additional absorption resulting from such matter has not been fairly well established. Robinson[60], for instance, cites various research reporting no additional absorption to absorption twice the water vapor absorption.

With regard to total absorption it appears that, in mid-latitudes at least, seasonal variations in absorption of global radiation may extend to a full order of magnitude. Climatologically, Munn[61] reports that, at Toronto, absorption of global radiation by water vapor alone varies between 6-9 per cent in winter to about 15 per cent in summer. For this reason comparison of radiation data between snow-covered and snow-free surfaces is not strictly justified.

Unfortunately, investigations into multiple reflection problems invariably neglect absorption.

4. Summary

That multiple reflection arises is a consequence of the interaction of the (global) solar radiation field with particulate matter of the atmosphere and the earth's surface. With regard to atmospheric matter, the interaction will be dependent upon the shape

---

59. Johnson, 1954, op. cit.

60. Robinson, G.D., 1963: Absorption of Solar Radiation by the Atmospheric Aerosol as Revealed by Measurements at the Ground, Arch. Meteor. Geophys. Biokl., Ser. B, V. 12, pp. 19-40.

61. Munn, R.E., 1966: Descriptive Micrometeorology, Academic Press, New York and London, 245 pp.

of the particle and certain characteristics of the particle such as its index of refraction and absorption index. For the special case of a spherical particle the dependence reduces to a dependence upon the radius of the particle.

Both the index of refraction and absorption index determine the scattering by the particle; the absorption index determines the absorption by the particle. Both parameters are wavelength dependent. Thus if the particle changes shape, or if its composition changes, for example, by condensation of water, then both the index of refraction and absorption index (which determines the absorption coefficient) will also change. These relations generally inhibit any rigorous theoretical evaluation of multiple reflection, especially so since there have been very few measurements, both in the laboratory and optical measurements, of the index of refraction and absorption index. Backscatterance, therefore, is a rather complex function of the size-density-and material nature characteristics of the atmospheric particle.

In general, backscatterance increases with increasing atmospheric anisotropy. This generalization, however, is only valid to the extent that absorption is either neglected or negligible. In recalling Möller's values for the intensification ratios at Moosonee and Toronto-Scarborough, it is observed that the values for the latter station were substantially lower than for the former. These differences are certainly due, in part, from differences in surface albedo, but also may arise from differences in absorption.

It becomes readily apparent, therefore, that the multiple reflection process at a locality is dependent upon the effeciency of the scattering and absorbing agents, which conceptually, includes the earth's surface.

CHAPTER III

METHODOLOGY

Recent developments in radiation climatology make it possible to calculate the instantaneous value of G^*/G_o^* without resorting to the functional relationships described in Chapter II but which, however, embody the concepts of scattering and absorption. Specifically, reference is made to H. and K. Lettau's[62] work on shortwave radiation climatonomy. Because this thesis employed the principles of climatonomy to calculate the intensification ratio, it is worthwhile to examine them in somewhat greater detail.

According to Lettau and Lettau "climatonomy denotes the mathematical explanation of the basic elements which determine the physical environment at any planetary surface. Mathematical explanation implies the use of numerical models which yield theoretical solutions in the form of a precise 'response function', or, output, in physical relationship to a precise 'forcing function', or, input.

"For any planet the intensity of the forcing function is determined by the absolute distance to the central sun, and its time structure by orbital elements and spin or the varying relative positioning of the considered planetary surface section with respect to the sun's flux-density. The climatonomic response function is governed

---

62. Lettau, H., and Lettau, K., 1969: Shortwave Radiation Climatonomy, Tellus, V. 21(2), pp. 208-222.

by the fundamental physical laws of radiation, heat conduction, and universal conservation principles.

"In climatonomy, total energies are more important than spectral distributions. Therefore, the discussion is restricted to values integrated with respect to wavelengths over the band-width of the solar spectrum."

The Mathematical Relations

It is convenient to make the mathematical relationships dimensionless by dividing any enrgy-flux densities by the atmospheric irradiance, $I_o \cos(Z)$ (Z = zenith angle of the sun). To guarantee a reasonable degree of completness and detail, nine variables must be considered. These may be divided into 3 groups:

(i) Non-dimensional values of shortwave fluxes

A = top albedo, or fraction returned to space,

G^* = global radiation, or, fraction received at ground level from sun and sky,

D^* = diffuse radiation, or, fraction received at the ground from the sky alone,

H^* = solar heating in the air, or, fraction absorbed by the atmosphere,

a = energy albedo of the lower boundary; or, $(1 - a)G^*$ = fraction absorbed by the lower boundary.

(ii) Contributions to the attenuation of non-dimensional beam radiation

σ = part of attenuation due to scatterers in the air,

α = part of attenuation due to absorbers in the air,

(iii) Coefficients of the scattering process

μ = fraction describing effective outward scattering to space;

or, $(1 - \mu)$ = fraction of effective downward scattering to the lower boundary,

κ = fraction describing backward scattering of that part of shortwave radiation which has been reflected at least once by the lower boundary.

Note that the term 'backward scattering' as used in the definition of κ has a meaning opposite to the sense that was used in Chapter II. Here backward scattered is taken to mean 'in the direction towards the earth's surface'.

The physical relationships between the nine dimensionless variables result in five budget equations. In what follows it is noted that the relationships refer to clear-sky conditions.

The first equation deals with the total shortwave energy. The fraction not returned to space must be equal to the sum of the absorption by the atmosphere (H^*) and by the ground $(1 - a)G^*$, i.e.,

$$1 - A = H^* + G^*(1 - a) \qquad (47)$$

The second equation considers beam radiation $(G^* - D^*)$. Its attenuation $(1 - G^* - D^*)$ must be equal to the depletion by absorbers and scatterers, namely,

$$1 - G^* - D^* = \alpha + \sigma \qquad (48)$$

The third equation deals with the radiation reflected back to space, the 'earth-shine'. The top albedo (A) is the sum of the outward directed part of primary scattering $(\mu\sigma)$ plus that part of ground-reflected global radiation which is neither absorbed in the air nor scattered back to the ground,

$$A = \mu\sigma + (1 - \alpha)aG^*(1 - \kappa\sigma) \qquad (49)$$

The fourth equation expresses the diffuse radiation arriving at the ground. It consists of the downward-directed part of primary scattering $(1 - \mu)\sigma$ and of that part of ground-reflected radiation that is reflected back towards the lower boundary,

$$D^* = (1 - \mu)\sigma + (1 - \alpha)aG^*\kappa\sigma \qquad (50)$$

The fifth equation is not independent. The overall balance of the preceding equations requires that the l.h.s. and the r.h.s. of eqns.(47) and (50), resp., must be equal, or,

$$H^* = \alpha(1 + aG^*) \qquad (51)$$

Eqn.(52) gives the heating function (H^*) as the sum of absorptions of: beam radiation plus ground-reflected radiation. For illustrative purposes FIG. 8 presents a schematic interpretation of eqns.(47) - (51).

With four independent equations and nine unknowns, five variables must be either observed independently, or partly observed and partly observed and partly prescribed by model assumptions, or externally given in order to calculate the remaining four variables.

The fundamental equations (47)-(51) can be transformed by eliminating certain variables. The elimination of D^* in eqn.(48) with the aid of eqn.(50) produces

$$G^* = (1 - \alpha - \mu\sigma)/(1 - a\kappa\sigma(1 - \alpha)) \qquad (52)$$

In the case of an ideally black earth's surface, with $a = 0$, eqn.(52) reduces to

$$G_o^* = 1 - \alpha - \mu\sigma \qquad (53)$$

Figure 8

A SCHEMATIC REPRESENTATION OF EQNS. (47)-(51)

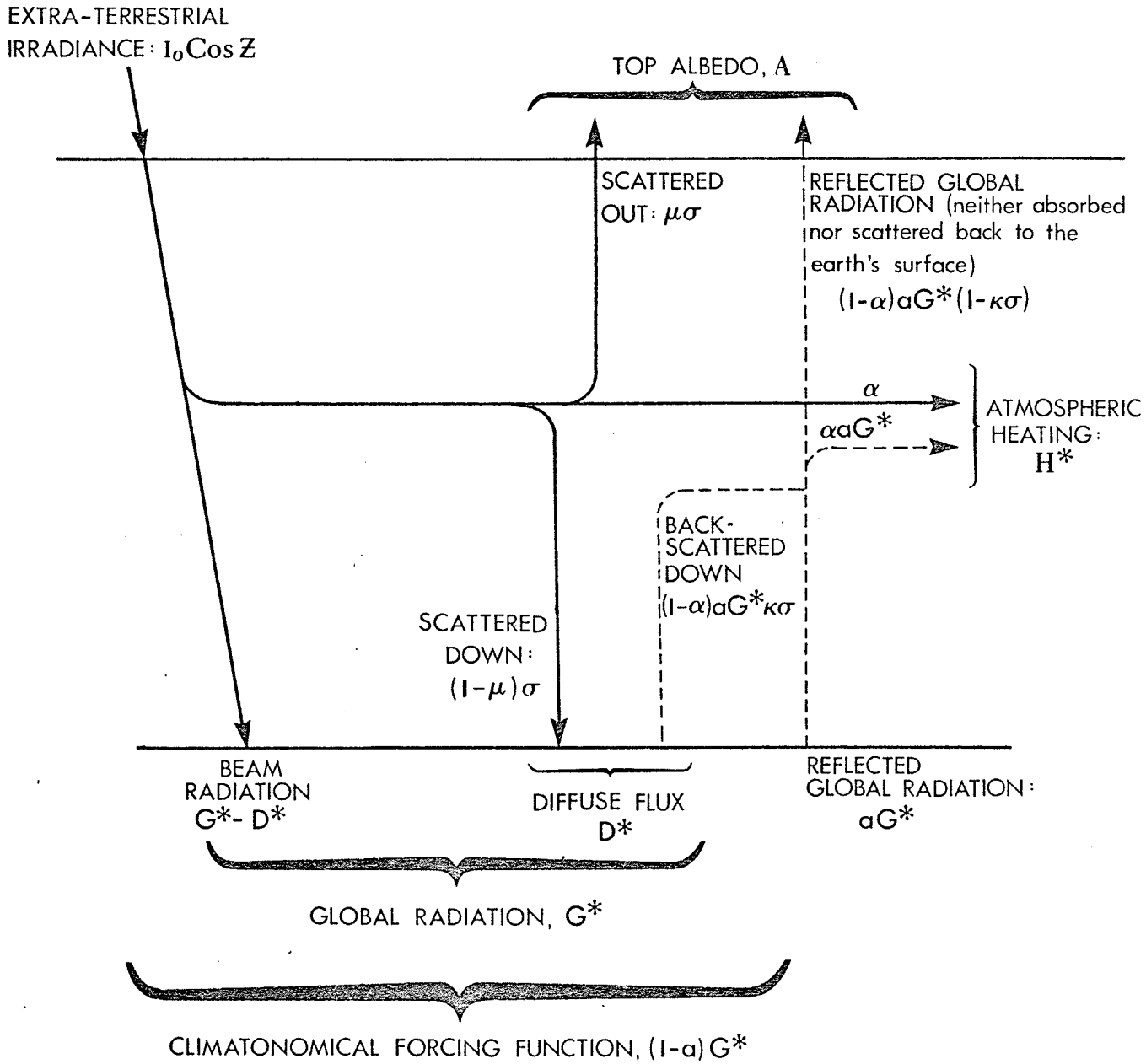

After Lettau and Lettau, 1969, op.cit.

Defining $d \equiv \kappa\sigma(1 - \alpha)$, eqn.(52) can be restated as

$$G^* = G_o^* / (1 - ad) \quad \text{or,} \quad G^*/G_o^* = (1 - ad)^{-1} \qquad (54)$$

which is Ångström and Tryselius' original equation (eqn.(2)). Climatonomy illustrates how backscatterance depends on the effeciency of scatterers and absorbers in the air, a fact illustrated in Chapter II.

If now a fraction, c, of the sky is covered by clouds the flux densities of the cloudless areas have a weight factor of (1 - c). In what follows let the subscripts o and c indicate values for the cloudless sky (with prescribed conditions for clear air attenuation and ground), and for cloudy sky, resp.

For the calculation of effective coefficients in partly cloudy air, it is assumed that the contributions by absorbers are additive, while contributions by scatterers are distributive, or must be prorated. Thus, in air with cloudiness c

$$\alpha = (1 - c)\alpha_o + c(\alpha_o + \alpha_c) = \alpha_o + c\alpha_c \qquad (55)$$

$$\sigma = (1 - c)\sigma_o + c\sigma_c = \sigma_o + c(\sigma_c - \sigma_o) \qquad (56)$$

From continuity principles, it follows that the top albedo is composed of a prorated contribution from the clear area and direct reflection from the cloud surface, plus diffuse radiation reflected from the ground, and reduced by what is either reflected back from the cloud-base or absorbed in the air. Hence,

$$A = (1 - c)A_o + c\left[A' + aG^*(1 - \alpha)(1 - A')\right] \qquad (57)$$

A corresponding development development for the heating function H^* yields

$$H^* = (1 - c)H_o^* + c\alpha(1 + aG^*) \qquad (58)$$

The sum of eqns.(57) and (58) is used to eliminate the term $(A + H_o^*)$ in eqn.(47). The resulting relation can be solved for G^*, viz,

$$G^* = \left\{1 - A_o - H_o^* + c(A_o + H_o^* - A^\dagger - \alpha)\right\} / \left\{1 - a + ca(1 - A^\dagger + \alpha A^\dagger)\right\} \qquad (59)$$

For the case of an ideally black earth's surface, eqn.(59) reduces to

$$G_o^* = 1 - A_o - H_o^* + c(A_o + H_o^* - A^\dagger - \alpha) \qquad (60)$$

Eqn.(59) can now be restated as

$$G^* = G_o^* / \left\{1 - a + ca(1 - A^\dagger + \alpha A^\dagger)\right\} \qquad (61)$$

Eqn.(61) is entirely compatible with eqn.(54), since the latter can be obtained from the former by setting $c = 0$ in eqn.(61). Thus for any given atmospheric and surface condition, the intensification ratio is given by

$$G^*/G_o^* \begin{cases} = 1 / \left\{1 - a + ac(1 - A^\dagger + \alpha A^\dagger)\right\} & 0 < c \leq 1 \qquad (62) \\ = 1 / \left\{1 - a\kappa\sigma(1 - \alpha)\right\} & c = 0 \qquad (63) \end{cases}$$

Eqns.(62) and (63) are the defining equations and were used to calculate the intensification ratio for this study. Before proceeding to a discussion of how the variables were calculated, it is informative to make a number of observations.

First, there exists a number of similarities and comparisons betweens climatonomy and the theoretical modelling as presented in Chapter II. Both approaches indicate that the diffuse flux is increased by a greater backscatterance due to surface reflection. For the case of an ideally black earth's surface, eqn.(50) reduces to

$$D^* = (1 - \mu)\sigma = D_o^* \qquad (64)$$

where the subscript o denotes the case for an ideally black earth's surface. When a > 0, the diffuse flux is increased by a larger backscatter. Employing eqn.(54) and the relation $d \equiv \kappa\sigma(1 - \alpha)$, eqn.(50) can be rewritten as

$$D^* = D_o^* + adG_o^* / (1 - ad) \qquad (65)$$

It is observed, however, that the results are obtained from two opposite 'directions'. In convential radiative transfer theory one starts out with the scattering functions and proceeds to calculate the resulting fluxes. In climatonomy, one starts out with the values of the pertinent fluxes, such as the diffuse and global radiations, and proceeds backwards to obtain the desired quantities.

Second, observe that grouping the two terms containing a in the denominator of the r.h.s. of eqn.(61) and factoring out a yields

$$G^* = G_o^* / \{1 - a(1 - c[1 - A' + \alpha A'])\} \qquad (66)$$

Thus, analogously to eqn.(54) an expression can be obtained which illustrates the functional nature of backscatterance of cloudy sky. Eqn.(66) demonstrates that, for a given cloud type, the backscatterance, and hence the intensification ratio decreases with increasing cloudiness.

This is somewhat contradictory to the notions of the intensification ratio presented in the introductory comments in Chapter I, since with increasing cloudiness one would expect a greater downward flux because of the greater basal area from which reflection could occur. It is important to realize, however, that this discussion is in terms of cloud amount and not density. As Haurwitz[63] has pointed out '... with larger values of cloudiness, the effect of density is very important'. This problem is given greater attention in Chapter IV.

In order to use the preceding relations it was found necessary to employ a number of approximations and empirical relationships. It remains, then, to discuss how values for the variables a, c, A', α, and κc were obtained.

The Variables

(i) - a, surface albedo

Hourly values for surface albedo were calculated exactly as follows. Values of global radiation, G^*, and reflected radiation, R, are given for each hour in the Monthly Radiation Summary. Then, by definition,

$$a = R/G^* \qquad (67)$$

(ii) - c, cloudiness

Hourly values of cloudiness, i.e., fraction of the sky covered by clouds, were obtained from the Daily Surface Weather Record for Toronto International Airport. While this station is approximately 7 miles to the south-west of Toronto MRS it was assumed that extrapolation to Toronto MRS was valid.

---

63. Haurwitz, 1945, op. cit.

This publication lists, for each hour, total cloud amount, cloud type, and cloud opacity. These values are also given for each cloud layer.

(iii) - $A^{\uparrow}$, cloud albedo

If the parameters of the scattering process are known, then the cloud albedo is given by

$$A^{\uparrow} = \mu^{\uparrow} \sigma_c \qquad (68)$$

where $\mu^{\uparrow}$ = fraction of upward scattering,
σ_c = scattering coefficient of the cloud

Because of variable thickness-density characteristics of clouds, both $\mu^{\uparrow}$ and σ_c are not likely to be independent of either the degree or type of cloudiness. Unfortunately, the relationship between these parameters of the scattering process and cloud type, specifically, cloud thickness, has not been extensively researched.

As an alternative to eqn.(68), this study employed mean values of cloud albedo reported by Vershinin[64]. These values are given in TABLE 7. Values of cloud albedo from TABLE 7 are somewhat higher than those given by Lettau and Lettau, especially for translucent types such as Ci, As, and Ac. As cloud-types of increasing opacity are considered the differences become appreciably smaller. This discrepancy may be partly explained by the fact that Lettau and Lettau's values refer to an average air mass of 1.2, while the values given in TABLE 7 represents a mean value, a value calculated and observed over a wide range of air mass values. Such differences are therfore understandable.

---

64. Vershinin, A. P., 1971: Justification of the Method of Computing Global Radiation over Short Periods of Time, Soviet Hydrology:Selected Papers, 1971(1), pp. 1-17.

TABLE 7 - ALBEDO VALUES FOR VARIOUS CLOUD TYPES. From Vershinin, 1971, op. cit.

Cloud-Type	Height, km	Thickness, km	Albedo, A'
Ci	8	-	0.36-0.74
Cs	7	-	0.36-0.74
Cc, Ci dense	6	-	0.70-0.75
As, trans	4-5	0.4	0.63
As, opaque	3	0.8	0.70
Ac, small waves	4-5	0.5	0.73
Ac, large waves	2-3	-	
Sc	1.2-1.5	0.4	0.60
Sc	0.6	0.8	0.68
Ns	1.0-1.5	2.1	0.80
Cu	1.2	0.5-3.0	0.30-0.80
Cb	1.0	2-3	0.86
St	0.4-1.0	0.7	0.64

In any event, TABLE 7 does illustrate the important feature that with increasing cloud opacity, the cloud albedo increases. This is in accord with several theoretical and empirical investigations of this problem[65,66].

It happened that several cloud types are recorded on the Daily Surface Weather Record, such as, for example, SF (Stratus Fractus), but for which no values are given in TABLE 7. In this case it was assumed that these cloud-types were derivatives of the parent cloud-type. Thus, SF clouds are treated as Stratus clouds.

(iv) - α, the absorption coefficient.

The absorption coefficient, α, is taken to include absorption by various sources, including: water vapor, w, ozone and other gases, g, and aerosols, a.

Symbolically,

$$\alpha = \alpha_w + \alpha_g + \alpha_a \qquad (69)$$

Because of the difficulty in assessing each of these coefficients individually several simplifications had to be introduced. Lettau and Lettau, using data summarized by Robinson[67], have shown that in industrial centers, such as Kew, U.K., that the ratio of absorption by water vapor to absorption by ozone and other gases and aerosols is approximately unity. In this case eqn.(69) can be restated as

---

65. Plass and Kattawar, 1968, op. cit.

66. Fritz, S., 1950: Measurements of the Albedo of Clouds, Bull. Amer. Meteor. Soc., V. 31(1), pp.

67. Robinson, 1963, op. cit.

$$\alpha \simeq 2\alpha_w \qquad (70)$$

The problem thus resolves to calculating α_w. If the precipitable water, w^*, and the corresponding air mass, M, are known, then α_w can be calculated from the relation

$$\alpha_w = 0.102(w^* M)^{0.276} \qquad (71)$$

Eqn.(71) is a semi-empirical relationship obtained by Lettau and Lettau using least squares technique on observations summarized by Yamamoto[68]. Eqn.(71) is very similar to such relationships obtained by Haltiner[69] and others.

Since values for M are easily obtained from various tables such as in the Smithsonian Meteorological Tables the problem remains to determine w^*.

If the vertical gradient of mixing gradient or the vertical gradient of dew point temperature, T_d, is known, then various graphical techniques can be applied to obtain w^*. Unfortunately, such soundings do not form part of the routine measurements taken at Toronto MRS or at nearby Toronto International Airport. Consequently, it was necessary to resort to a statistical relationship from which w^* could be estimated.

According to McKay[70] and several authors '...surface dew points

---

68. Yamamoto, G., 1962: Direct Absorption of Solar Radiation by Atmospheric Water Vapor, Carbon Dioxide, and Molecular Oxygen, J. Atmos. Sci., V. 19, pp. 182-188.

69. Haltiner, G.J., 1971: Numerical Weather Prediction , Wiley and Sons, Inc., New York, 317 pp.

70. McKay, G., 1970: Precipitation, Section II of Handbook on the Principles of Hydrology, D.M.Gray (ed.), pp. 2.1-2.111, published by the Secretariat, Canadian National Committee for the International Hydrological Decade, National Research Council of Canada, Ottawa, Canada.

are highly correlated with the amount of water vapour contained in the atmosphere above the measuring point, particularly under circumstances which favor atmospheric lifting...'. Unfortunately, the mathematical relationship between T_d and w^* is not given.

The relationship between T_d (the independent variable) and w^* (dependent variable) was formally examined, statistically, for the Canadian station Trout Lake (53° 50' N, 89°52' W) for the period 1 Jan/68 - 31 Dec/69, a sample of 608 values. Values of w^* for 1200h GMT were obtained from the Monthly Bulletin - Canadian Upper Air Data, while 0700h ET (i.e., 1200h GMT) values of T_d were obtained from the Daily Weather Map (U.S. Dept. of Commerce, Weather Bureau).

FIG. 9 illustrates a plot of w^* versus T_d. In general the plot may be described as a power function. Polynomial regression analysis yielded a second degree polynomial as the best-fitting equation:

$$\hat{w}^* = 2.54 \{ 0.14063 + 4.67513 \times 10^{-3}(T_d) + 1.60818 \times 10^{-4}(T_d)^2 \} \quad (72)$$

In eqn.(72) the factor 2.54 is a conversion factor which arises from the fact that the units of the original data were in inches, whereas eqn.(71) requires that w^* be in cm.

Hourly optical air mass values were calculated exactly. A discussion of this calculation is given is conjunction with the discussion on radiation values. Suffice it is to mention here that a computer programme was written up which calculated the hourly extra-atmospheric irradiance and the mid-hour zenith angle, Z. Once Z had been determined, the corresponding value of M was obtained employing Bemporad's formula as given in TABLE 137 (OPTICAL AIR MASS CORRESPONDING TO DIFFERENT ZENITH ANGLES OF THE SUN) of the Smithsonian Meteorological Tables. Values of

Figure 9

SCATTER DIAGRAM OF PRECIPITABLE WATER, W* AS A FUNCTION OF DEW POINT TEMPERATURE, Td.

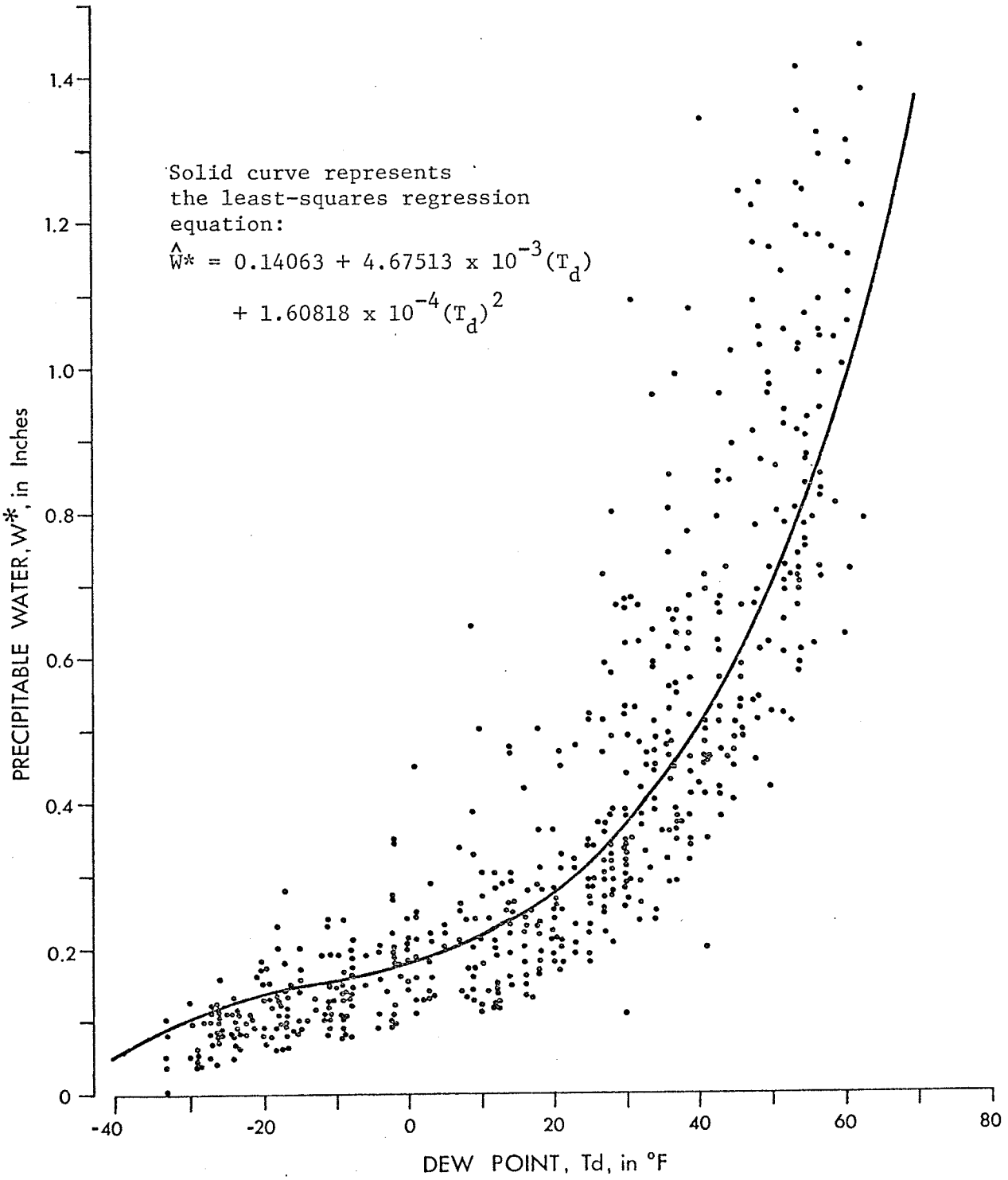

M were then corrected for surface pressure differences by a factor p/p_o, where p is the observed surface pressure and p_o is the corresponding sea-level pressure. These pressure values are given in the Daily Surface Weather Record.

The above considerations of the absorption coefficient may be summarized by the following expression:

$$\alpha = 2(0.102\,[2.54\,\hat{w}^{*}M]^{0.276}) \qquad (73)$$

Strictly speaking, eqn.(73) represents absorption in a cloudless atmosphere. According to eqn.(55) if a fraction (c) of the sky is clouded over, then the absorption is increased by an amount $c\alpha_c$, where α_c is the absorption coefficient of the particular cloud-type under consideration.

Various researchers, such as Fritz and McDonald[71], Neiburgur[72], and others, have shown that absorption of solar radiation by clouds is quite low, ranging, generally, from 0.00 for optically thin clouds such as Ci and As to coefficients of about 0.10 for well-developed clouds of vertical extent such as Ns and Cb. There appeared to be very little disagreement between the values given in the literature and those given by Lettau and Lettau. To this end this study employed the various absorption coefficients as given by Lettau and Lettau. These values are given in TABLE 8

TABLE 8 - ABSORPTION COEFFICIENTS OF VARIOUS CLOUD-TYPES. From Lettau and Lettau, 1969, op. cit.

Cloud-Type	Ci, Cs	Ac	As	Sc	St	Ns, N, Cu, Cc, Cb
α_c	0.00	0.01	0.03	0.05	0.07	0.10

71. Fritz, S., and McDonald, T.H., 1951: Measurements of Absorption of Solar Radiation by Clouds, Bull. Amer. Meteor. Soc., V. 32(6), pp.

(v) - $\kappa\sigma$, parameters of the scattering process

In the absence of direct measurement, these parameters must be externally prescribed or calculated from the fundamental equations eqns.(47) - (50). While it is possible to calculate these parameters exactly, it was found necessary to prescribe a value for both κ and σ.

It is noted that σ can be calculated from eqn.(48), provided α can be accurately assesed. Because of the uncertainty in the determination of the (total) absorption coefficient, inaccuracies will result whether one uses eqn.(48) or if some statistical relation is used to calculate σ. Moreover, values of the diffuse flux were not available for the period 1 Feb - 26 April due to instrument malfunction. For this period it would have been necessary to employ some form of statistical relationship.

This study made the assumption that the particulate matter in such an industrial-urban setting as Toronto would be more efficient as an absorber of global radiation than as a scatterer. Lettau and Lettau's calculations of Robinson's[73] data from Kew, an environment not unlike that of Toronto, illustrates that the ratio of the absorption coefficient to the scattering coefficient is $\simeq 4/3$. Because of a dearth of systematic studies examining this ratio at a location, this study assumes that this ratio equals 4/3 at Toronto MRS. Thus the accuracy in determining σ depends on the accuracy of the determination of total absorption.

It was also found necessary to externally prescribe κ, although it is shown in Chapter V that, utilizing certain transformations of the fundamental equations, it is possible to calculate both κ and μ exactly.

---

72. Neiburgur, M., 1949: Reflection, Absorption, and Transmission of Insolation by Stratus Clouds, J. Meteor, V. 6, pp. 98-104.
73. Robinson, 1963, op. cit.

(vi) - Radiation Values

Although it is unecessary to calculate the extra-atmospheric irradiance, since these values do not enter directly into any of the computations, there is the important advantage of working with dimensionless quantities. Moreover, it proved very easy to obtain these values in calculations of the optical air mass.

From the fundamental relationship quoted by Sellers[74]

$$\cos(Z) = \sin(\phi)\sin(\delta) + \cos(\phi)\cos(\delta)\cos(h) \qquad (74)$$

where Z = sun's zenith angle
ϕ = latitude of the station
δ = solar declination
h = hour angle

mid-hourly values of Z could be calculated. Daily values of δ for the year 1970 were obtained from the Ephemeris of the Sun (U.S. Naval Observatory), while ϕ is a constant ($= 43^{\circ}48'$) and h is assigned a value according to time of day. Since the trace of Z is symmetrical about solar noon it was only necessary to calculate cos(Z) between either sunrise and solar noon or between solar noon and sunset. This study adopted the latter.

A computer programme was then written up which read in daily values of δ, R, the radius vector, and DIFF, the equation of time for that day. The programme then calculates the time at which solar noon occurred, then proceeds to calculate the sun's zenith angle mid-way between solar noon and the first full hour after solar noon. i.e., 1300h local apparent time.

On an hourly basis, except near sunrise and sunset, cos(Z) is

---

74. Sellers, 1969, op.cit.

very nearly a linear function of time of day. This fact was used to calculate Q, the extra-atmospheric irradiance. Thus if it can be assumed that the mid-hourly zenith angle is constant for that hour, then

$$Q = \left(1.98 \cos(Z) \ / R^2 \right) \times 60 \ \text{ly hr}^{-1} \qquad (75)$$

where 1.98 is the value of the solar constant.

Having completed this calculation, the hour angle is increased by 15° and the calculations are repeated for the next hour. The process continues until the last complete hour the sun is above the horizon is encountered. The test of whether this is indeed the last complete hour is accomplished by comparing the computed mid-hour zenith angle to the quantity (sunset - $\frac{1}{2}$hour). The comparison is a valid one since both quantities are angular measurements, specifically, radians. The daily values if sunset are calculated from the relationship quoted by Sellers[75]

$$\text{sunset} = \cos^{-1}(-\tan(\phi)\tan(\delta)) \qquad (76)$$

The programme then proceeds to calculations for the following day. The programme and the results are presented in APPENDIX I.

The remaining radiation quantities, namely, G,D, and R, are recorded at the earth's surface. These values were obtained from the Monthly Radiation Summary for the months Jan - June/70 inclusive.

A computer programme was then written to analyze the data. This is given in APPENDIX II. The calculations were carried out on an hourly basis, since,in general, both cloudiness and cloud-type are not constant throughout the day. When the hourly values were obtained for a particular day, the mean was calculated. This is referred to as the daily mean value. There were a total of 1750 hourly observations that could be utilized for the analyses.

CHAPTER IV

RESULTS

In terms of theoretical predictions the overall results appear very satisfactory. Thus there is observed a distinct winter maximum of G^*/G_o^* and a distinct summer minimum. Examination of G^*/G_o^* in terms of such factors as cloudiness, both with respect to type and degree, zenith angle, etc., however, does not permit many broad generalizations to be advanced.

In FIG. 10 the daily mean values of G^*/G_o^* are plotted (dashed curve). Included in this diagram is a plot of the 5-day running-mean G^*/G_o^* and the daily surface albedo (dotted curve). This diagram illustrates a number of interesting features. Of primary interest are the maximum values of G^*/G_o^* occurring during January when surface albedo is a maximum (mean daily surface albedo in Jan. $\simeq$ 0.84). It is also of interest to note that there is very little variation in the surface albedo values. On the other hand, the maximum variation in G^*/G_o^* occurs at this time of year.

As the snow-pack begins to decay in February and March, there is a consequent lowering of the surface albedo and a subsequent decrease in G^*/G_o^*. Observe the general synchroneity of the daily plots of G^*/G_o^* and the surface albedo as of 13 March. With the disappearance of the snow cover on 18 March, G^*/G_o^* approaches its minimum value. Note the increases in G^*/G_o^* on several occasions after 18 March on which light snowfalls were recorded.

The station was completely snow-free as of 4 April. Both surface

Figure 10

INTENSIFICATION RATIO, G^*/G_o^*

Plotted As A Function Of Time Of Year

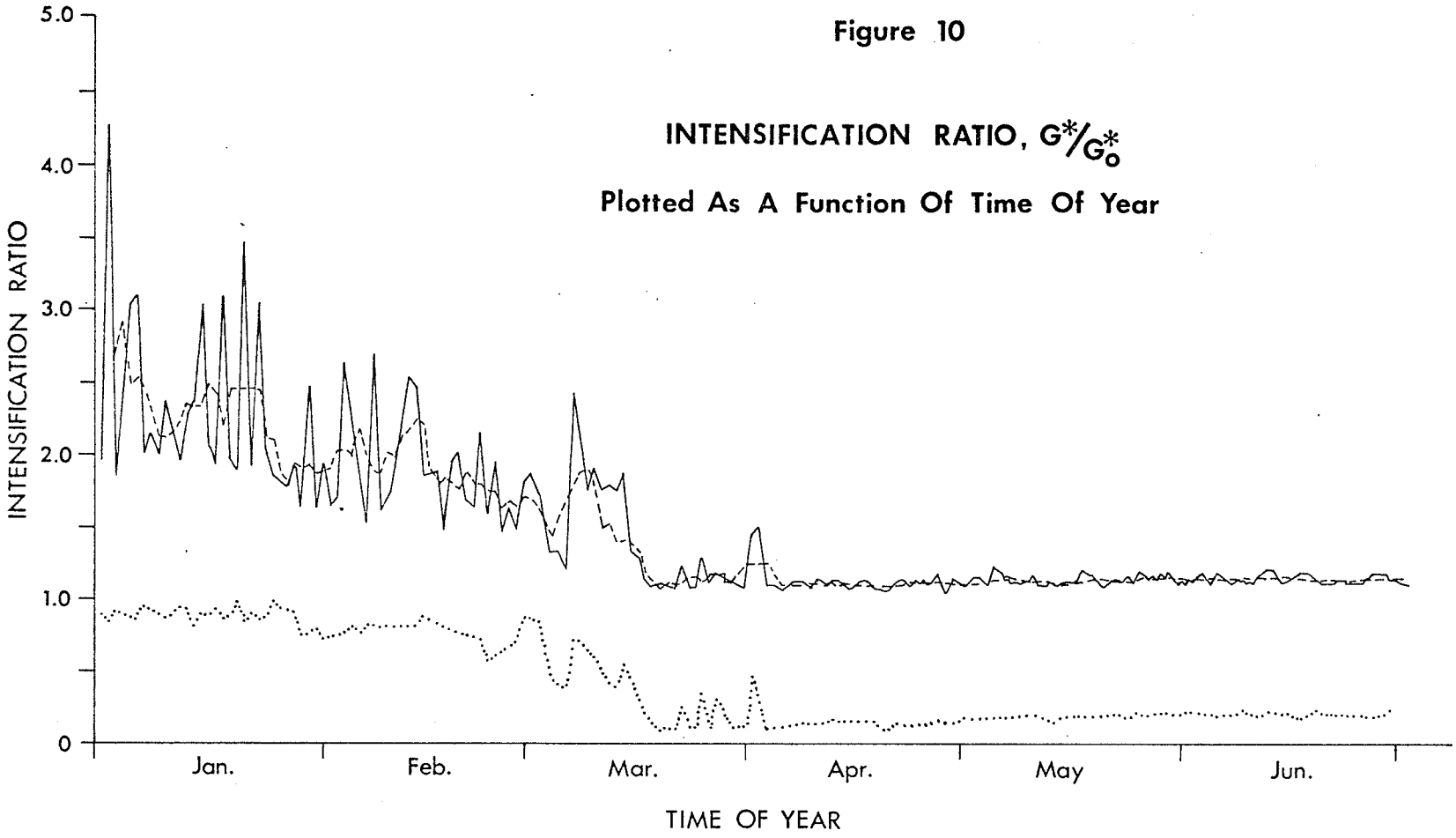

——— Daily mean values
----- Five-day running means of daily mean values
····· Daily surface albedo

albedo and G^*/G_o^* display very little variation from the beginning of the snow-free period to the end of the observation period. This is perhaps the most striking feature of G^*/G_o^* during the snow-free period. In fact, the daily curve and the 5-day running-mean curve are almost coincident. This is in spite of the fact that there was no apparent systematic change in either type or degree of cloudiness during the observation period. Cumulus clouds, for instance, are observed almost as frequently in January as they are in June. This illustrates that the degree of multiple reflection, and hence, the global radiation receipt, is rather sensitive to cloudiness over a snow-covered surface.

The intensification ratio was then examined in terms of cloudiness, both with respect to the type and the degree of cloudiness. The hourly values of G^*/G_o^* were first grouped according to various cloud amounts. Values of c = 0.0, 0.2, 0.4,..., 1.0 were chosen. FIGS. 11 - 16 illustrate plots of the frequency distributions for each of the values of c chosen, while some basic statistics are summarized in TABLE 9.

It is observed that G^*/G_o^* is a minimum for the case of c = 0.0, which is in accord with theory. However, the values for this case are very low. The mean value for this case is 1.0114. This is a value comparable to the Rayleigh case, and substantially less than the clear-sky, but turbid conditions as calculated by Feigel'son et al[76]. On the other hand, Lettau and Lettau's calculations of the backscatterance for Kew, U.K., also indicate very small values, values close to the Rayleigh case.

---

76. Feigel'son et al, 1960, op. cit.

Figure 11

FREQUENCY DISTRIBUTION OF G^*/G^*_o
FOR C=0.0

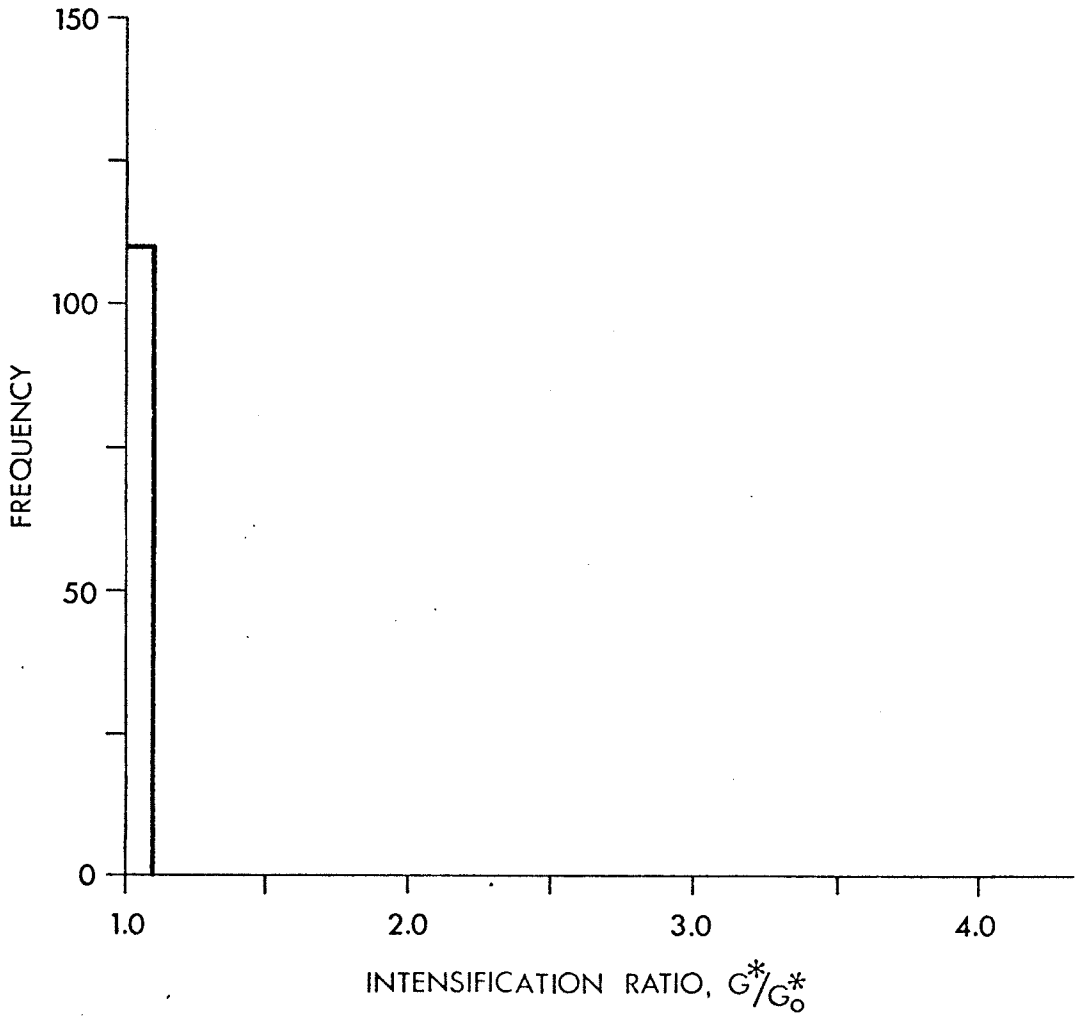

Figure 12

FREQUENCY DISTRIBUTION OF G^*/G^*_o

FOR C = 0.2

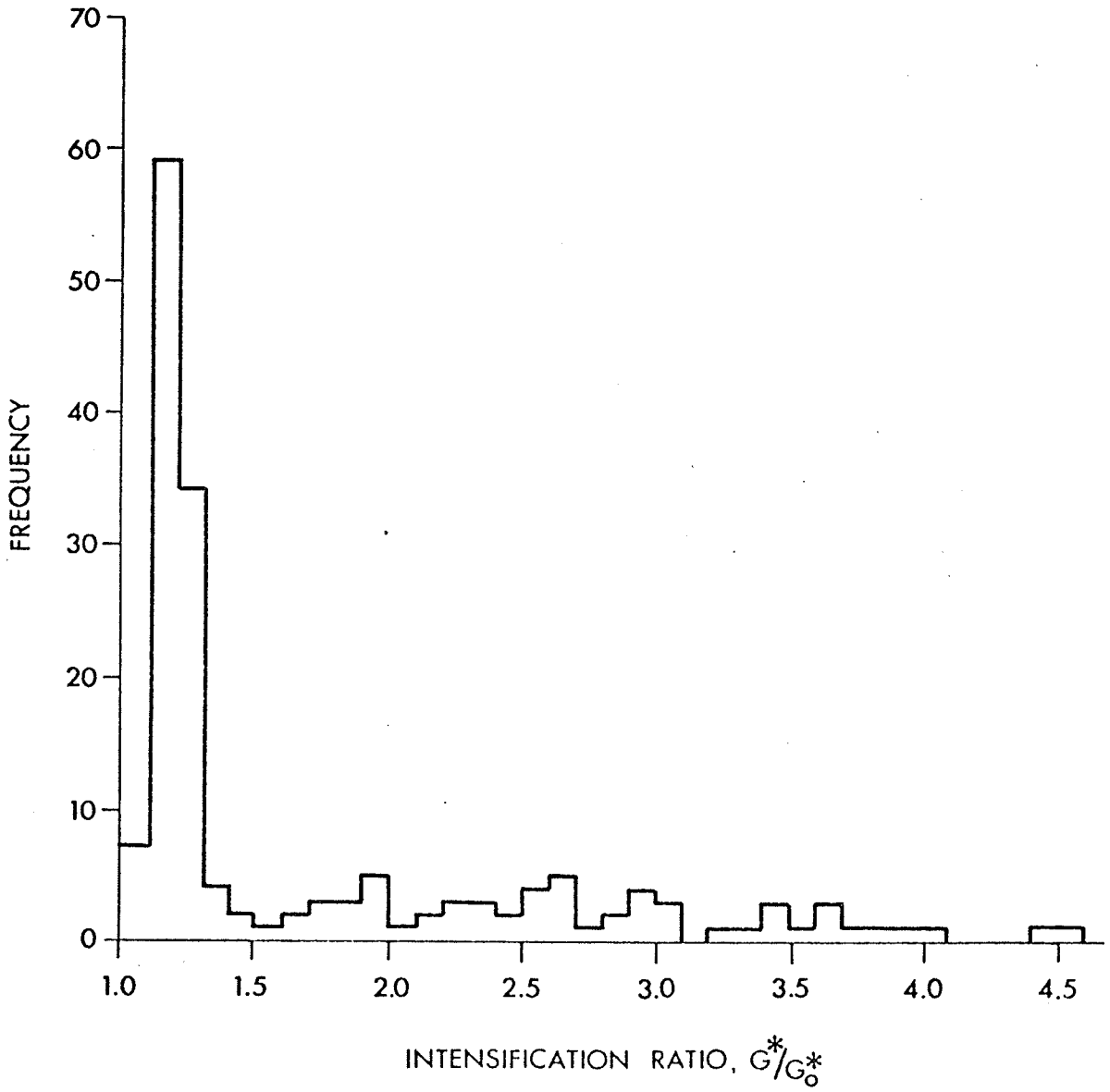

Figure 13

FREQUENCY DISTRIBUTION OF INTENSIFICATION RATIO
FOR C = 0.4

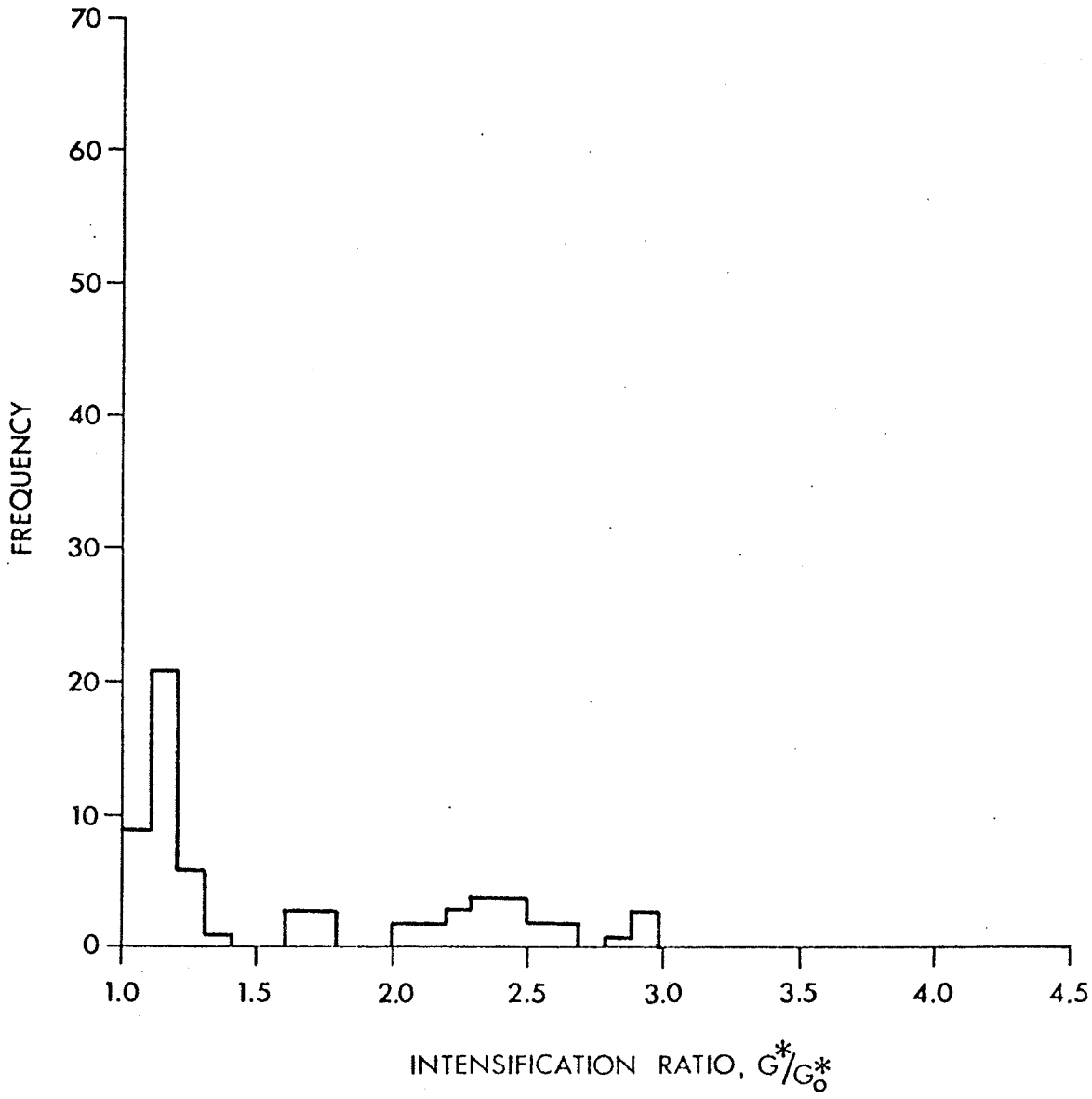

Figure 14

FREQUENCY DISTRIBUTION OF G^*/G^*_o

FOR C = 0.6

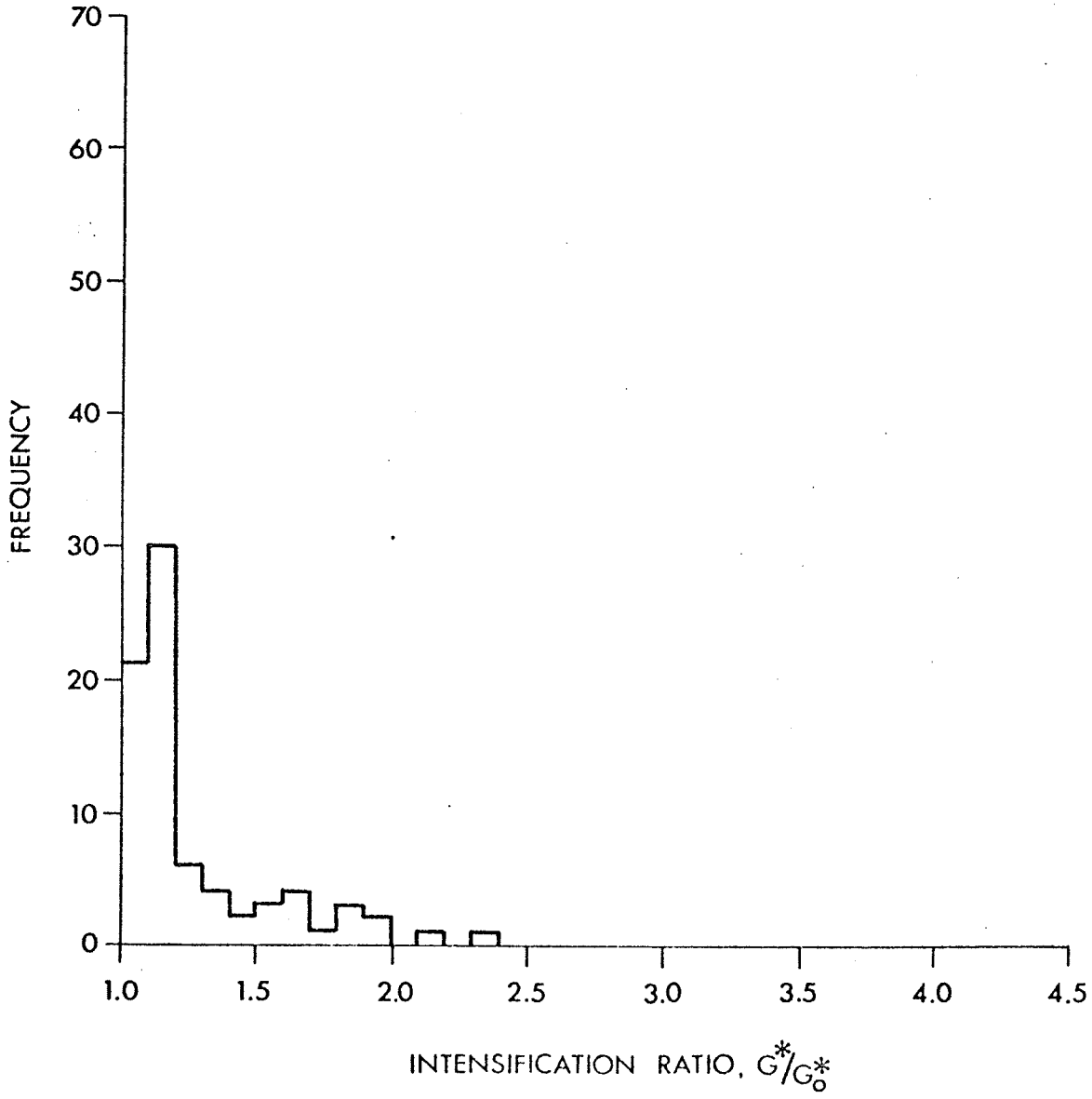

Figure 15

FREQUENCY DISTRIBUTION OF G^*/G^*_o

FOR C = 0.8

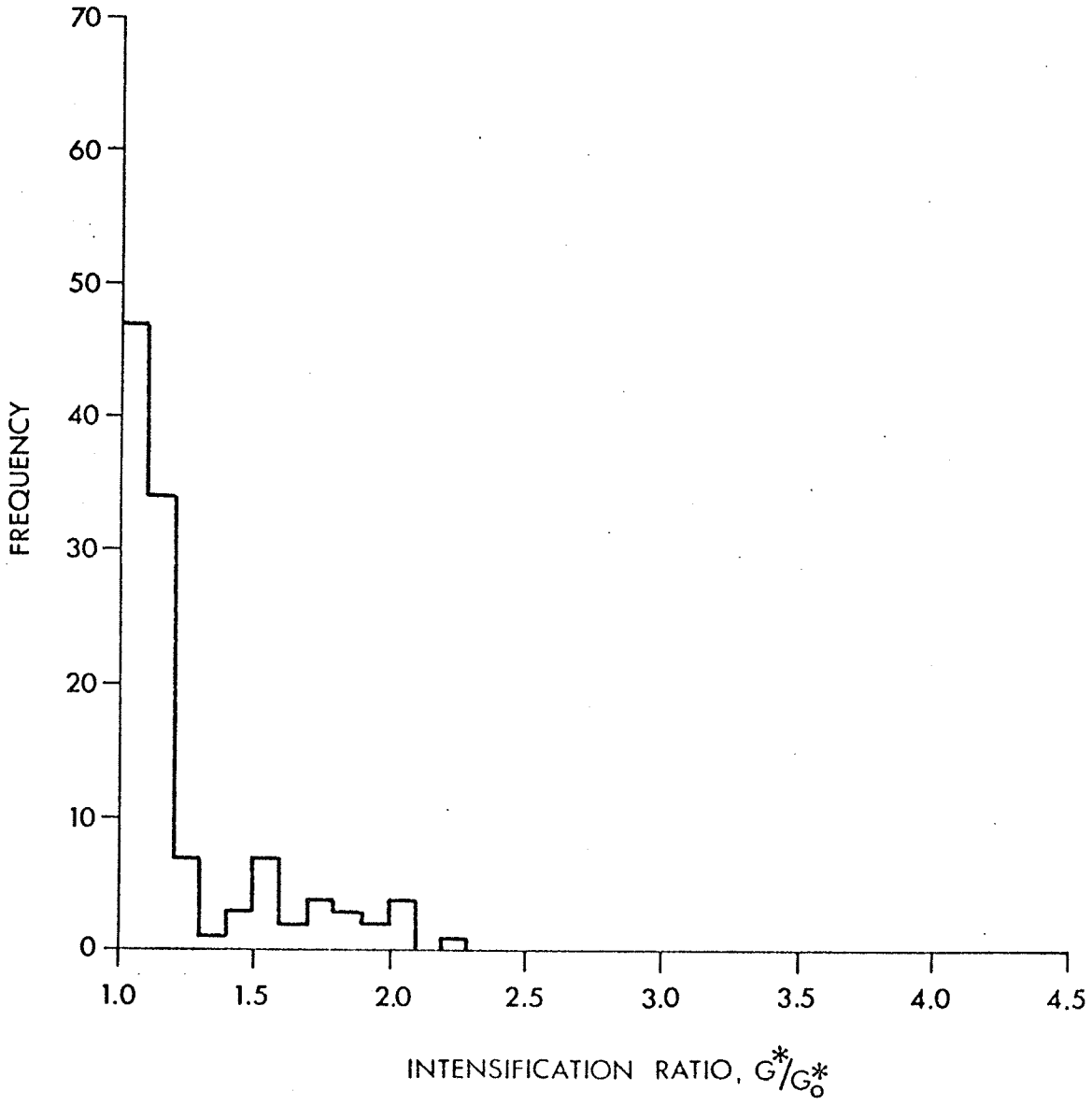

Figure 16

FREQUENCY DISTRIBUTION OF G^*/G^*_o
FOR C = 1.0

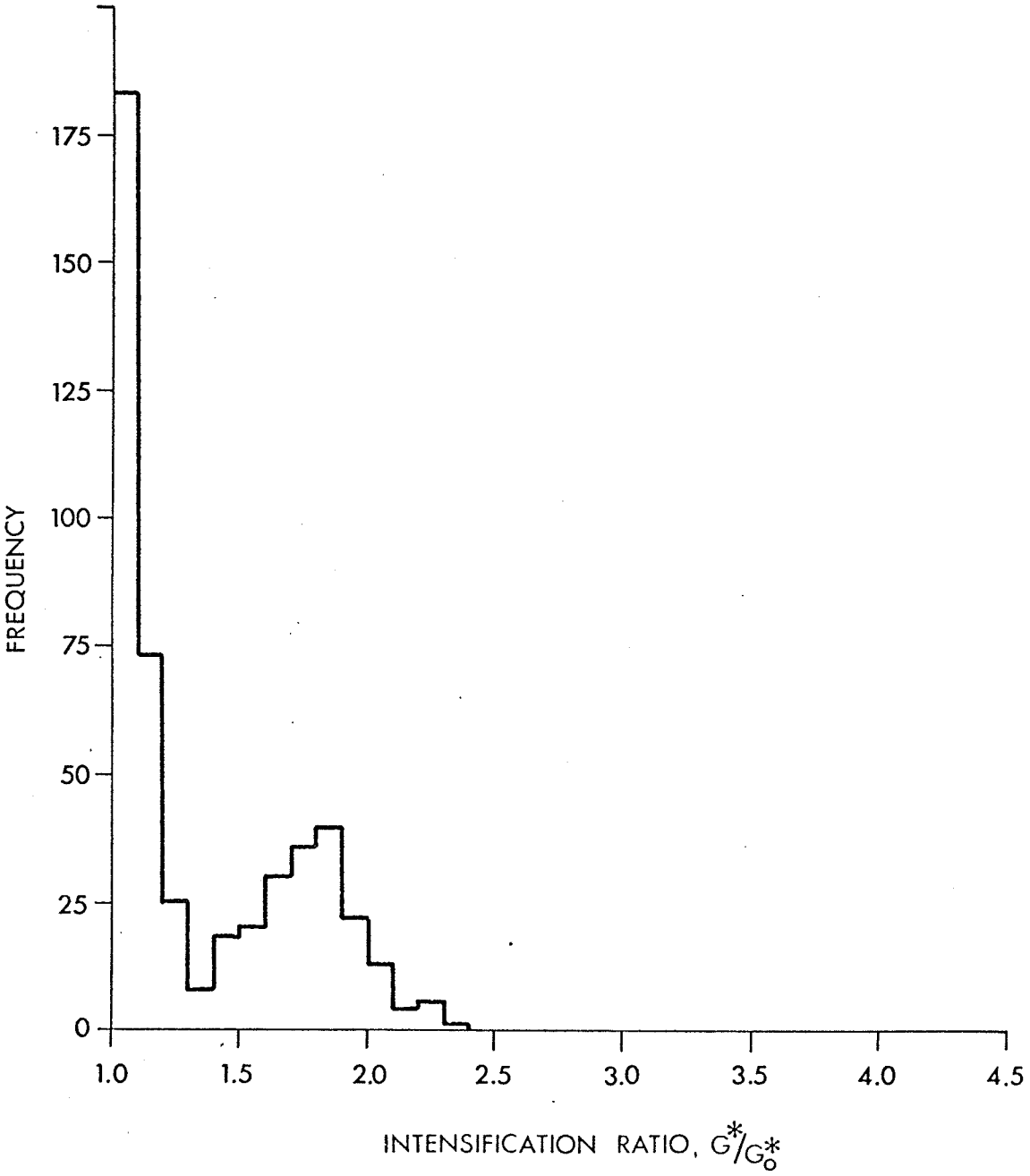

TABLE 9 - SUMMARY OF SOME BASIC STATISTICS OF THE INTENSIFICATION RATIO AS A FUNCTION OF CLOUDINESS.

Cloudiness (Amount)	Sample Size	Sample Mean	Sample Stnd. Dev.	Coef. of Var. (%)	Median
c = 0.0	110	1.0114	0.0086	0.85	1.01
c = 0.2	166	1.7484	0.8993	51.44	1.23
c = 0.4	63	1.6043	0.5986	37.32	1.20
c = 0.6	80	1.2969	0.3202	24.69	1.14
c = 0.8	115	1.2537	0.2875	22.93	1.12
c = 1.0	487	1.3826	0.3557	25.73	1.16

When the frequency distributions for $c > 0$ are considered it is first observed that, for each case, there is a high frequency of observations centered in the lowest class intervals. For cases of small cloudiness the distributions are often discontinuous. As cases of increasing cloudiness are considered, the range decreases and the distributions begin to approach a bimodal distribution, which is clearly evident in FIG. 16.

When the values of G^*/G_o^* are considered in terms of values of c, it is observed that that maximum values of the intensification ratios are associated with minimum values of c,† which is in accord with the climatonomical prediction. However, for $c \simeq 0.8$, the intensification ratio begins to increase with increasing cloudiness. Why this happens cannot be ascertained precisely. One very likely consideration, however, is that the optical parameters of the mostly clouded sky, such as the optical thickness, degree of forward- and backward- scattered radiation, i.e., the scattering functions, assume a greater importance than the actual amount of cloudiness.

Müller[77] has stated that '... it is well known that global radiation with scattered cloud is, on the average, 2 to 3 times larger with scattered clouds than with overcast sky...'. Clearly, this observation is tenable only if multiple reflection is substantially enhanced for the former case. The ratio of mean intensification ratio for $c = 0.2$ to the mean intensification ratio for $c = 1.0$ is 1.32. Obviously, reflection from the sides, and to a lesser extent, the base of the cloud, of clouds is an important mechanism in the multiple reflection process.

---

77. Müller, 1965, op. cit.

† For $c > 0$.

It is interesting to note that when the actual global radiation receipts are considered, Haurwitz[78] has found that when all values of cloudiness are considered, for the case that density = 1 (on a scale 0 to 4) that the mean value of global radiation is highest for the case when c = 0.1 - 0.3, greater, in fact, than for the cloudless case, although the differences are small (57.6 ly/hr for c = 0.1-0.3 versus 57.5 ly/hr for c = 0). When clouds of increasing density are considered this pattern is not maintained and the expected pattern of decreasing global radiation receipts with increasing cloudiness emerges, with the maximum global radiation being recorded for the case of c = 0. It is also to be noted that the above results were obtained for the case of air mass = 1.

When the case of air mass = 3 is considered, slightly different features arise. Global radiation receipt, for either density = 1 or 3, is a maximum for the clear sky case and decreases with increasing cloudiness. When clouds of density = 1 are considered, it is observed that the mean global radiation receipts are greater for the case of c = 0.8-0.9 than for the case of c = 0.4-0.7. Other factors unchanged, these observations tend to support the correctness of the results derived in this study.

The values of G^*/G_o^* were next grouped according to cloud-type. Only those hours in which one cloud-type was recorded were utilized for this part of the analysis. Because the majority of hours were observed to contain more than one cloud-type, the sample size is necessarily small.

FIGS. 17 - 22 illustrate the frequency distributions for the six

---

78. Haurwitz, 1945, op. cit.

Figure 17

FREQUENCY DISTRIBUTION OF G^*/G^*_o FOR CIRRUS CLOUDS

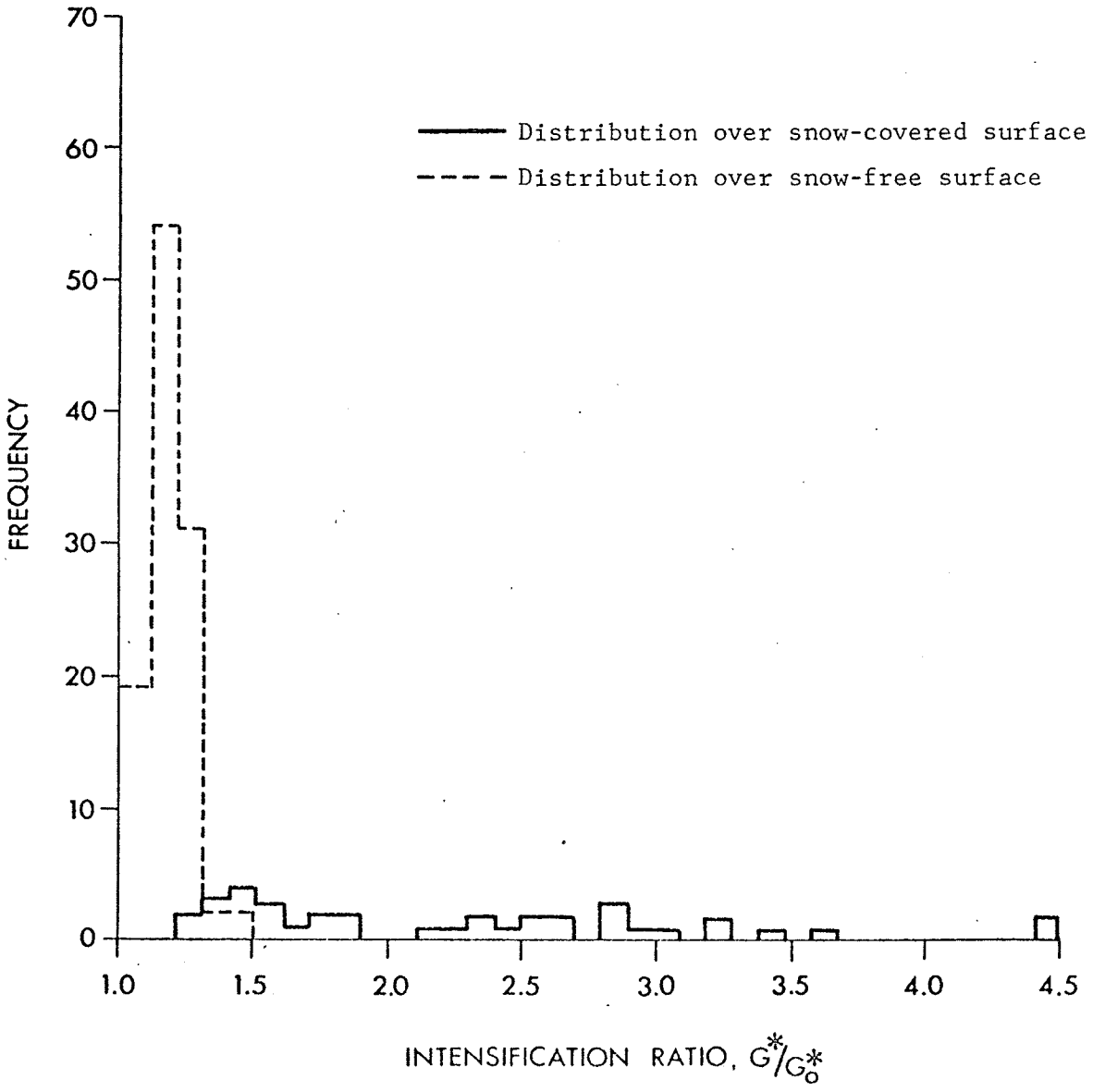

Figure 18

FREQUENCY DISTRIBUTION OF G^*/G^*_o WITH RESPECT TO ALTO-CUMULUS CLOUDS

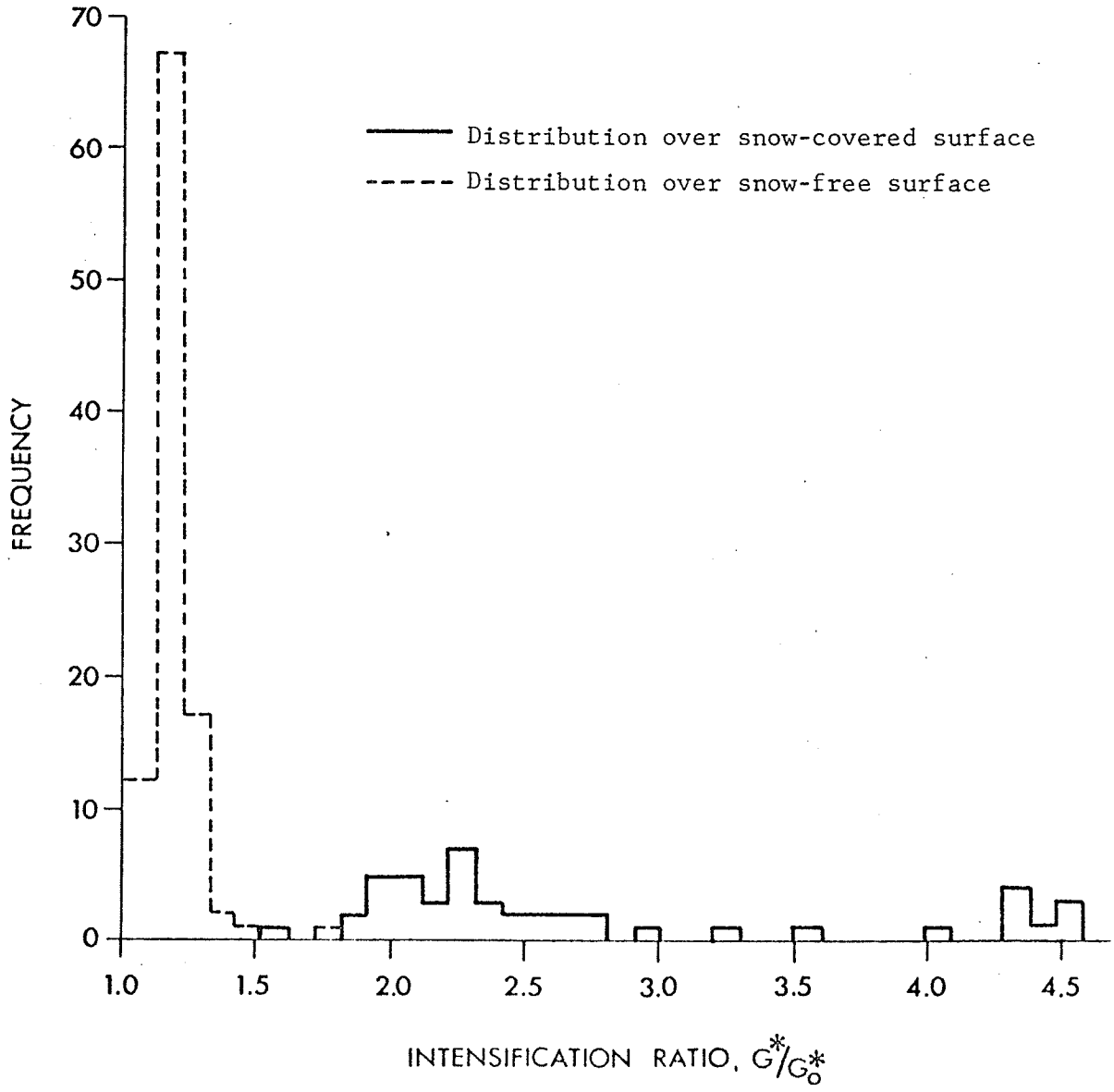

Figure 19

FREQUENCY DISTRIBUTION OF G^*/G^*_o WITH RESPECT TO CIRRO-STRATUS CLOUDS

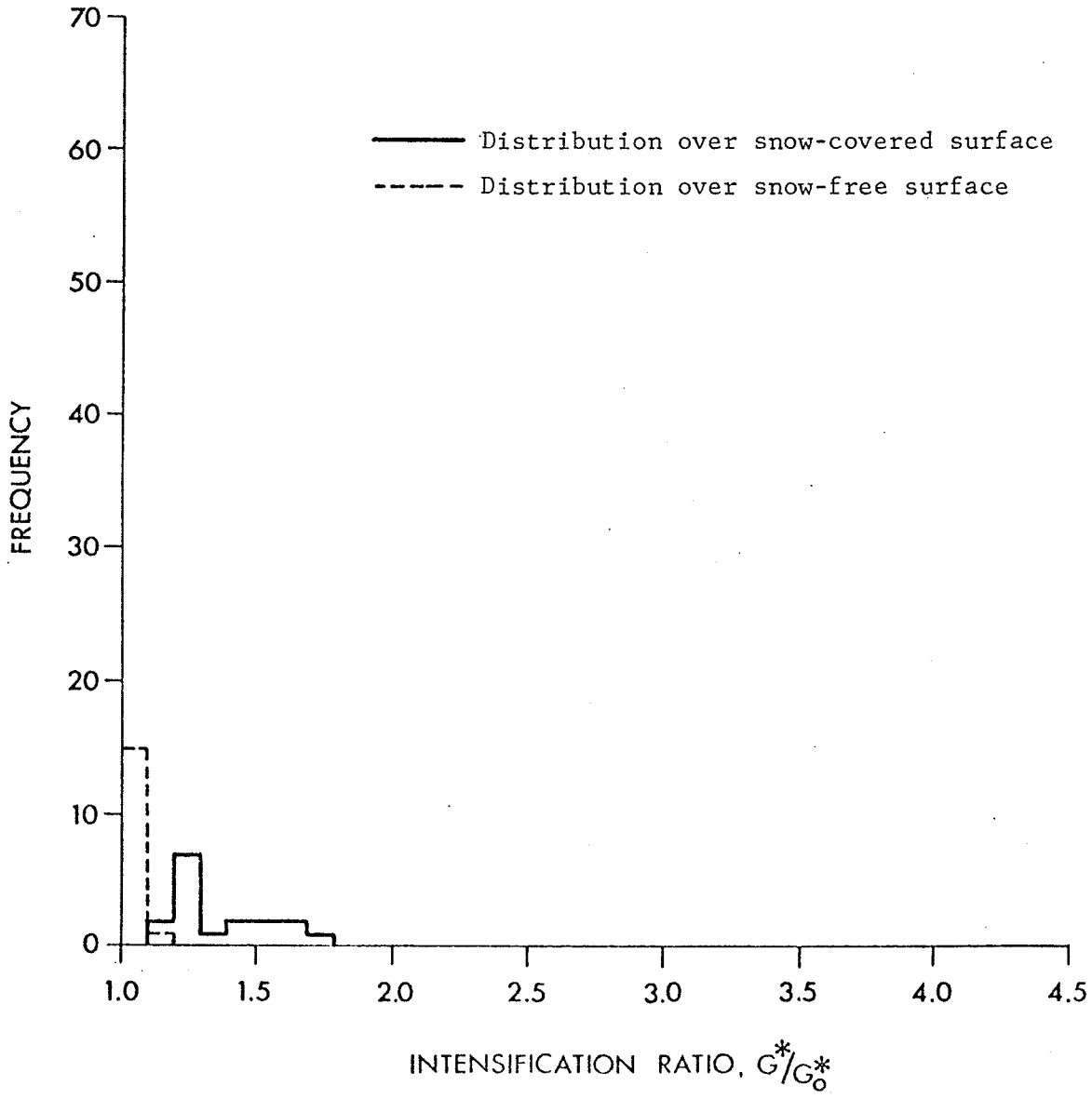

Figure 20

FREQUENCY DISTRIBUTION OF G^*/G^*_o WITH RESPECT TO STRATO-CUMULUS CLOUDS

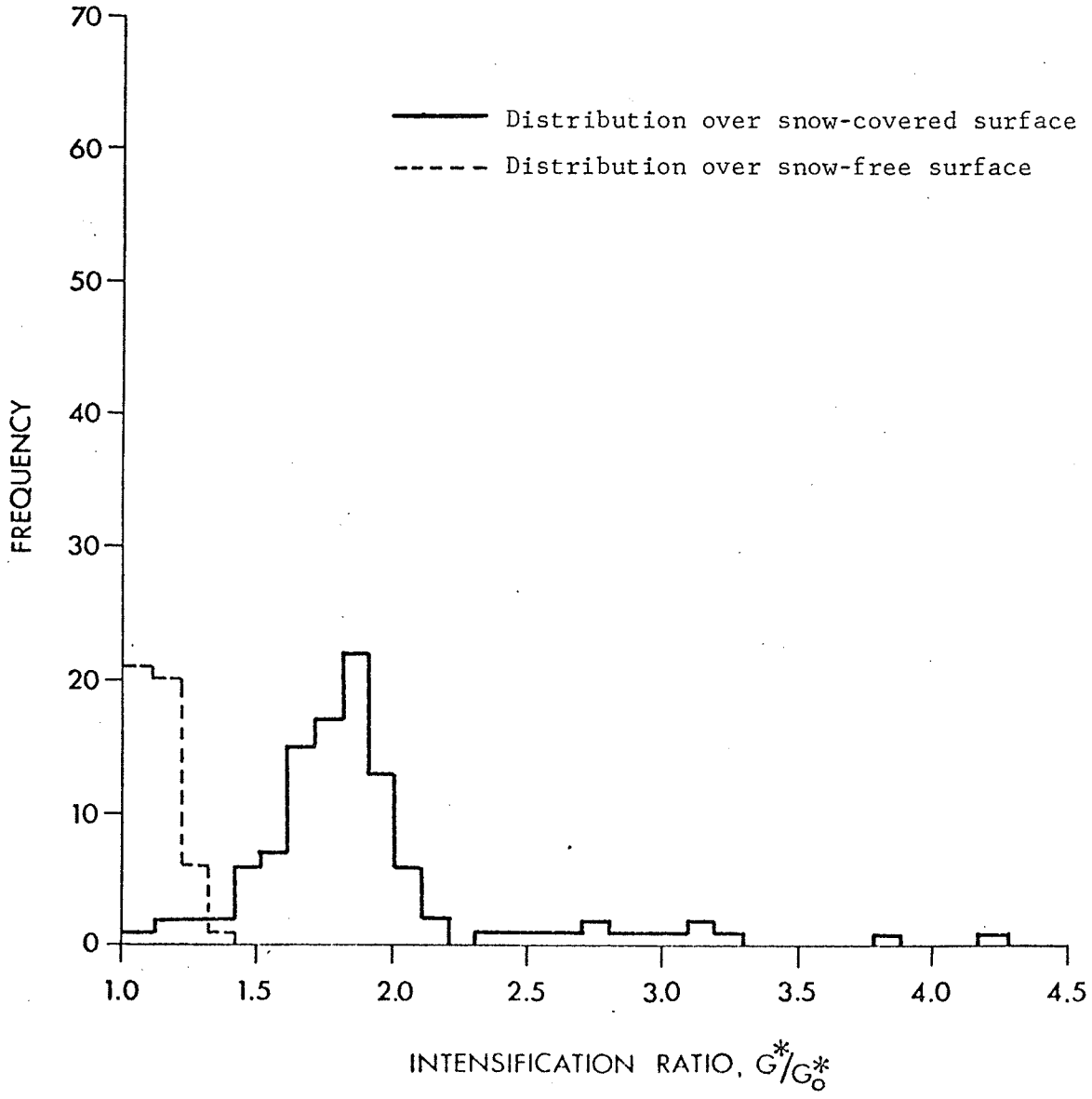

Figure 21

FREQUENCY DISTRIBUTION OF G^*/G^*_o WITH RESPECT TO STRATUS CLOUDS

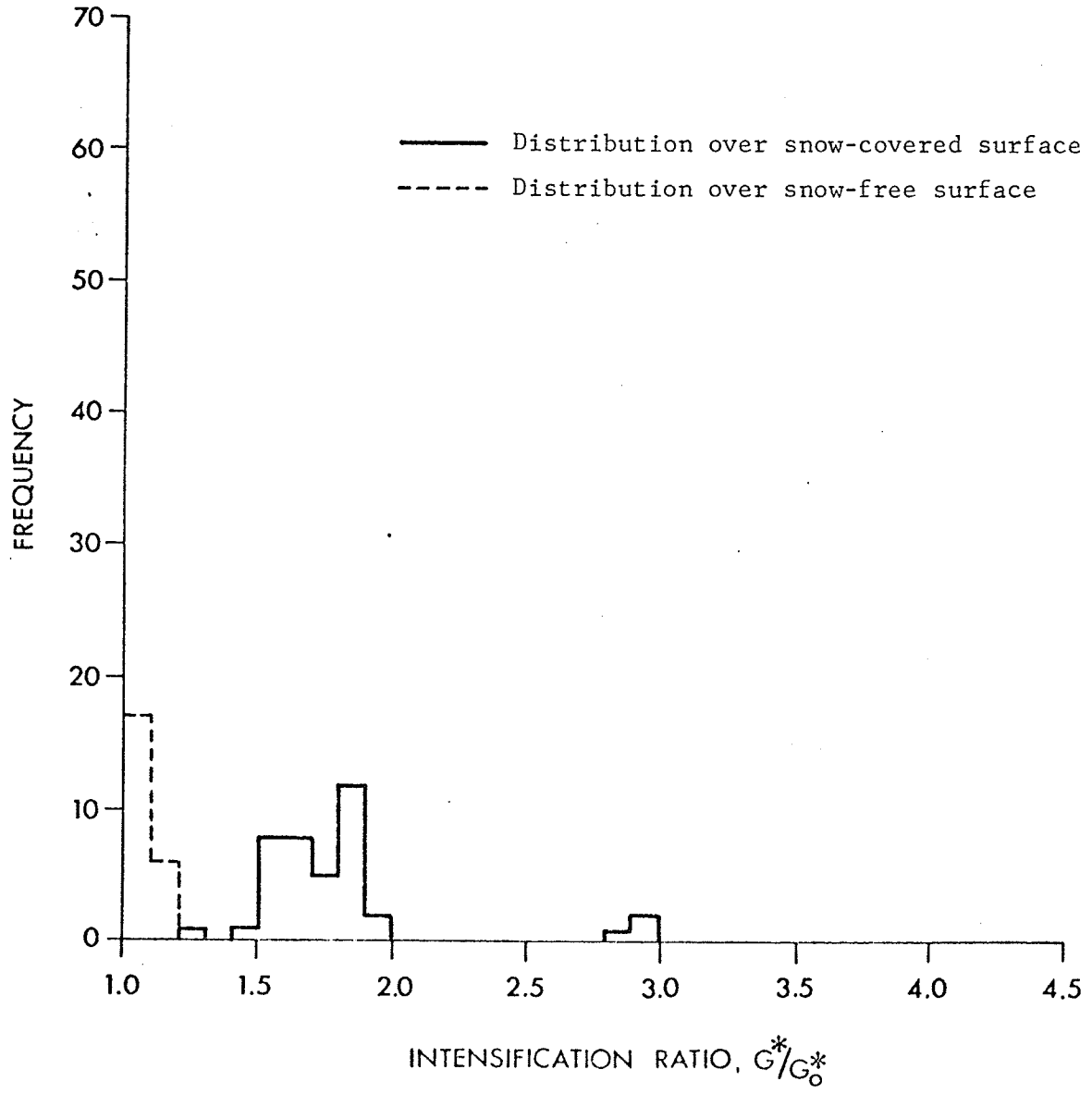

Figure 22

FREQUENCY DISTRIBUTION OF G^*/G^*_o WITH RESPECT TO CUMULUS CLOUDS

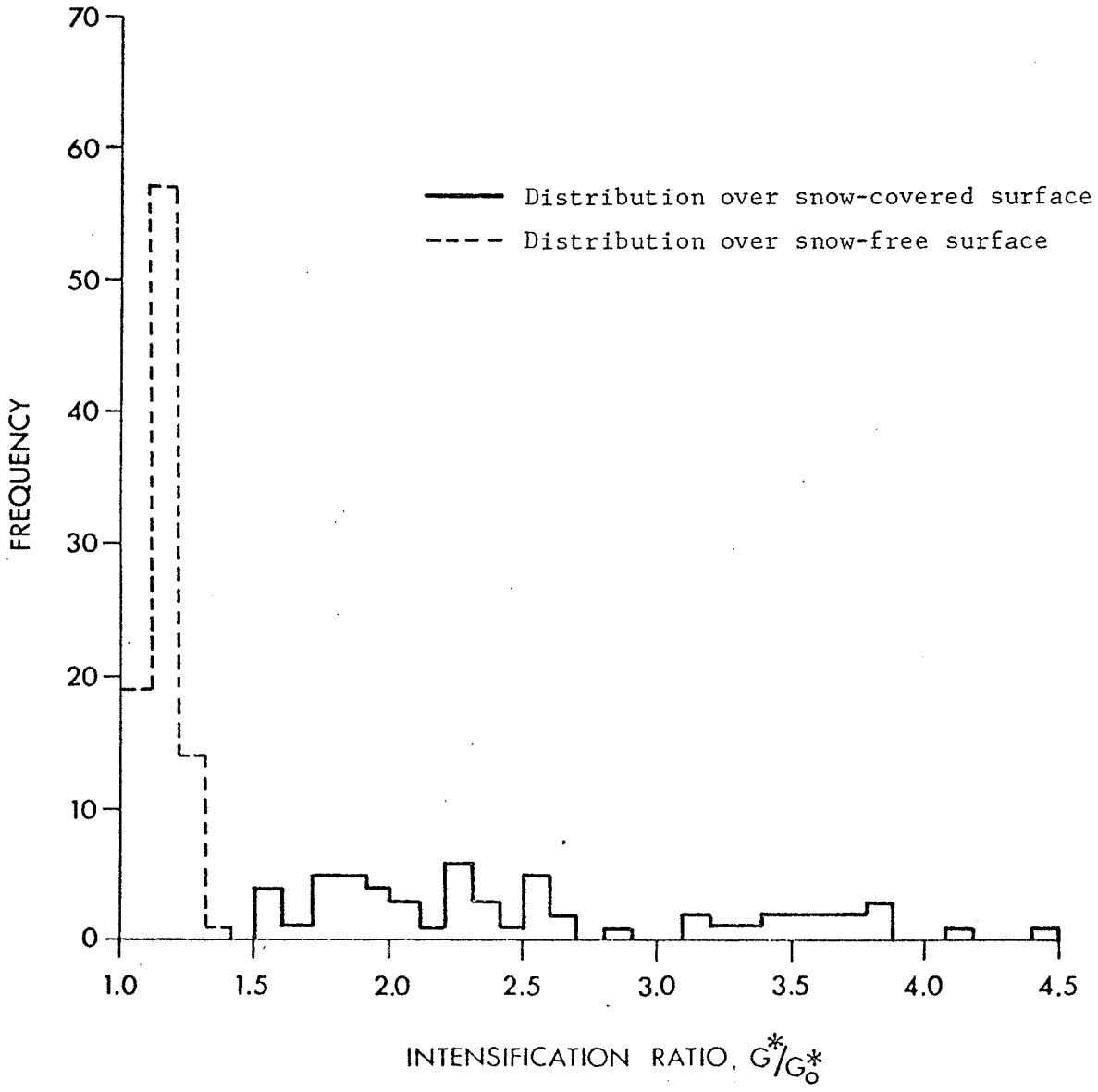

cloud-types: i) Ci; ii)- Ac; iii)- Cs; iv)- Sc; v)- St; and vi)- Cu. The distributions are given both for the case of snow-free and snow-covered surface. Some basic statistics are summarized in TABLES 10 and 11.

For the distributions over snow-covered surface there is witnessed a considerable variation for all cloud-types. Over a snow-free surface this variation is considerably reduced.

In terms of absolute comparisons it is observed that clouds of vertical extent, namely Ac and Cu, are associated with the greatest (mean) G^*/G^*_o. Clouds of horizontal development, viz., Sc and St, have lower intensification ratios. This result is not surprising since these cloud-types posses a far smaller (total) surface area, in comparison to clouds of vertical extent, for reflection of diffuse radiation to occur. The value for St clouds is less than the value for Sc clouds, probably due to the greater absorption that occurs with St clouds.

For optically thin clouds an interpretation is difficult to give. Certainly Cs clouds conform to the expected pattern that G^*/G^*_o should decrease with decreasing opacity.The value for the Cs cloud-type, in fact, are the lowest observed. On the other hand, Ci clouds have values close to those for clouds of vertical extent.

In a tentative manner, the data from TABLES 10 and 11 were utilized to calculate the (mean) backscatterance for the various cloud-types. These data are given in TABLE 12. The results conform to theory, with one exception: clouds of vertical extent have the greatest backscatterances, while clouds of vertical extent have a lower value (St < Sc), while the optically thinest clouds, except for Ci, have the smallest backscatterances.

TABLE 10 - SUMMARY OF SOME BASIC STATISTICS OF THE INTENSIFICATION RATIO FOR VARIOUS CLOUD-TYPES (Case of a snow-covered surface).

Cloud-type	Sample Size	Sample Mean	Sample Stnd. Dev.	Coef. of Var. (%)	Median
Cirrus	37	2.3886	0.9508	39.8	2.36
Alto-Cumulus	46	2.7239	0.9668	39.5	2.31
Cirro-Stratus	17	1.3682	0.1889	13.8	1.26
Strato-Cumulus	110	1.9278	0.6036	31.3	1.82
Stratus	40	1.7942	0.3507	19.6	1.75
Cumulus	60	2.6142	0.8750	33.5	2.31

TABLE 11 - SUMMARY OF SOME BASIC STATISTICS OF THE INTENSIFICATION RATIO FOR VARIOUS CLOUD-TYPES (Case of snow-free surface).

Cirrus	117	1.1713	0.0678	5.8	1.16
Alto-Cumulus	100	1.1559	0.0830	7.2	1.13
Cirro-Stratus	16	1.0631	0.0166	1.6	1.06
Strato-Cumulus	48	1.1250	0.0553	4.9	1.11
Stratus	23	1.0896	0.0287	2.6	1.09
Cumulus	91	1.1497	0.0591	5.1	1.14

TABLE 12 - CALCULATED MEAN BACKSCATTERANCES FOR VARIOUS CLOUD-TYPES

Cloud-Type	Ci	Ac	Cs	Sc	St	Cu
Mean Intensification Ratio	2.04	2.40	1.28	1.72	1.64	2.38
Mean Backscatterance	0.693	0.793	0.297	0.569	0.530	0.788

In order to obtain a comprehensive analysis of the intensification ratio, both in terms of cloud amount and opacity, G^*/G_o^* was examined as a function of opacity and the sun's zenith angle (optical air mass). The values of opacity which are given in the Daily Surface Weather Record is a measure of both cloud amount and the opacity of the cloud. Unfortunately, a precise definition of the term opacity could not be obtained from the Canadian Meteorological Service. Thus it is not known to what extent this measure corresponds to the optical thickness τ^*. The (total) opacity for each hour was considered. In this manner the entire data set could be utilized. The range of opacity is from 0 (clear sky), 1, 2, 3, ..., 10 (complete overcast). The values of the intensification ratio were grouped into each of these classes and then subgrouped according to zenith angle. For zenith angle, an interval of 15° was chosen. The lowest class limit is 20°, since this is the minimum zenith angle observed. These intervals correspond to mean zenith angles of 27.5°, 42.5°, 57.5°, and 72.5°. The pertinent data are summarized in TABLE 13 and schematically in FIG. 23.

With but three exceptions the intensification ratio increases with increasing zenith angle which conforms to Feigel'son's et al[79] theoretical calculations for the clear, but turbid, atmosphere.

For a given zenith angle interval, the intensification ratio is a minimum for opacity = 0. Maximum values are observed for opacity = 1. The values then decrease to a secondary minimum at opacity $\simeq$ 6-7 for small zenith angles to $\simeq$ 4-5 for large zenith angles.

Recalling Haurwitz's[80] study, it is observed that, for large zenith angles, the global radiation receipts are larger for the case of high cloudiness (c = 0.8-0.9) than for the case of partly clouded sky (c = 0.4-0.7), which is also the pattern established by the

TABLE 13 - COMPUTED MEAN INTENSIFICATION RATIO AS A FUNCTION OF OPACITY AND THE SUN'S ZENITH ANGLE, Z.

	Mean Zenith Angle				
	27.5	42.5	57.5	75.0	Mean
Opacity = 0	1.01	1.04	1.13	1.02	1.05
= 1	1.16	1.34	2.00	2.19	1.67
= 2	1.15	1.19	1.75	2.06	1.56
= 3	1.12	1.13	1.60	1.76	1.40
= 4	1.11	1.14	1.38	1.36	1.25
= 5	1.10	1.11	1.31	1.41	1.23
= 6	1.10	1.11	1.31	1.48	1.25
= 7	1.09	1.11	1.34	1.42	1.24
= 8	1.11	1.09	1.40	1.51	1.28
= 9	1.10	1.11	1.40	1.48	1.28
= 10	1.10	1.12	1.42	1.64	1.32
Mean	1.10	1.14	1.46	1.58	

Figure 23

MEAN INTENSIFICATION RATIOS AS A FUNCTION OF OPACITY AND ZENITH ANGLE

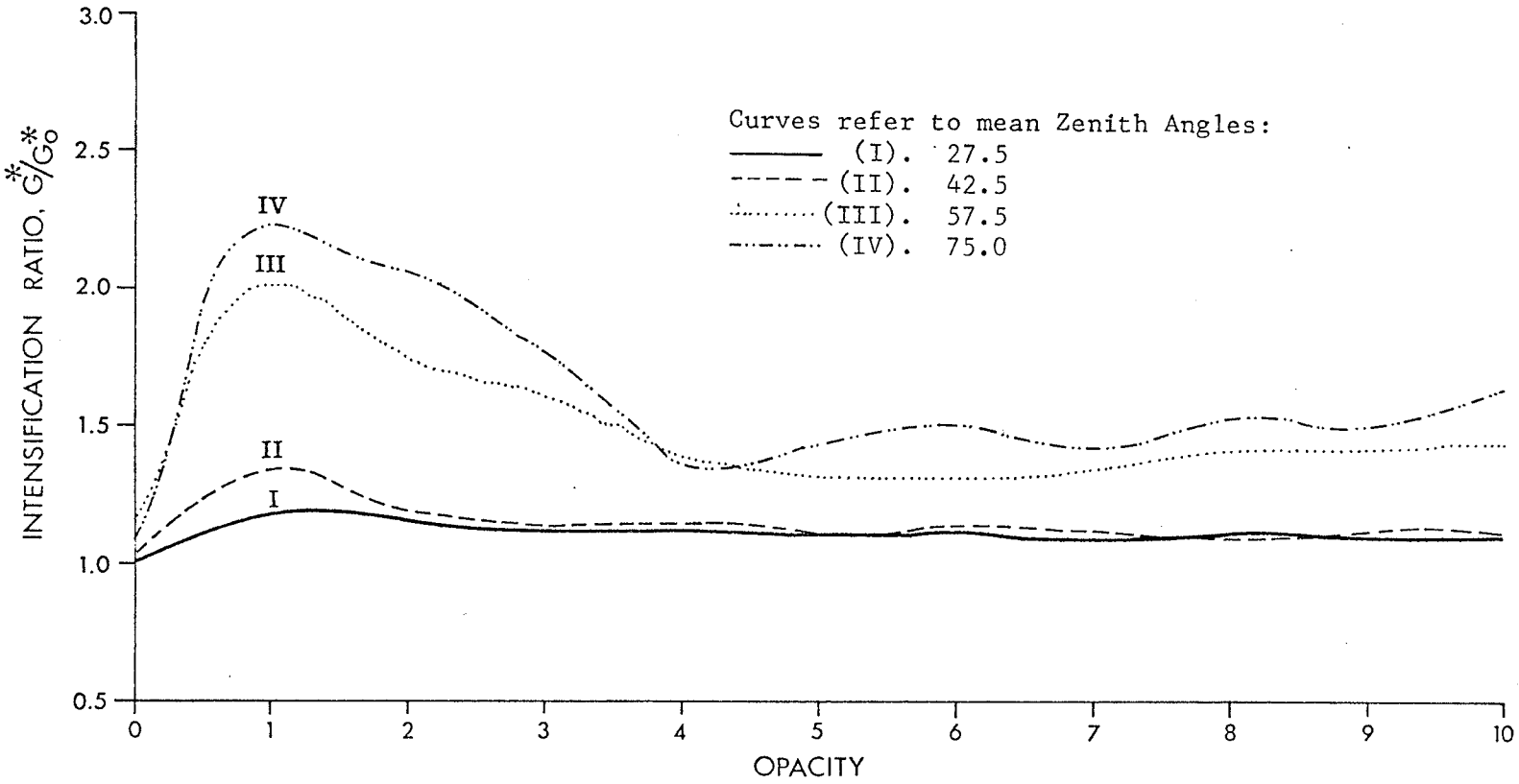

the intensification ratio. Referring to either TABLE 13 of FIG. 23, it is observed that this feature is not manifested for the case of small zenith angles.

In summary, it is apparent that the role of cloudiness in the multiple reflection process remains a rather complex one. The computations suggest that G^*/G_o^* is dependent upon both the type and degree of cloudiness, as well as the sun's zenith angle.

In a final and exploratory manner can any inferences be drawn about the relationship between the multiple reflection process and the global solar radiation estimation equations? The answer is apparently very little.

In the first instance, a mean plot of the seasonal regime of the intensification ratio has not been obtained. The plot given in FIG. 10 is only one of a number of possible plots and only suggests what the mean values would be. Moreover, the plot is incomplete: only half a years data has been analysed. No indication of the plot for the second half of the year is given. Time constraints and the tremendous mass of input data prohibited a more complete analysis from being undertaken.

Second, it proved impossible to calculate the regression coefficients of the (linear) estimation equation for this station because sunshine records appear intermittently for this station. An attempt was made to use the sunshine records of a downtown Toronto station, some 15 miles to the south-east. But on quite a number of occasions it happened that when the sunshine duration was zero at the there was a full day of sunshine at Toronto MRS. It therefore proved safer to abandon this plan than to proceed with it. Out of these

79. Feigel'son et al, 1960, op. cit.
80. Haurwitz, 1945, op. cit.

considerations the following discussion is necessarily qualitative in nature.

Recalling Chapter I, the global radiation estimation equation is of the following form:

$$Q/Q_o = f(n/N) \qquad (77)$$

where the variables are defined as before. Mention has already been made of empirical investigations which illustrate that the regression coefficients are inversely related. And, moreover, this research illustrates that over a snow-covered surface $\hat{a}$ is a maximum and $\hat{b}$ is a minimum, while over a snow-free surface the reverse is true, i.e., $\hat{a}$ is a minimum and $\hat{b}$ is a maximum. Since it is $\hat{b}$ which determines the regression line, attention will be concentrated on it.

Mathematically, $b = d(Q/Q_o) / d(n/N)$. Over a snow-covered surface it has been shown that there are wide variations in the intensification ratio associated with cloudiness, and hence, with the relative sunshine duration, neglecting, for the moment, the fact that in winter surface albedo fluctuations are greater than in summer. This would lead one to suspect that $\hat{b}$ should be a maximum in winter and a minimum in summer, since intensification is nearly constant in summer, despite the wide variations in cloudiness that occur. The consequence is that $\hat{a}$ would now be a minimum in winter and a maximum in summer.

Such qualitative reasoning yields a regime for the regression coefficients that contradict a large body of empirical evidence. Part of this divergence may be explained as follows. The methodology employed in this study necessitated several assumptions and approximations. For

instance, the coefficients of the scattering process are held constant and not treated as variables as they ought to have been. And while the total absorption was allowed to vary, it could only vary as did the absorption coefficient of water vapor, since a fixed relationship between water vapour absorption and all other absorption is assumed. It is possible, therefore, that much of the variability in the intensification ratio, over a snow-covered surface, arises due to the attenuation in the cloud-free atmosphere and not from cloudiness. Hence the effect of multiple reflection on the global radiation receipt, with respect to cloudiness, may be the same for either snow-free or snow-covered surfaces. And thus the reasoning of a winter maximum and summer minimum for $\hat{b}$ may be fallacious.

In summary, the relationship between multiple reflection and the global radiation estimation equations remains rather nebulous, and is likely to remain so until such time that the attenuation in the cloud-free atmosphere can be more definitively ascertained.

CHAPTER V

SOME METHODOLOGICAL PROBLEMS RECONSIDERED

In applying climatonomy to investigate the climatology of multiply reflected global radiation, a number of theoretical and statistical/observational results are verified. Such success may be attributed to the correctness of climatonomy. It is instructive to observe, however, that in this study's application of climatonomy several assumptions and approximations were necessitated; thus the intensification ratio follows a regime that occurrs as a result of seasonal variations in surface albedo and water vapour absorption. A more realistic appraisal of G^*/G_o^* would have treated the scattering and absorbing processes as variables and not as constants. It is of some importance, therefore, to be aware of the limitations which were brought about in the application of climatonomy to calculate the intensification ratio and how some of these limitations might be potentially resolved.

There exist three fundamental aspects that require further examination. These may be termed: i) - absorption in the cloudless atmosphere; ii) - parameters of the scattering process in the cloudless atmosphere; iii) - absorption-scattering relationships in cloudy atmospheres.

1 - Absorption in the cloudless atmosphere

Because the total absorption in the cloudless atmosphere represents a summation of several absorption coefficients, one might proceed, initially,

by attempting to calculate the individual coefficients and then summing to obtain the total absorption coefficient. And, while α_w may be determined to within reasonably accurate limits, it does not appear possible, at present, to accurately establish the magnitudes of α_g and α_a.

A comprehensive theoretical investigation of absorption and emission of radiation by atmospheric gases, such as, for example, by Goody[81], and others, indicate a rather complex spectrum of absorption by the various gases. FIG. 24 represents Langley's interpretation of the infra-red portion of solar radiation. The major complicating factor in this diagram is that the toal absorption by an individual gas is dependent upon the total pressure, temperature, and density of the absorbing gas, all of which vary with altitude.

About the only firm generalization to be advanced is that such atmospheric absorption is low, especially in the presence of appreciable amounts of water vapour. Lettau's and Lettau's calculations for the three stations used in their study indicate that the ratio of gaseous absorption to total absorption is gnerally low, less than 10^{-1}, or, approximately 1 to 2 percent of the extra-atmospheric irradiance.

Much the same commentary can be applied for the case of aerosol absorption, except that in this case there exists even more uncertainty. Refrence has already been made to Johnson's statement that the absorption spectra of aerosols are poorly known. As well, the few laboratory and optical measurements that have been made further prohibit the advancement of any firm conclusions. Robinson[82] has also pointed out that various

---

81. Goody, R.M., 1964: Atmospheric Radiation, Oxford University Press, 436 pp.

82. Robinson, 1963, op. cit.

Figure 24

GENERALIZED SCHEMA OF ABSORPTION SPECTRUM OF SOLAR RADIATION

After Langley, 1900

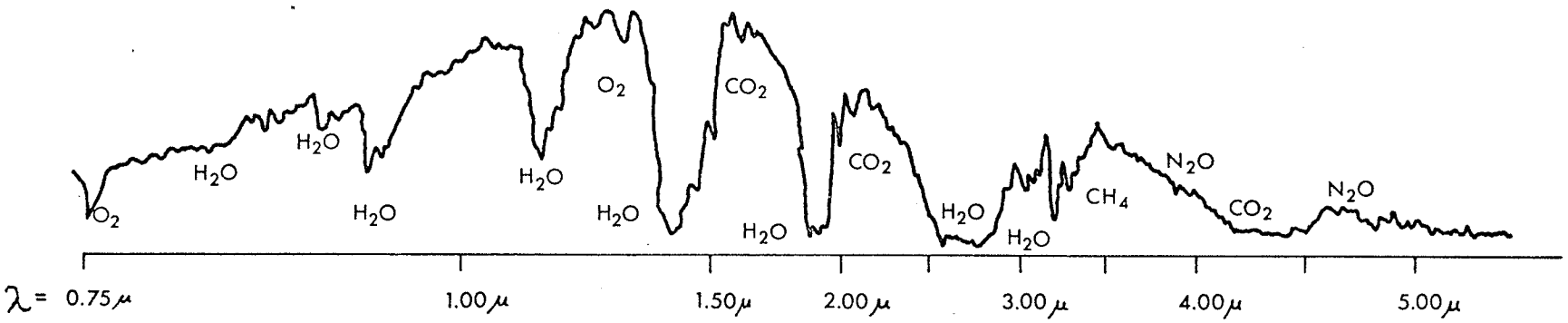

From: Goldberg, 1958, op.cit.

research into the problem of aerosol absorption illustrates that there is no additional absorption to an absorption twice that of water vapour. Such results clearly point to the necessity of considering the quality and quantity of the aerosol at a particular station.

It is likely, however, that in an industrial-urban setting, aerosols do lead to an increased absorption of global radiation. It well known, for instance, from studies of urban climates that the relative humidity is greater in the urban area than in the surrounding countryside. In this event particles emitted into the urban atmosphere may begin to assume many important properties of water vapour, such as its index of refraction and absorption. Consequently, aerosol absorption may be a function of water vapour absorption.

In order to expedite this research, and since no information is given concerning the particulate matter in the atmosphere for this station, this study assumed that all non-water vapour absorption was related to water vapour absorption in the form

$$(\alpha_g + \alpha_a) / \alpha_w = k \qquad (78)$$

where k is some constant and the ratio of the l.h.s. of eqn.(78) shall be referred to as the absorption ratio. Such a formulation allows one to calculate the total absorption as a function of the water vapour absorption.

Such a formulation, however, has two serious limitations. In the first instance it is implicitly assumed that all non-water vapour absorption increases with increasing water vapour. But aerosol absorption is controlled to a greater extent by the quality and quantity of aerosols. The significance of this lies in the fact that, at Toronto, the greatest

concentration of particulate matter occurs in January, a time when water vapour absorption is likely to be at a minimum. Consequently, the absorption ratio may not be a constant but rather a complex function of time of year.

The second limitation stems from a lack of knowledge of the absorption ratio. Even assuming that it is a constant, there is a great paucity of systematic studies examining this ratio with respect to both time and space. This study assumed that Lettau and Lettau's calculations for Kew were representative of other industrial areas and for any time of year which, from the preceding considerations, is not likely to be true.

It would therefore be of some utility to carry out studies sytematically examining the absorption ratio. If airborne measurements of the top albedo are available, then climatonomy could be employed to obtain a good estimate of this ratio. The method involves transformation of some of the fundamental equations which relate the top albedo, A, to the total absorption, α, surface albedo, a, and global radiation, G^*.

Specifically, solving for κc from eqns.(49) and (50), equating the two resultant expressions, and then solving for A yields

$$A = (1 - \alpha)(1 + aG^*) - G^* \qquad (79)$$

Using the airborne value for A and substituting in eqn.(79), one can solve for α, assuming, of course, that the corresponding values of a and G^* are given. Then calculating α_w by the methods outlined in Chapter III, and subsequent subtraction from α yields $(\alpha_g + \alpha_a)$.

2. Parameters of the scattering process in the cloudless atmosphere.

Closely related to the preceding considerations for absorption is that for the scattering process. If total absorption can be accurately determined, then it is possible to calculate the parameters of the scattering process exactly rather than externally prescribing them.

This study made two major assumptions. The first concerns the relationship between scattering and absorption. The second assumption concerns the nature of κ. With regard to the former assumption, the limitations are obvious. This assumption implies that the total scattering is a function of absorption and not with respect to the particulate load in the atmosphere. Thus in this study inaccuracies in the determination of the total absorption are transmitted to calculations of the total scattering coefficient σ.

With regard to the second assumption, mention has already been made of the fact that the size distribution ϑ^* varies both with respect to time of day and time of year. Because of this the parameter κ is not likely to be constant.

Provided α may be accurately determined, for example, by the method outlined in the preceding section, then σ may be obtained as a subtraction term in eqn.(48), provided the other values are given. Both κ and μ may be obtained exactly as follows. Substituting the value of A obtained from airborne techniques and substituting this value into eqn.(49), it is observed that, taken together with eqn.(50), there is given a set of two linear equations in two unknowns, namely κ and μ. Matrix algebra can then be utilized to solve for both κ and μ.

3. Absorption-scattering relationships in cloudy atmospheres.

There are several aspects of this problem which merit further expansion. The first concerns the measurements of cloudiness itself. Values of cloudiness for a given hour are instantaneous values. It is assumed that this value remains constant for that hour. Realistically, this is not true. Cloudiness can and does change with great rapidity. Clouds which originate through glaciation processes, such as Cirrus clouds, can evolve and degenerate with great rapidity. The development of Cumulus clouds on a humid summer day is another example. Still another example would be the passage of frontal systems, particularly cold fronts.

One approach to minimize the error that could arise from this feature would be to consider only those hours in which the following hour had the same value of cloudiness. The major disadvantage to this approach is that the sample size would be reduced. Moreover, there is no guarantee that, during the hour, there were no changes in cloudiness.

A second approach would be to consider the instantaneous value of the intensification ratio. This would have involved calculating the instantaneous extra-atmospheric irradiance for the beginning of the hour, a simple enough task. The corresponding instantaneous value of c is given. But it would become necessary to prorate the value of the global radiation, because global radiation values are given in terms of an hourly value. Therefore, unless the instantaneous global radiation values are given, it becomes necessary to prorate the hourly value. Such prorating, however, is likely to be fraught with many difficulties. Even the simplest form of prorating, dividing the global radiation by 60 to obtain the instantaneous value, implicitly assumes a constant value for cloudiness. The two approaches thus encounter the same problem.

A second problem concerns the albedo-absorption-transmission characteristics of individual cloud-types. This study assumes that these properties are constant for a given cloud-type. There are a large number of both theoretical and observational studies which illustrate that this is not quite realistic. FIG. 25 illustrates the case for St and Sc clouds. For a given cloud-type both absorption and cloud albedo increase with increasing cloud thickness. This is thus a recognizable source of variation in G^*/G_o^* when examined in terms of cloudiness. To correct this situation it would be desirable to know the statistical relationship between the scattering parameters and cloud thickness. Unfortunately, these relationships are not very well established. Clouds of horizontal extent are the most frequently used models: little is known of high clouds, such as Cirrus clouds, or of clouds of vertical extent.

A third aspect concerns the problem of cloud stratification. The methodology employed in this study assumes that, even though there may be more than one cloud-type present, the cloud medium could be treated as a single layer. This assumption as well is not quite realistic. It is observed that clouds are stratified, sometimes up to 4 or 5 layers. Among other consequences, such stratification may substantially increase the top albedo through increased multiple reflections occurring between the various layers and/or altering the absorption relations in the lowest layers.

The absolute accuracy of this study's application of climatonomy is thus in doubt. It is certainly dependent upon the accuracy of several assumptions that have been utilized to expedite the research. And doubtless better estimates of the climatology of multiply reflected global radiation

Figure 25

ALBEDO OF STRATUS AND STRATO-CUMULUS CLOUDS
AS A FUNCTION OF CLOUD THICKNESS

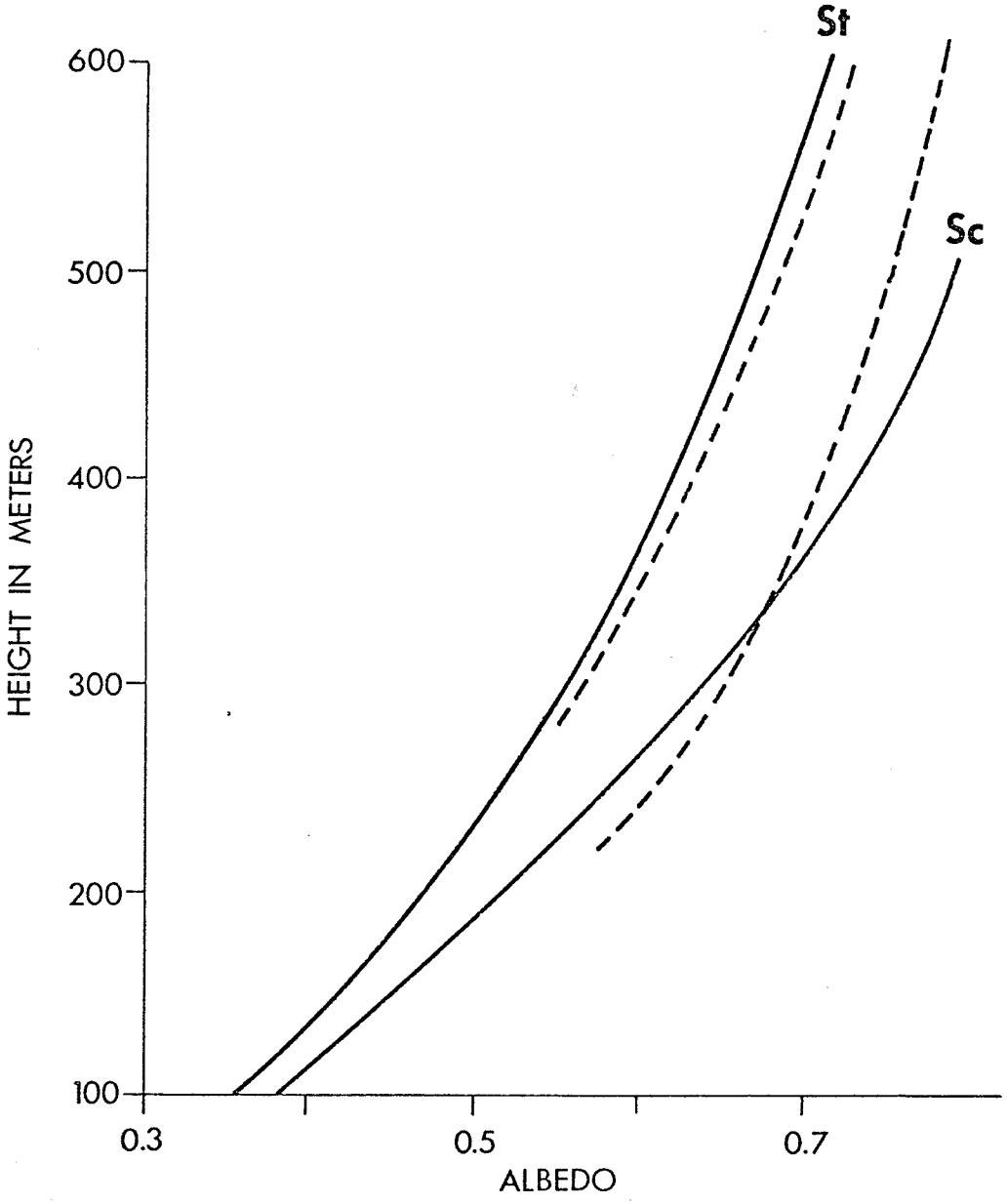

Solid curves refer to calculations by Feigel'son (1966, op.cit.)

Dashed curve refers to measurements by Chel'tsov

From: Feigel'son, 1966, op.cit.

will be obtained when successively better approximations or even direct measurement or evaluation of the attenuating processes can be performed. It is comforting to observe, however, that, as crude as our application of climatonomy has been, many results are inaccord with both theory and observation.

CHAPTER VI

SUMMARY AND CONCLUSIONS

Applying climatonomy to calculate the intensification ratio, G^*/G^*_o, illustrates that a number of theoretical and statistical and/or observational evidence is substantiated. Thus, the intensification ratio is observed to be a maximum over a snow-covered surface and a minimum over a snow-free surface regardless of atmospheric conditions.

The calculated (mean) backscatterances agree, in the main, with the theoretical prediction that they should increase with clouds of increasing opacity. The major exception is the case of Cirrus clouds.

The intensification ratio is a minimum for the case of cloudless sky, as predicted by theory. Maximum intensification ratios occur with very small amounts of cloudiness, and not with total overcast as was thought in Chapter I. The computed values, when examined as a function of the sun's zenith angle generally conform to the theoretical prediction that they should decrease with decreasing zenith angle. When the intensification ratio is examined as a function of both type and degree of cloudiness no general trend is evidenced and the relations between intensification and cloudiness remain rather complex. It may hardly be expected, therefore, that any definitive relations between global radiation receipt and cloudiness can be advanced. Thus the results of empirical studies of global radiation receipt in relation to cloudiness, such as by Haurwitz[83], and Vowinckel and Orvig[84], and others

---

83. Haurwitz, 1945, op. cit.
84. Vowinckel, E., and Orvig, S., 1962: Relation between Solar Radiation Income and Cloud Type in the Arctic, J. Appl. Meteor., V. 1, pp.552-559.

are readily undertandable.

There were two rather unexpected results. The first concerns the increase in magnitude of the intensification ratio with increasing opacity after a secondary minimum at opacity $\simeq$ 5-8. This feature illustrates that with increasing cloudiness the effect of density does become rather important, as Haurwitz has pointed out. The second unexpected result was the finding of rather high intensification ratios, and consequently, backscatterances, associated with Cirrus clouds. The result is surprising especially since Cirrus clouds are the optically thinest clouds.

For the station under consideration then, the climatology of multiply reflected global radiation might be described as follows. During winter a number of factors conspire to produce maximum intensification of global radiation at the earth's surface: a generally high surface albedo due to a snow surface, low absorption both by the surface, because of the high albedo, and by the atmosphere, because of the generally low water vapor concentration at this time of year, and a large mean solar zenith angle, because of the station's latitudinal position. During the summer all these tendencies are reversed producing minimum intensification of global radiation.

Finally, with regard to the statistical problem of (relative) global radiation receipts in relation to the (relative) duration of sunshine, no firm conclusions can be drawn. Certainly, previous research is correct in defining the snow-melt period as a critical changeover event. This study suggests, however, that $\hat{b}$ should be a maximum during winter and a minimum during the summer months, the reverse of what has been found through regression analysis. Our reasoning for this type of regime, however, might be fallacious since a major portion of the

variation in the intensification ratio during the period of snow-cover is attributed to variations in cloudiness, when in fact, it may also be due to differences in attenuation. In this event, the effect of cloudiness may be the same for any time of the year. Unfortunately, the question of the accuracy of the computations is in doubt and thus imposes a rather severe restriction on the employement of extensive statistical analyses. Moreover, it proved impossible to calculate the regression constants for this station, since the required data was not available. And consequently, no firm conclusions can be drawn.

This study suggests several avenues for further research. There is first a need to determine aerosol and atmospheric absorption more definitively, both with respect to the absolute magnitude and the temporal variations at a location. Obviously, the absorption ratio is a prime factor in climatic differentiation. This study points to the necessity of a fuller understanding of it.

Closely allied to the above problem is the necessity for a greater understanding of the ratio α/σ, not only with respect to cloud-free and cloudy atmospheres, but in geographical terms as well.

Finally, there is a need to more fully ascertain the statistical relationships between scattering-absorption parameters and cloudiness, especially in terms of height-thickness-density characteristics and to other features such as cloud stratification.

* * * * *

APPENDIX I

This appendix summarizes the computer programming necessary for the evaluation of (mid) hourly optical air mass values and hourly extra-terrestrial solar radiation flux values.

The programme is fairly simple, especially with regard to input data. Only three variables are required; i - daily values of solar declination in degrees (in decimal form); ii - daily values of the earth's radius vector; iii - daily values of the equation of time in degrees (in decimal form).

The local mean solar time must be supplied for the station. The programme then calculates the true solar time and then obtains the mid-hourly zenith angle and begins calculations for 13:00h. local apparent time, and continues thus for each complete hour before sunset. Hence, the time since the last full hour and sunset is not included. Only a few statements would be required to include these part hours.

The programme includes as output several parameters although only 2 are of interest. This was done for purposes of internal checking only. Only slight adjustmensts to the print statement are required to delete these extraneous output.

The programme was written for the IBM 365 computer using FORTRAN IV with the WATFIV compiler.

```
C       THIS IS A PROGRAMME TO CALCULATE THE HOURLY EXTRA-TERRESTRIAL
C       SOLAR RADIATION FLUX AT NORTH LATITUDE 43 DEGREES, 48 MINUTES.
        REAL L, MIDHRA
        L = 0.76445
100     READ 2, DATE, R, DIFF
C       DATE = SOLAR DECLINATION IN DEGREES, R = RADIUS VECTOR,
C       DIFF = EQUATION OF TIME IN DEGREES
2       FORMAT(3F10.5)
        IF(R.EQ.0) GO TO 101
C       THE LAST CARD OF THE DATA DECK SHOULD HAVE R = 0.00000. THIS
C       IS A STOPPER CARD.
        SOLARN = -0.06981 + (DIFF/57.29577)
C       SOLARN = SOLAR NOON. MULTIPLICATION OR DIVISION  BY THE
C       FACTOR 57.29577 IS THE CONVERSION FACTOR FOR CHANGING
C       DEGREES TO RADIANS OR VICE VERSA.
        SD = DATE/57.29677
C       SD = SOLAR DECLINATION
        SINT = SIN(L)*SIN(SD)
        COST = COS(L)*COS(SD)
        S = -TAN(L)*TAN(SD)
        Y = ARCOS(S)
        SUNSET = (Y * 57.29577)/15.
        MIDHRA = SOLARN + 0.13090
C       MIDHRA = MID-HOUR ANGLE
5       Z = SINT + COST(COS(MIDHRA))
C       Z = THE COSINE OF THE MID- HOUR ANGLE
        Q = (( 1.98 * Z)/ R*R) * 60.
C       Q IS THE EXTRA-TERRESTRIAL SOLAR RADIATION FLUX FOR THAT HOUR
        T = (MIDHRA * 57.29577)/15.
C       T IS THE TIME IN HOURS
        ZENITH = ( ARCOS(Z) * 57.29577)
```

```
      PRINT8, SD, SUNSET, T, ZENITH, Q
8     FORMAT(' ', F10.5,5X,F7.5,5X,F7.5,5X,F10.5,5X,F6.2)
      MIDHRA = MIDHRA + 0.26180
      IF( MIDHRA.LE.Y - 0.13090) GO TO 5
      GO TO 100
101   STOP
      END
$ENTRY
```

****

TIME	EXTRA-TERRESTRIAL SOLAR RADIATION, Q. / MID-HOURLY OPTICAL AIR MASS, M } FOR HOUR ENDING AT All times are local apparent times; Q in langleys							
DATE	13:00 12:00	14:00 11:00	15:00 10:00	16:00 9:00	17:00 8:00	18:00 7:00	19:00 6:00	20:00 5:00
Jan 1	47 2.55	43 2.77	34 3.39	21 5.60				
Jan 2	47 2.55	43 2.77	35 3.39	21 5.60				
Jan 3	47 2.55	43 2.77	35 3.39	21 5.60				
Jan 4	47 2.55	44 2.65	35 3.39	22 5.12				
Jan 5	47 2.55	44 2.65	35 3.39	22 5.12				
Jan 6	48 2.45	44 2.65	36 3.39	22 5.12				
Jan 7	48 2.45	44 2.65	36 3.21	23 5.12				
Jan 8	48 2.45	45 2.65	36 3.21	23 5.12				
Jan 9	48 2.45	45 2.65	36 3.21	23 5.12				
Jan 10	49 2.45	45 2.65	37 3.21	24 5.12				
Jan 11	49 2.45	46 2.55	37 3.21	24 4.72				
Jan 12	49 2.45	46 2.55	37 3.21	24 4.72				

DATE	13:00 12:00	14:00 11:00	15:00 10:00	16:00 9:00	17:00 8:00	18:00 7:00	19:00 6:00	20:00 5:00
Jan 13	49 2.36	46 2.55	38 3.05	25 4.72				
Jan 14	50 2.36	47 2.55	38 3.05	25 4.72				
Jan 15	50 2.36	47 2.55	39 3.05	25 4.72				
Jan 16	50 2.36	47 2.45	39 3.05	26 4.37				
Jan 17	51 2.39	48 2.45	39 3.05	26 4.37	10 10.39			
Jan 18	51 2.27	48 2.45	40 2.90	27 4.37	10 10.39			
Jan 19	52 2.27	49 2.45	40 2.90	27 4.37	11 10.39			
Jan 20	52 2.27	49 2.45	41 2.90	28 4.37	11 10.39			
Jan 21	52 2.27	49 2.36	41 2.90	28 4.07	11 10.39			
Jan 22	53 2.27	50 2.36	42 2.77	29 4.07	12 8.90			
Jan 23	53 2.19	50 2.36	42 2.77	29 4.07	12 8.90			
Jan 24	54 2.19	51 2.36	42 2.77	29 4.07	13 8.90			
Jan 25	54 2.19	51 2.36	43 2.77	30 3.82	13 8.90			
Jan 26	55 2.19	52 2.27	43 2.77	30 3.82	13 8.90			
Jan 27	55 2.12	52 2.27	44 2.65	31 3.82	14 7.77			
Jan 28	56 2.12	53 2.27	44 2.65	31 3.82	15 7.77			
Jan 29	56 2.12	53 2.19	45 2.65	32 3.59	15 7.77			

DATE	13:00 12:00	14:00 11:00	15:00 10:00	16:00 9:00	17:00 8:00	18:00 7:00	19:00 6:00	20:00 5:00
Jan 30	56 2.12	54 2.19	45 2.65	32 3.59	15 7.77			
Jan 31	57 2.06	55 2.19	46 2.55	33 3.59	16 6.88			
Feb 1	57 2.06	55 2.19	47 2.55	33 3.59	17 6.88			
Feb 2	58 2.06	55 2.19	47 2.55	34 3.59	17 6.88			
Feb 3	59 2.00	56 2.12	48 2.45	34 3.39	17 6.88			
Feb 4	59 2.00	56 2.12	48 2.45	35 3.39	18 6.88			
Feb 5	60 2.00	57 2.06	49 2.45	35 3.39	18 6.18			
Feb 6	60 2.00	57 2.06	49 2.45	36 3.39	19 6.18			
Feb 7	61 1.94	58 2.06	50 2.36	36 3.21	19 6.18			
Feb 8	61 1.94	58 2.06	50 2.36	37 3.21	20 5.60			
Feb 9	62 1.94	59 2.00	51 2.36	38 3.21	20 5.60			
Feb 10	62 1.88	60 2.00	51 2.27	38 3.05	21 5.60			
Feb 11	63 1.88	60 2.00	52 2.27	39 3.05	21 5.60			
Feb 12	64 1.88	61 1.94	52 2.27	39 3.05	22 5.12			
Feb 13	64 1.83	61 1.94	53 2.27	40 3.05	22 5.12			
Feb 14	65 1.83	62 1.94	53 2.19	40 2.90	23 5.12			
Feb 15	65 1.83	62 1.88	54 2.19	41 2.90	23 5.12			
Feb 16	66 1.78	63 1.88	55 2.19	41 2.90	24 4.72			

DATE	13:00 12:00	14:00 11:00	15:00 10:00	16:00 9:00	17:00 8:00	18:00 7:00	19:00 6:00	20:00 5:00
Feb 17	66 1.78	64 1.88	55 2.12	42 2.77	25 4.72			
Feb 18	67 1.78	64 1.83	56 2.12	42 2.77	25 4.72			
Feb 19	68 1.74	65 1.83	56 2.12	43 2.77	26 4.72			
Feb 20	68 1.74	65 1.83	57 2.06	44 2.65	26 4.37			
Feb 21	69 1.74	66 1.78	58 2.06	44 2.65	27 4.37			
Feb 22	69 1.70	67 1.78	58 2.06	45 2.65	27 4.37			
Feb 23	70 1.70	67 1.78	59 2.00	45 2.65	28 4.37			
Feb 24	71 1.66	68 1.74	59 2.00	46 2.55	28 4.07			
Feb 25	71 1.66	68 1.74	60 2.00	46 2.55	29 4.07			
Feb 26	72 1.66	69 1.74	60 1.94	47 2.55	29 4.07			
Feb 27	73 1.62	70 1.70	61 1.94	47 2.45	30 3.82			
Feb 28	73 1.62	70 1.70	62 1.94	48 2.45	30 3.82			
Mar 1	74 1.62	71 1.66	62 1.88	49 2.45	31 3.82			
Mar 2	74 1.59	71 1.66	63 1.88	49 2.45	31 3.82			
Mar 3	75 1.59	72 1.66	63 1.88	50 2.36	32 3.59	11 10.39		
Mar 4	76 1.55	73 1.62	64 1.83	50 2.36	32 3.59	12 8.90		
Mar 5	76 1.55	73 1.62	64 1.83	51 2.36	33 3.59	12 8.90		
Mar 6	77 1.55	74 1.62	65 1.83	51 2.36	33 3.59	13 8.90		

DATE	13:00 12:00	14:00 11:00	15:00 10:00	16:00 9:00	17:00 8:00	18:00 7:00	19:00 6:00	20:00 5:00
Mar 7	77 1.52	74 1.59	65 1.83	52 2.27	34 3.39	13 8.90		
Mar 8	78 1.52	75 1.59	66 1.78	52 2.27	34 3.39	14 7.77		
Mar 9	79 1.52	75 1.59	67 1.78	53 2.27	35 3.39	14 7.77		
Mar 10	79 1.49	76 1.55	67 1.78	53 2.19	35 3.39	14 7.77		
Mar 11	80 1.49	77 1.55	68 1.74	54 2.19	36 3.21	15 7.77		
Mar 12	81 1.46	77 1.52	68 1.74	54 2.19	36 3.21	16 6.88		
Mar 13	81 1.46	78 1.52	69 1.74	55 2.12	37 3.21	16 6.88		
Mar 14	82 1.46	78 1.52	69 1.70	55 2.12	37 3.21	16 6.88		
Mar 15	82 1.44	79 1.48	70 1.70	56 2.12	38 3.05	17 6.88		
Mar 16	83 1.44	79 1.48	70 1.70	56 2.12	38 3.05	18 6.88		
Mar 17	83 1.41	80 1.48	71 1.66	57 2.06	39 3.05	18 6.18		
Mar 18	84 1.41	80 1.46	71 1.66	57 2.06	39 3.05	18 6.18		
Mar 19	85 1.41	81 1.46	72 1.66	58 2.06	40 2.90	19 6.18		
Mar 20	85 1.39	82 1.46	73 1.62	58 2.06	40 2.90	19 6.18		
Mar 21	86 1.39	82 1.44	73 1.62	59 2.00	41 2.90	20 5.60		
Mar 22	86 1.37	83 1.44	73 1.62	59 2.00	41 2.90	20 5.60		
Mar 23	87 1.37	83 1.44	74 1.59	60 2.00	42 2.77	21 5.60		
Mar 24	87 1.37	84 1.41	74 1.59	60 2.00	42 2.77	21 5.60		

DATE	13:00 12:00	14:00 11:00	15:00 10:00	16:00 9:00	17:00 8:00	18:00 7:00	19:00 6:00	20:00 5:00
Mar 25	88 1.34	84 1.41	75 1.59	61 1.94	42 2.77	22 5.60		
Mar 26	88 1.34	85 1.39	75 1.59	61 1.94	43 2.77	22 5.12		
Mar 27	89 1.34	85 1.39	76 1.55	62 1.94	44 2.65	23 5.12		
Mar 28	90 1.32	86 1.39	76 1.55	62 1.94	44 2.65	23 5.12		
Mar 29	90 1.32	86 1.37	77 1.55	63 1.88	44 2.65	23 5.12		
Mar 30	91 1.30	87 1.37	77 1.52	63 1.88	45 2.65	24 4.72		
Mar 31	91 1.30	87 1.37	75 1.52	63 1.88	45 2.65	24 4.72		
Apr 1	92 1.28	88 1.34	78 1.52	64 1.83	46 2.55	25 4.72		
Apr 2	92 1.28	88 1.34	79 1.49	64 1.83	46 2.55	25 4.72		
Apr 3	93 1.28	89 1.34	79 1.49	65 1.83	46 2.55	25 4.72		
Apr 4	93 1.27	89 1.32	80 1.49	65 1.83	47 2.55	26 4.37		
Apr 5	94 1.27	90 1.32	80 1.49	66 1.78	47 2.45	26 4.37		
Apr 6	94 1.27	90 1.32	81 1.46	66 1.78	48 2.45	27 4.37		
Apr 7	94 1.25	90 1.30	81 1.46	66 1.78	48 2.45	27 4.37		
Apr 8	95 1.25	91 1.30	81 1.46	67 1.78	49 2.45	28 4.37		
Apr 9	95 1.25	91 1.30	82 1.44	67 1.74	49 2.45	28 4.07		
Apr 10	96 1.23	92 1.28	82 1.44	68 1.74	49 2.45	28 4.07		
Apr 11	96 1.23	92 1.28	83 1.44	68 1.74	50 2.36	29 4.07		

DATE	13:00 12:00	14:00 11:00	15:00 10:00	16:00 9:00	17:00 8:00	18:00 7:00	19:00 6:00
Apr 12	97 1.22	93 1.28	83 1.44	69 1.74	50 2.36	29 4.07	
Apr 13	97 1.22	93 1.27	83 1.41	69 1.70	51 2.36	30 3.82	
Apr 14	98 1.22	93 1.27	84 1.41	69 1.70	51 2.27	30 3.82	
Apr 15	98 1.20	94 1.27	84 1.41	70 1.70	51 2.27	30 3.82	
Apr 16	98 1.20	94 1.27	85 1.41	70 1.70	52 2.27	31 3.82	
Apr 17	99 1.20	95 1.25	85 1.39	71 1.70	52 2.27	31 3.82	
Apr 18	99 1.19	95 1.25	85 1.39	71 1.66	52 2.27	32 3.82	
Apr 19	100 1.19	95 1.25	86 1.39	71 1.66	53 2.27	32 3.59	
Apr 20	100 1.19	96 1.23	86 1.39	72 1.66	53 2.19	32 3.59	
Apr 21	100 1.18	96 1.23	86 1.37	72 1.66	54 2.19	33 3.59	11 10.39
Apr 22	101 1.18	96 1.23	87 1.37	72 1.62	54 2.19	33 3.59	12 8.90
Apr 23	101 1.18	97 1.22	87 1.37	73 1.62	54 2.19	34 3.59	12 8.90
Apr 24	101 1.17	97 1.22	87 1.37	73 1.62	55 2.19	35 3.39	12 8.90
Apr 25	102 1.17	97 1.22	88 1.34	73 1.62	55 2.12	35 3.39	13 8.90
Apr 26	102 1.17	98 1.22	88 1.34	74 1.62	56 2.12	35 3.39	13 8.90
Apr 27	102 1.15	98 1.20	88 1.34	74 1.59	56 2.12	35 3.39	14 7.77
Apr 28	103 1.15	98 1.20	89 1.34	74 1.59	56 2.12	36 3.39	14 7.77
Apr 29	103 1.15	99 1.20	89 1.34	74 1.59	56 2.12	36 3.21	14 7.77

DATE	13:00 12:00	14:00 11:00	15:00 10:00	16:00 9:00	17:00 8:00	18:00 7:00	19:00 6:00
Apr 30	103 1.14	99 1.20	89 1.32	75 1.59	57 2.06	36 3.21	15 7.77
May 1	104 1.14	99 1.18	89 1.32	75 1.59	57 2.06	37 3.21	15 7.77
May 2	104 1.14	100 1.18	90 1.32	76 1.59	57 2.06	37 3.21	15 7.77
May 3	104 1.14	100 1.18	90 1.32	76 1.55	58 2.06	37 3.21	16 6.88
May 4	105 1.13	100 1.18	91 1.30	76 1.55	58 2.06	38 3.05	16 6.88
May 5	105 1.13	101 1.18	91 1.30	77 1.55	59 2.00	38 3.05	17 6.88
May 6	105 1.13	101 1.18	91 1.30	77 1.55	59 2.00	38 3.05	17 6.88
May 7	105 1.12	101 1.18	91 1.30	77 1.52	59 2.00	39 3.05	17 6.88
May 8	106 1.12	101 1.18	92 1.30	77 1.52	59 2.00	39 3.05	17 6.88
May 9	106 1.12	102 1.17	92 1.28	77 1.52	60 2.00	39 3.05	18 6.18
May 10	106 1.12	102 1.17	92 1.28	78 1.52	60 2.00	40 3.05	18 6.18
May 11	106 1.11	102 1.17	92 1.28	78 1.52	60 2.00	40 2.90	19 6.18
May 12	107 1.11	102 1.17	93 1.28	78 1.52	60 1.94	40 2.90	19 6.18
May 13	107 1.11	102 1.15	93 1.28	79 1.52	61 1.94	41 2.90	19 6.18
May 14	107 1.11	103 1.15	93 1.27	79 1.49	61 1.94	41 2.90	20 5.60
May 15	107 1.10	103 1.15	93 1.27	79 1.49	61 1.94	41 2.90	20 5.60
May 16	108 1.10	103 1.15	94 1.27	79 1.49	62 1.94	41 2.90	20 5.60
May 17	108 1.10	103 1.15	94 1.27	80 1.49	62 1.94	42 2.77	21 5.60

DATE	13:00 12:00	14:00 11:00	15:00 10:00	16:00 9:00	17:00 8:00	18:00 7:00	19:00 6:00
May 18	108 1.10	104 1.14	94 1.27	80 1.49	62 1.88	42 2.77	21 5.60
May 19	108 1.09	104 1.14	94 1.27	80 1.49	62 1.88	42 2.77	21 5.60
May 20	108 1.09	104 1.14	94 1.25	80 1.46	63 1.88	43 2.77	22 5.60
May 21	108 1.09	104 1.14	95 1.25	81 1.46	63 1.88	43 2.77	22 5.12
May 22	109 1.09	104 1.13	95 1.25	81 1.46	63 1.88	43 2.77	23 5.12
May 23	109 1.09	105 1.13	95 1.25	81 1.46	64 1.88	44 2.65	23 5.12
May 24	109 1.09	105 1.13	95 1.25	81 1.46	64 1.83	44 2.65	23 5.12
May 25	109 1.09	105 1.13	95 1.25	82 1.46	64 1.83	44 2.65	23 5.12
May 26	109 1.09	105 1.13	96 1.23	82 1.46	64 1.83	44 2.65	24 5.12
May 27	109 1.09	105 1.13	96 1.23	82 1.44	64 1.83	45 2.65	24 4.72
May 28	110 1.09	105 1.13	96 1.23	82 1.44	65 1.83	45 2.65	24 4.72
May 29	110 1.09	105 1.12	96 1.23	82 1.44	65 1.83	45 2.65	24 4.72
May 30	110 1.08	106 1.12	96 1.23	82 1.44	65 1.83	45 2.65	24 4.72
May 31	110 1.08	106 1.12	96 1.23	83 1.44	65 1.83	45 2.65	25 4.72
Jun 1	110 1.08	106 1.12	97 1.23	83 1.44	66 1.78	46 2.55	25 4.37
Jun 2	110 1.08	106 1.12	97 1.22	83 1.44	66 1.78	46 2.55	25 4.37
Jun 3	110 1.08	106 1.12	97 1.22	83 1.44	66 1.78	46 2.55	26 4.37
Jun 4	110 1.08	106 1.12	97 1.22	83 1.41	66 1.78	46 2.55	26 4.37

DATE	13:00 12:00	14:00 11:00	15:00 10:00	16:00 9:00	17:00 8:00	18:00 7:00	19:00 6:00
Jun 5	110 1.08	106 1.11	97 1.22	83 1.41	66 1.78	47 2.55	26 4.37
Jun 6	111 1.07	106 1.11	97 1.22	84 1.41	66 1.78	47 2.55	26 4.37
Jun 7	111 1.07	107 1.11	97 1.22	84 1.41	67 1.78	47 2.55	27 4.37
Jun 8	111 1.07	107 1.11	98 1.22	84 1.41	67 1.78	47 2.55	27 4.37
Jun 9	111 1.07	107 1.11	98 1.22	84 1.41	67 1.78	47 2.55	27 4.37
Jun 10	111 1.07	107 1.11	98 1.22	84 1.41	67 1.78	47 2.45	27 4.37
Jun 11	111 1.07	107 1.11	98 1.22	84 1.41	67 1.78	48 2.45	27 4.37
Jun 12	111 1.07	107 1.11	98 1.20	85 1.41	67 1.74	48 2.45	27 4.37
Jun 13	111 1.07	107 1.11	98 1.20	85 1.41	68 1.74	48 2.45	28 4.37
Jun 14	111 1.07	107 1.11	98 1.20	85 1.41	68 1.74	48 2.45	28 4.37
Jun 15	111 1.07	107 1.11	98 1.20	85 1.41	68 1.74	48 2.45	28 4.37
Jun 16	111 1.07	107 1.11	98 1.20	85 1.41	68 1.74	48 2.45	28 4.07
Jun 17	111 1.07	107 1.11	98 1.20	85 1.39	68 1.74	48 2.45	28 4.07
Jun 18	111 1.07	107 1.10	98 1.20	85 1.39	68 1.74	49 2.45	28 4.07
Jun 19	111 1.07	107 1.10	98 1.20	85 1.39	68 1.74	49 2.45	28 4.07
Jun 20	111 1.07	107 1.10	98 1.20	85 1.39	68 1.74	49 2.45	28 4.07
Jun 21	111 1.07	108 1.10	99 1.20	85 1.39	68 1.74	49 2.45	29 4.07
Jun 22	111 1.07	108 1.10	99 1.20	85 1.39	68 1.74	49 2.45	29 4.07

DATE	13:00 12:00	14:00 11:00	15:00 10:00	16:00 9:00	17:00 8:00	18:00 7:00	19:00 6:00
Jun 23	111 1.07	108 1.10	99 1.20	85 1.39	68 1.74	49 2.45	29 4.07
Jun 24	111 1.07	108 1.10	99 1.20	85 1.39	68 1.74	49 2.45	29 4.07
Jun 25	111 1.07	108 1.10	99 1.20	85 1.39	68 1.74	49 2.45	29 4.07
Jun 26	111 1.07	108 1.10	99 1.20	85 1.39	69 1.74	49 2.36	29 4.07
Jun 27	111 1.07	108 1.10	99 1.20	86 1.39	69 1.74	49 2.36	28 4.07
Jun 28	111 1.07	108 1.10	99 1.20	85 1.39	69 1.74	49 2.45	29 4.07
Jun 29	111 1.07	108 1.10	99 1.20	85 1.39	69 1.74	49 2.45	29 4.07
Jun 30	111 1.07	107 1.10	99 1.20	85 1.39	68 1.74	49 2.45	29 4.07

* * * * *

APPENDIX II

This appendix summarizes the computer programme that was utilized to calculate the hourly intensification ratio. It was written for the IBM 365 computer using FORTRAN IV with the WATFIV compiler. The programme assumes a three-layer cloud model. For each cloud layer there must be supplied: N_i - the cloud amount, which must be in integer form; B_i - the absorption coefficient for that cloud-type; and L_i - the corresponding cloud albedo. If any of these values are zero, leave blank. For the last variable on the punch card (i.e., the variable 'I') the value is 1 (one) for the last hour of the day; all other hourly values are zero, or leave blank. Finally, the last card of the data deck has DATE = 000000. This is a stopper card. Input of total cloudiness, K, must be in integer form. All other variables for input are as defined in the text.

```
      REAL M, MCOR, N1, N2, N3, L1, L2, L3
      INTEGER OP, DATE
      SUM = 0.
      KOUNT = 0
2     READ5,DATE,K,Q,G,R,D,OP,TD,K1,B1,L1,K2,B2,L2,K3,B3,L3,M,P,PO,I
5     FORMAT(I6,I2,4F4.0,I2,F4.0,3(I2,2F3.2),F5.2,2F6.1,I1)
      IF (DATE.EQ.0) GO TO 7
      A = R/G
      GSTAR = G/Q
      WSTAR = 2.54*(.14063 + .0046751*TD + .0001608*(TD**2))
      MCOR = M*(P/PO)
      ALPHAW = .104*((WSTAR*MCOR)**.276)
      ALPHAO = 2.0*ALPHAW
      C = K/10
```

```
      N1 = K1/10.
      N2 = K2/10.
      N3 = K3/10.
      IF ( C ) 6,6,9
C     PROGRAMME FOR CALCULATIONS IN CLEAR SKY
6     SIGMA = .75*ALPHAW
      H = .375
      GRATIO = 1./(1. - (A*H*SIGMA*(1. - ALPHAO)))
      BACKSC = (1. - (1./GRATIO))/A
1     PRINT8, DATE, K, OP, A, BACKSC, GRATIO
8     FORMAT(' ', I6,5X,2(I2, 5X), 2(F5.3, 5X), F8.3)
      GO TO 40
C     CALCULATIONS FOR CLOUDY ATMOSPHERE
9     ALPHAC = N1*B1 + N2*B2 + N3*B3
      ALPHA = ALPHAO + ALPHAC
      AP = N1*L1 + N2*L2 + N3*L3
      GRATIO = 1./(1. - A + A*C*(1. - AP + ALPHA*AP))
      BACKSC = (1. - (1./GRATIO))/A
      GO TO 1
40    IF (I.LE.1) SUM = SUM + GRATIO
      IF (I.LE.1) KOUNT = KOUNT + 1
      IF (I.EQ.0) GO TO 2
      IF (I.EQ.1) AVG = SUM/KOUNT
      PRINT 38, AVG
38    FORMAT(' ',F5.2)
      SUM = 0.
      KOUNT = 0
      GO TO 2
7     STOP
      END
$ENTRY
```

* * * * * * *

(Note: The value of AVG is the daily mean value of the intensification ratio)

BIBLIOGRAPHY

Ångström, A., 1925: Solar and Terrestrial Radiation, Quart. J. Roy. Meteor. Soc., V. 50, pp. 121-126.

_____, 1929: On the Atmospheric Transmission of Sun Radiation and on Dust in the Air (I), Geography. Ann., V. 12(1), pp. 156-166.

_____, 1929(b): On the Atmospheric Transmission of Sun Radiation(II), Geography. Ann., V. 12(2), pp. 130-158.

_____, 1970: On Determinations of the Atmospheric Turbidity and their Relation to Pyrheliometric Measurements, Advances in Geophysics, V. 16, (Ch. 9) pp. 269-284.

_____, and Tryselius, O., 1934: Total Radiation from Sun and Sky at Abisko, Geography. Ann., V. 16, pp. 53-69.

Atwater, M.A., 1970: Planetary Albedo Changes Due to Aerosols, Science, V. 1, pp. 64-66.

_____, 1971: The Radiation Budget for Polluted Layers of Urban Environment, J. Appl. Meteor., V. 10, pp. 205-214.

Bennett, I., 1965: A Method for Preparing Maps of Mean Daily Global Radiation, Arch. Met. Geophys. Biokl., Ser. B, V. 13, pp. 216-248.

Black, J.N., Bonython, C.W., and Prescott, J.A., 1954: Solar Radiation and the Duration of Sunshine, Quart. J. Roy. Meteor. Soc., V. 80, pp. 231-235.

Budyko, M.I., 1956: The Heat Balance of the Earth's Surface (Trans. from the Russian by N.A. Stepanova, U.S. Dept. of Commerce, Washington, D.C., 1958), Gidrometeorologicheskoe Izdatel'stvo (GMIZ), Leningrad, 1956.

_____, 1969: The Effect of Solar Radiation Variations on the Climate of the Earth, Tellus, V. 21, 611-619.

Bullrich, K., 1964: Scattered Radiation in the Atmosphere, Advances in Geophysics, V. 10, pp. 99-260.

Catchpole, A.J.W., and Moodie, W., 1971: Multiple Reflection in Arctic Regions, Weather, V. 26(4), pp. 157-163.

Chandrasekhar, S., 1950: Radiative Transfer, Clarendon Press, Oxford.

Charlson, R.J., Ahlquist, N.C., and Horvath, H., 1968: On the Generality of Correlation of Atmospheric Aerosol Mass Concentration and Light Scatter, Atmos. Envir., V. 2, pp. 455-464.

Danielson, R.E., Moore, D.R., and van de Hulst, H.L., 1968: The Rransfer of Visible Radiation Through Clouds, J. Atmos. Sci., V. 26, pp. 1078-1087.

Dave, J.V., and Sekera, Z., 1959: Effect of Ozone on the Total Sky and Global Radiation, J. Meteor., V. 16, pp. 211-212.

Deirmendjian, D., and Sekera, Z., 1954: Global Radiation Resulting from Multiple Scattering in a Rayleigh Atmosphere, Tellus, V. 6, pp. 382-398.

Dreidger, H.L., 1969: An Analysis of the Relationship between Total Daily Solar Radiation Receipt and Total Daily Duration of Sunshine at Winnipeg, 1950-1967. Unpublished M.A. Thesis, University of Manitoba, Winnipeg, Canada.

_____, and Catchpole, A.J.W., 1970: Estimation of Solar Radiation Receipt from Sunshine Duration at Winnipeg, Meteor. Mag., V. 99, pp. 285-291.

Feigel'son, E.M., Malchevich, M.S., Kogan, S. Ya., Koronotova, T.D., Glazova, K.S., and Kutznetsova, M.A., 1960: Calculations of the Brightness of Light in the Case of Anisotropic Scattering, Part 1, (Trans. from the Russian), Consult. Bureau, New York.

Feigel'son, E.M., 1964: Light and Heat Radiation in Stratus Clouds, (Trans. from the Russian by IPST, Jerusalem, 1966), GMIZ, Leningrad, 244 pp.

Fischer, K., 1970: Measurements of Absorption of Visible Radiation by Aerosol Particles, Atmos. Physics, V. 43, pp. 244-254.

Fowle, F.E., 1915: Astrophysics Journal, V. 42

Fritz, S., 1950: Measurements of the Albedo of Clouds, Bull. Amer. Meteor. Soc., V. 31(1).

_____, 1951: Solar Radiant Energy and its Modifications by the Earth and its Atmosphere, in Compendium of Meteorology, American Meteorological Society, Boston, Mass., pp. 13-50.

_____, 1954: Scattering of Solar Energy by Clouds of 'Large Drops', J. Meteor., V. 11, pp. 291-300.

_____, 1955: Illuminance and Luminance under Overcast Skies, J. Opt. Soc. Amer., V. 45(10), pp. 820-825.

_____, and McDonald, T.H., 1949: Average Solar Radiation in the United States, Heating and Ventillating, V. 46(7), pp. 61-64.

_____, and _____, 1951: Measurements of Absorption of Solar Radiation by Clouds, Bull. Amer. Meteor. Soc., V. 32(6).

Gibbons, M.G., Langbridge, F.I., Nichols, I. R., and Rudkin, R.L., 1961: Transmission and Scattering Properties of the Nevada Desert Atmosphere, J. Opt. Soc. Amer., V. 51, pp. 6.

Glover, J., and McCulloch, 1958(a): The Empirical Relation between Solar Radiation and Hours of Bright Sunshine in the High Altitude Tropics, Quart. J. Roy. Meteor. Soc., V. 84, pp. 56 - 60.

_____, and _____, 1958(b): The Empirical Relation between Solar Radiation and Hours of the Bright Sunshine, Quart. J. Roy. Meteor. Soc., V. 84, pp. 172-175.

Goldberg, L., 1958: The Absorption Spectrum of the Atmosphere,(Ch. 9), pp. 434-490 in The Earth as a Planet, G.P. Kuiper (ed.), The University of Chicago Press, Chicago, 751 pp.

Haltiner, G.J., 1971: Numerical Weather Prediction, Wiley and Sons, Inc., New York, 470 pp.

_____, and Martin, F.L., 1957: Dynamical and Physical Meteorology, McGraw Hill, New York, 470 pp.

Hamon, R.W., Weiss, L.L., and Wilson, W.T., 1954: Insolation as an Empirical Function of Daily Sunshine Duration, Mon. Weath. Rev. , V. 83, pp. 141-146.

Hansen, J.E., 1969: Exact and Approximate Solutions for Multiple Scattering by Cloudy and Hazy Planetary Atmospheres, J. Atmos. Sci., V. 26, pp. 478-487.

Haurwitz, B., 1945: Insolation in Relation to Cloudiness and Cloud Density, J. Meteor., V. 2, pp. 154-166.

Johnson, J.C., 1954: Physical Meteorology, The M.I.T. Press, Cambridge, Mass., 393 pp.

Kimball, H.H., 1919: Variations in the Total and Luminous Radiation with Geographical Position in the United States, Mon. Weath. Rev., V. 47, 769-793.

Korb, G., 1961: Absorption von Sonnenstrahlung, Wolken. Wiss. Mitt., Meteorol. Inst., München, Nr. 6, 175 pp.

Lettau, H., and Lettau, K., 1969: Shortwave Radiation Climatonomy, Tellus, V. 21(2), pp. 208-222.

Loewe, F., 1963: On the Radiation Economy, Particularly in Ice- and Snow-Covered Regions. Contribution no. 44 of the Institute of Polar Studies, The Ohio State University, Columbus, Ohio.

Mateer, C.L., 1955(a): Average Insolation in Canada during Cloudless Days, Canad. J. Tech., V. 33, pp. 12-32.

_____, 1955(b): A Preliminary Estimate of Average Insolation in Canada, Canad. J. Agri. Sci., V. 35, pp. 579-594.

Mie, G., 1908: A Contribution to the Optics of Turbid Media, Especially Colloidal Metalic Suspensions, Ann. Physik, fourth series, V. 25, pp. 377-445.

Möller, F., 1965: On the Backscatterance of Global Radiation by the Sky, Tellus, V. 17(3), pp. 350-355.

Monteith, J.L., 1962: Attenuation of Solar Radiation: A Climatological Study, Quart. J. Roy. Meteor. Soc., V. 88, pp. 508-521.

Munn, R.E., 1966: Descriptive Micrometeorology, Academic Press, New York and London, 245 pp.

____, and Bolin, B., 1971: Global Air Pollution- Meteorological Aspects, Atmos. Envir., V. 5, p. 363.

Neiburgur, M., 1949: Reflection, Absorption, and Transmission of Insolation by Stratus Clouds, J. Meteor., V. 6, pp. 98-104.

Neumann, J., 1954: Insolation in Relation to Cloud Amount, Mon. Weath. Rev., V. 82, pp. 137-139.

Plass, G., and Kattawar, G., 1968(a): Influence of Single Scattering Albedo on Reflected and Transmitted Light from Clouds, J. Appl. Opt., V. 7(2), pp. 361-367.

____, and _____, 1968(b): Monte Carlo Calculations of Light Scattering from Clouds, J. Appl. Opt., V. 7(3), pp. 415-419.

____, and _____, 1968(c): Radiant Intensity of Light Scattered from Clouds, J. Appl. Opt., V. 7(4), pp. 699-704.

____, and _____, 1968(d): Influence of Particle Size Distribution on Reflected and Transmitted Light from Clouds, J. Appl. Opt., V. 7(5), pp. 869-878.

____, and _____, 1968(e): Calculations of Reflected and Transmitted Radiance for Earth's Atmosphere, J. Appl. Opt., V. 7(6), pp.1129-1135.

Pochop, L.O., Shanklin, M.D., Horner, D.A.,1968: Sky Cover Influence on Total Hemispheric Radiation During Daylight Hours, J. Appl. Meteor., V. 7(3), pp. 484-489.

Rasool, S.I., and Schneider, S.H., 1971: Atmospheric Carbon Dioxide and Aerosols: Effects of Large increases on Global Climate, Science, V. 173, pp. 138-141.

Rayleigh, Lord, 1899: On the Transmission of Light Through an Atmosphere Containing Small Particles in Suspension and the Origin of the Blue in the Sky, Philos. Mag., V. 47, pp. 375-384.

Robinson, G.D., 1958: Some Observations from Aircraft of Surface Albedo and the Albedo and Absorption of Clouds, Arch. Met. Geophys. Biokl., V.9, Ser. B, pp. 28-41.

Robinson, G.D., 1963: Absorption of Solar Radiation by the Atmospheric Aerosol as Revealed by Measurements at the Ground, Arch. Met. Geophys. Biokl., Ser B, V. 12, pp. 19-40.

_____, 1970: Some Meteorological Aspects of Radiation and Radiation Measurement, Advances in Geophysics, V. 16, pp. 285-306.

Robinson, N., 1966: Solar Radiation, Elsevier, Amsterdam, 347 pp.

Schneider, S.H., 1971: A Comment on Climate: The Influence of Aerosols, J. Appl. Meteor., V. 10, pp. 840-841.

Sekera, Z., and Blanche, G., 1952: Tables Relating to Rayleigh Scattering of Light in the Atmosphere, Scientific Report No. 3, Contract AF 19(122)-239, Air Force Cambridge Research Center, Cambridge, Mass.

Sellars, W.D., 1969: Physical Climatology, The University of Chicago Press Chicago and London, 272 pp.

Study of Man's Impact on Climate (SMIC), Report of, 1971: Inadvertent Climate Modification, The M.I.T. Press, Cambridge, Mass. 308 pp.

Tanaka, M., 1971(a): Radiative Transfer in Turbid Atmospheres: I - Matrix Analysis for the Problem of Diffuse Reflection and Transmission, J. Meteor. Soc. Japan, V. 49(4), pp. 296-311.

_____, 1971(b): II - Angular Distribution of Intensity of Solar Radiation Diffusely Reflected and Transmitted by Turbid Atmospheres, J. Meteor. Soc. Japan, V. 49(5), pp. 321-332.

_____, 1971(c): III - Degree of Polarization of the Solar Radiation Reflected and Transmitted by Turbid Atmospheres, J. Meteor. Soc. Japan, V. 49(5), pp 321-342.

Titus, R.L., and Truhlar, E.J., 1969: A New Estimate of Global Solar Radiation in Canada, Atmospheric Branch, Dept. of the Environment, Government of Canada, 17 pp.

Tverskoi, P.N., 1962: Physics of the Atmosphere, (Trans. from the Russian by IPST, Jerusalem, 1965), GMIZ, Leningrad, 560 pp.

Twomey, S., Jacobowitz, H., and Howell, H.B., 1966: Matrix Methods for Multiple Scattering Problems, J. Atmos. Sci., V. 23, pp. 289-296.

Vershinin, I., 1973: Justification for Computing Solar Radiation over Short Periods of Time, Soviet Hydrology: Selected Papers, pp. 1-17.

Vowinckel, E., and Orvig, S., 1962: The Relation between Solar Radiation and Cloud Type in the Arctic, J. Appl. Meteor., V. 1, pp. 552-559.

Wallen, C.C., 1966: Global Solar Radiation and Potential Evapotranspiration in Sweden, Tellus, V. 18(4), pp. 786-800.

Yamamoto, G., 1962: Direct Absorption of Solar Radiation by Atmospheric Water Vapour, Carbon Dioxide, and Molecular Oxygen, J. Atmos. Sci., V. 19, pp. 182-188.